![UiA University of Agder logo]

Optimal capacity density of offshore wind farms

An analysis for the prospective wind energy projects in the North Sea

AKANSHA JHA

SUPERVISORS

Sathyajith Mathew
Stefan Goossens
Dhruvit Berawala

Abstract

The North Sea and Norwegian continental shelf have been identified to possess some of the world's best wind resources. Nine countries, including Norway, have signed the Ostend Declaration and established their offshore wind development targets for 2050. However, space constraints, current consumption, siting regulations, and spatial planning risks accentuate the need for finding an optimum design parameter, i.e., capacity density (MW/km^2) for offshore wind farms. A thorough understanding of this optimization problem seems to be missing in the offshore wind energy industry including leading offshore wind developers. Achieving an optimal capacity density involves a collaborative effort while also considering the potential economic and environmental benefits of the project. This master's thesis aims to create guidelines and identify the levers that drive the optimal capacity density of an offshore wind farm in the North Sea by assessing wind characteristics, evaluating net annual energy production, computing economic indices, and performing sensitivity analysis.

The work emphasizes better understanding of the input and output parameter sensitivities pertaining to techno-economic factors under eleven different scenarios using PyWake simulation and cross-linking the simulation results to create a sensitivity analysis tool for economic indices. The focus is on in-depth study to document the procedure involved in identifying the optimal windfarm capacity density and not simply objectifying the results based on the most accurate wake model.

The study found that different offshore wind developers may reach different optimum capacity densities depending on their assumptions, methodologies and technologies used for estimation and reporting the financial metrics. For example, the study shows that the choice of wake model can lead to a significantly different optimum capacity density between 4.76 and 9.10 MW/km^2 with the motive to maximize profit using a conservative and optimistic approach. Moreover, some developers may have more advanced or sophisticated methods for wind farm simulation and power production estimation, leading to more accurate and precise capacity density estimates. Based on a comprehensive analysis of various parameters and their impact on sensitivity, the optimal capacity density is anticipated to lie between 3.62 and 6.05 MW/km^2 for a typical wind farm located in the North Sea. In some extreme cases where wind resources are scarce or strike prices are below levelized energy cost, the optimal capacity density could be as low as 2.64 MW/km^2.

Abstrakt (Norsk)

Nordsjøen og norsk kontinentalsokkel er identifisert for å besitte noen av verdens beste vindressurser. Ni land, inkludert Norge, har signert Ostend-deklarasjonen og etablert sine havvindutviklingsmål for 2050. Plassbegrensninger, strømforbruk, lokaliseringsbestemmelser og arealplanleggingsrisiko fremhever imidlertid behovet for å finne en optimal designparameter, dvs. kapasitetstetthet (MW/km^2) for havvindparker. En grundig forståelse av dette optimaliseringsproblemet ser ut til å mangle i offshore vindenergiindustrien, inkludert ledende offshore vindutviklere. Å oppnå en optimal kapasitetstetthet innebærer en samarbeidsinnsats samtidig som man vurderer de potensielle økonomiske og miljømessige fordelene ved prosjektet. Denne masteroppgaven tar sikte på å lage retningslinjer og identifisere driverne for den optimale kapasitetstettheten til en havvindpark i Nordsjøen ved å vurdere vindkarakteristikker, evaluere netto årlig energiproduksjon, beregne økonomiske indekser og utføre sensitivitetsanalyse.

Arbeidet legger vekt på bedre forståelse av sensitiviteten til input og output parametre knyttet til teknoøkonomiske faktorer under elleve forskjellige scenarier ved bruk av PyWake-simulering og krysskobling av simuleringsresultatene for å lage et sensitivitetsanalyseverktøy for økonomiske indekser. Fokuset er på dybdestudier for å dokumentere prosedyren involvert i å identifisere den optimale vindparkens kapasitetstetthet og ikke bare objektivisere resultatene basert på den mest nøyaktige vakemodellen.

Studien fant at forskjellige havvindutviklere kan oppnå forskjellige optimale kapasitetstettheter avhengig av deres forutsetninger, metoder og teknologier som brukes for estimering og rapportering av økonomiske beregninger. For eksempel viser studien at valg av kjølvannsmodell kan føre til en vesentlig forskjellig optimal kapasitetstetthet mellom 4,76 og 9,10 MW/km2 med motivet for å maksimere profitt ved å bruke en konservativ og optimistisk tilnærming. Dessuten kan noen utviklere ha mer avanserte eller sofistikerte metoder for vindparksimulering og kraftproduksjonsestimat, noe som fører til mer nøyaktige og presise estimater av kapasitetstetthet. Basert på en omfattende analyse av ulike parametere og deres innvirkning på følsomheten, forventes optima å ligge mellom 3,62 og 6,05 MW/km^2 for en typisk vindpark lokalisert i Nordsjøen. I noen ekstreme tilfeller der vindressursene er knappe eller strikeprisene er under energikostnad over levetiden (LCOE), kan den optimale kapasitetstettheten være så lav som 2,64 MW/km^2.

Preface

This thesis marks the completion of Master of Science education in Renewable Energy at University of Agder. As a Mechanical Engineering graduate with work experience in the oil & gas industry, this project helped me leverage my prior knowledge and develop competence in the field of offshore wind. In this thesis, we focus on the optimal capacity density analysis for future offshore wind farms, aiming to determine the maximum power that can be generated while minimizing the cost and environmental impact.

The target readers for this thesis includes researchers and professionals in the field of renewable energy, as well as policymakers and stakeholders interested in the development of offshore wind farms. The thesis provides a comprehensive overview of the optimal capacity density analysis framework and its applications to offshore wind farms.

One of the key challenges in this research was the availability and uncertainty of detailed financial data, so assumptions were made where applicable. Furthermore, the computation requirements for performing wake simulation with a greater number of turbines were substantial, which presented a significant computational challenge.

This research would not have been possible without the guidance and support of my supervisors. I would like to express my sincere gratitude to Prof. Sathyajith Mathew at the Faculty of Engineering and Science, UiA and Mr. Stefan Goossens and Dr. Dhruvit Berawala at Offshore Wind Technology, Equinor ASA for their valuable insights, advice, and encouragement throughout this project. Their expertise and dedication have been instrumental in the successful completion of this thesis.

I hope that this thesis contributes to the understanding of the optimal capacity density analysis for future wind farm development and inspires further research in this field.

Akansha Jha

Grimstad, 22.05.2023

Individual/group Mandatory Declaration

The individual student or group of students is responsible for the use of legal tools, guidelines for using these and rules on source usage. The statement will make the students aware of their responsibilities and the consequences of cheating. Missing statement does not release students from their responsibility.

1.	I/We hereby declare that my/our report is my/our own work and that I/We have not used any other sources or have received any other help than mentioned in the thesis.	☑
2.	I/we further declare that this thesis: - has not been used for another exam at another department/university/university college in Norway or abroad; - does not refer to the work of others without it being stated; - does not refer to own previous work without it being stated; - have all the references given in the literature list; - is not a copy, duplicate or copy of another's work or manuscript.	☑
3.	I/we am/are aware that violation of the above is regarded as cheating and may result in cancellation of exams and exclusion from universities and colleges in Norway, see Universitets- og høgskoleloven §§4-7 og 4-8 og Forskrift om eksamen §§ 31.	☑
4.	I/we am/are aware that all submitted theses may be checked for plagiarism.	☑
5.	I/we am/are aware that the University of Agder will deal with all cases where there is suspicion of cheating according to the university's guidelines for dealing with cases of cheating.	☑
6.	I/we have incorporated the rules and guidelines in the use of sources and references on the library's web pages.	☑

Publishing Agreement

Authorization for electronic publishing of the thesis.

Author(s) have copyrights of the thesis. This means, among other things, the exclusive right to make the work available to the general public (Åndsverkloven. §2).

All theses that fulfill the criteria will be registered and published in Brage Aura and on UiA's web pages with author's approval.

Theses that are not public or are confidential will not be published.

I hereby give the University of Agder a free right to

make the task available for electronic publishing: ☑JA ☐NEI

Is the thesis confidential? ☐JA ☑NEI

 (confidential agreement must be completed and signed by the Head of the Department)

   - If yes:

Can the thesis be published when the confidentiality period is over? ☐JA ☐NEI

Is the task except for public disclosure? ☐JA ☑NEI

(contains confidential information. see Offl. §13/Fvl. §13)

Table of Contents

List of Figures

List of Tables

Notation

Symbols	Unit	Variables
A	km^2	Offshore area
a	years or y	annuity
a_c	years or y	annuity based on construction years
a_o	years or y	Annuity based on operation
a_{oc}	years or y	Annuity based on operation + construction
AEP_{net}	MWh/y	Net Annual Energy production
c	m/s	Weibull scale factor
C	€/y	Cash flow
CF_{net}	-	Net Capacity factor
CRF	y^{-1}	Capital recovery factor
D	m	Rotor diameter
E_T	kWh	gross AEP
H	m	Hub height
i	%	inflation rate
k	-	Weibull shape factor
n	-	Velocity power proportionality
n	-	minimum no. of divisions for creating grids in the Layout
n_c	years or y	Construction years
n_o	years or y	Economic Lifetime / operational years of a wind turbine
P_R	kW	Rated power
P_v	kW	Power at wind speed V
R	%	Weighted-average cost of capital or Nominal discount rate
r	%	interest rate or real discount rate
S	D	Average wind turbine spacing or Minimum spacing ‖ (ALONG) Wind direction
T	-	No. of wind turbines
V	m/s	wind speed
V_C	m/s	Cut-out speed
V_I	m/s	Cut in speed
V_R	m/s	Rated speed
η	%	Efficiency afer additional Losses

Abbreviations

AEP	Annual energy production
BP	BastankhahGaussian wake model (wake model)
CapEx	Capital expenditures or overnight capital cost
CD	Wind farm Power density or capacity density
CF	Capacity factor
CfD	Contract for Difference
ECN	Energy Research Centre of the Netherlands
IEA37SBG	IEA37SimpleBastankhahGaussian (wake model)
IRENA	International Renewable energy Agency
IRR	Internal rate of return
LCOE	Levelized cost of electricity
NCS	Norwegian continental shelf
NOJLocal	Local Jensen (wake model)
NOJ	Original Jensen (wake model)
NPV	Net present value
NREL	National Renewable Energy Laboratory
NSWPH	North Sea Wind Power Hub
O&M	Operation, Maintenance and Service
OpEx	Operational expenditures per year
RPD	Rotor power density or Specific Power
TotEx	Present value of Total Expenditure
TurboNOJ	Turbulence Optimized Park (wake model) or TurbOPark or Turbo Jensen
WACC	Weighted-average cost of capital or Nominal discount rate
WD	Wind direction
WFP	Wind farm power or rating
WS	Wind speed
WT	Wind turbine
WTP	Wind turbine nominal power or rating

1. Introduction

Offshore wind has emerged as a key enabler in the global energy transition towards a green shift during the past few decades, and in the future, it shall play a pivotal role in meeting the continuously rising demand for renewable power, promoting decarbonization as well as the future energy mix. The North Sea and Norwegian continental shelf (NCS) have some of the world's most brilliant wind resources. In collaboration with evolving technology (such as larger wind turbines, better design, and higher efficiency), the richer wind resources can be tapped efficiently [1]. Recent reports indicate that nine countries, including Norway, have signed the Ostend Declaration and are committed to jointly producing at least 120GW of offshore wind energy by 2030 and 300GW by 2050 [2]. The mission is to decarbonize the power sector and transform the North Sea into a sustainable energy hub or "green power plant". Norway has set a goal to install a minimum of 3.1 GW of offshore wind capacity, with 50% floating wind projects by 2030. Additionally, the country plans to identify areas that are suitable for the development of 30 GW of offshore wind by 2040, which will be open for bidding [3],[4].

In general, the North Sea has been utilized for various industries and functions over the years, including oil and gas platforms, telecommunication cables, pipelines, shipping lanes, military zones, fishing areas, sand mining, and natural habitats. Due to the limited available space with present consumption, only a small percentage of the remaining offshore space can accommodate the required gigawatt, considering utilized power density and water depth available for the fixed bottom (target water depth ≤ 55m) [5]. This raises the question of the maximum number of wind turbines that can be installed in a given offshore area while still maintaining high levels of energy production efficiency (referred to as optimal capacity density).

When planning for new offshore wind farms, several techno-economic and social factors need to be addressed. The social aspects include the natural environment, wildlife impact, noise pollution, property values, and public concerns such as the impact on the landscape and the overall aesthetics of the area. Financial analysts and domain experts consider criteria such as available wind resources, costs, subsidies, and market interest rates. Ultimately, determining the optimal capacity density for a wind farm involves a collaborative effort involving the concerns and priorities of the local community while also considering the potential economic and environmental benefits of the project. The purpose of this master's thesis is to identify the levers that drive the optimal capacity density of an offshore wind farm in the North Sea with the following objectives:

1) Identifying an optimized layout based on the wind characteristics at the site, developing scenarios according to capacity densities, and evaluating net annual energy production (AEP_{net}) depending on different types of wake models. The site assessment and study on PyWake models were carried out as preliminary work during the energy research project. (Refer to Energy Research project under the appendix)

2) Computing the economic indices such as levelized cost of energy (LCOE), net present value (NPV), and internal rate of return (IRR) for the selected range of capacity densities while extrapolating the cost estimates and finding the optimized result.

3) Performing sensitivity analysis based on the input parameters such as wind resource, capital expenditure (CapEx), operating expenses (OpEx), the weighted average cost of capital

(WACC), inflation rates, operational and construction timelines, and additional losses (such as non-availability, performance, electrical, environmental, and curtailment losses).

In various analyses conducted in the North Sea, it has been determined that the optimal capacity density for a wind farm, considering the Levelized Cost of Energy (which represents the average cost of electricity generation, accounting for all expenses over the lifespan of an energy source), can range between 3.6 and 7.5 MW/km^2, depending on the specific location. While previous studies have focused exclusively on optimizing for the levelized cost of energy (LCOE), this report aims to investigate whether optimizing for other parameters, such as net present value (NPV) and internal rate of return (IRR), yields similar results. The project's novelty lies in establishing a comprehensive guideline for the prospective offshore wind industry, particularly focusing on wind farm development along the Norwegian coastlines (or Norwegian continental shelf). The sensitivity analysis tool developed within the scope of this thesis incorporates a range of variations for the uncertainty of financial, operational, and wind data; and computes the results using two different methods. The tool encompasses three distinct economic indicators, evaluates eleven capacity density scenarios, and employs eight PyWake models to simulate the results. Moreover, Python^{TM} programming is implemented to generate plots, perform time-series analysis and produce results in this work.

The thesis is carried out in collaboration with the Wind Energy Technology team of Equinor and there is currently no timeline or specific plan to develop the offshore wind project at the given site. The findings performed are solely intended for the study and research purposes; and relies exclusively on publicly available information. Instances where information was not available or highly uncertain, simplification and assumptions were made to facilitate the analysis and address the research objectives effectively.

2. Research Questions

The research questions addressed in this study aim to provide answers to the following:

1) How does the capacity density of an offshore wind farm influence economic indices like Net Present Value (NPV), Levelized cost of energy (LCOE), and IRR (Internal rate of return)?
   - How does the variable that we are optimizing for (NPV, IRR or LCOE) influence the optimum? How far apart does optima lie?
   - How do the input assumptions influence the curve on a general level?
2) How can we find the optimal capacity density and what is the optimal value of a typical offshore wind farm?
3) How do different wake models influence the expected optimal capacity density?
4) How does the optimal capacity density change with the wind resource?

3. Literature Review and Technical Analysis

The determination of a reasonable capacity density requires an in-depth assessment of wind resource at the site, wind turbines to be installed and wake simulation. The section covers the technical aspects and pre-analysis for a windfarm project development on the theoretical level, starting with the essential terms involved. Studies on the European offshore wind capacity density and further expected developments are reviewed and summarized.

3.1 Technical terms and definitions

Wind farm rating or wind farm power

The term wind farm rating or wind farm power (WFP) typically refers to the total installed capacity or power rating of the windfarm. The rating is measured in megawatts (MW) or gigawatts (GW). It is alternatively referred to as plant size in this work and can be determined with the number and rating of wind turbines installed.

Turbine spacing

The distances between neighboring turbines in a wind farm is defined as turbine spacing. The inter turbine spacing is usually preferred in the prevailing wind direction to improve the overall efficiency of the windfarm [6]. It is an important factor to consider when designing and planning wind farms, as the spacing can affect the efficiency and overall performance of the turbines. Proper spacing is necessary to avoid velocity deficit and turbulence caused by wind wakes from adjacent turbines, which can lead to decreased power output, increased maintenance costs, and shortened turbine lifespan. A typical windfarm practically implements the turbine spacing in the range of 5D to 15D in the direction of prevailing wind, where D is the rotor diameter of a turbine [6].

Annual energy production (AEP) and Net annual energy production (AEP$_{net}$)

Annual energy production (AEP) refers to the total amount of energy generated by a wind farm, over the course of a year while net annual energy production (AEP_{net}) considers the actual usable energy output after accounting for external losses and other operational factors. AEP_{net} considers factors such as wake losses, availability, curtailment, transmission/distribution losses etc. and provides a more accurate assessment of the actual energy available for consumption or sale, taking into account the efficiency and performance of the wind farm. The terms are typically measured in megawatt-hours (MWh) [6],[7].

Capacity factor

Capacity factor (CF) is an important index for evaluating the performance of a windfarm and is defined as the ratio of actual energy production over a certain period, typically a year, to theoretical production (refer to eq. (3.1)) [6]. While the capacity factor is a unitless quantity, it is occasionally expressed as a percentage. It is a measure of efficiency and productivity of the wind farm. The capacity factor discussed in this work specifically pertains to wake losses, while the net capacity factor (CF_{net}) includes additional external losses too. Studies indicate the capacity factor ranges from 0.30 to 0.62 in the North Sea with an average wind speed of 7 to 8.5m/s [5].

$$CF_{net} = \frac{AEP_{net}}{WFP \cdot 8760} \tag{3.1}$$

Capacity density

The term capacity density (CD) of a windfarm, sometimes referred to as windfarm power density is defined as the ratio of windfarm's nameplate power capacity to its ground area or offshore space. The wind farm area is often calculated from a closed polygon connecting the wind turbines on the perimeter of the layout. Capacity density is expressed in megawatt per square kilometer (MW/km^2) [6].

The installed wind farm power density or the nominal capacity density may differ from the output power density. The former represents nameplate power capacity per unit area and the latter refers to power output per unit area [8]. In this report, the referred capacity density is in terms of the nominal value denoted by the following equation:

$$CD = \frac{WFP}{A}$$
(*MW/km^2*)   (3.2)

Specific power

Specific power alternatively referred to as rotor power density (RPD) is the nameplate generation capacity rating of a wind turbine (or nominal power) per unit rotor swept area [6]. It is expressed in watt per square meter (W/m^2) and can be represented by the following equation where D is the diameter of the wind turbine:

$$RPD = \frac{WFP}{\frac{\pi D^2}{4}}$$
(*W/m^2*)   (3.3)

3.2 Studies on capacity density

Optimal capacity density reflects design principles that seek to maximize wind farm efficiency and energy production while minimizing the cost of energy and environmental impact, with lower capacity density generally resulting in lower turbine interaction losses. Turbine spacing has been identified as the dominant driver of capacity density. The capacity factor decreases if the turbines are placed close to one another due to mutual interference. On the other hand, if the turbines are spaced too far apart, valuable wind resources may go untapped, the overall cost of a wind project per wind farm rating may escalate, and land utilization could be inefficient. Moreover, an excessively high density of turbines can detrimentally affect the environment by disrupting wildlife and altering the visual landscape (for offshore wind farms closer to shore). However, it's important to note that real-life wind projects are affected by regulations that can significantly impact the average capacity density [9].

Figure 3.1 depicts the actual and projected capacity densities of multiple offshore wind markets in five European countries, as reported [9]. The optimal capacity density of a wind farm varies depending on the specific power and turbine ratings. The average capacity density for the United Kingdom, Denmark, the Netherlands, and Germany ranges from 4 to 6 MW/km^2. Existing offshore wind farms in the chart exhibit varying capacity densities, falling within the range of approximately 3 and 14 MW/km^2. Another study conducted in 2021 with eleven offshore wind farms located in the North Sea (including the UK, Germany, and Denmark), signifies mean capacity density as 7.2 (range between 3.3 and 20.2 MW/km^2) [8]. All these studies imply that the capacity density is being overestimated and will decrease up to an optimum limit in the coming years, especially in countries with more seabed availability and where the decision on installed capacity stays with the developer [9].

a) Size and maturity of capacity density[1]

b) mean and range of windfarm capacity density per market
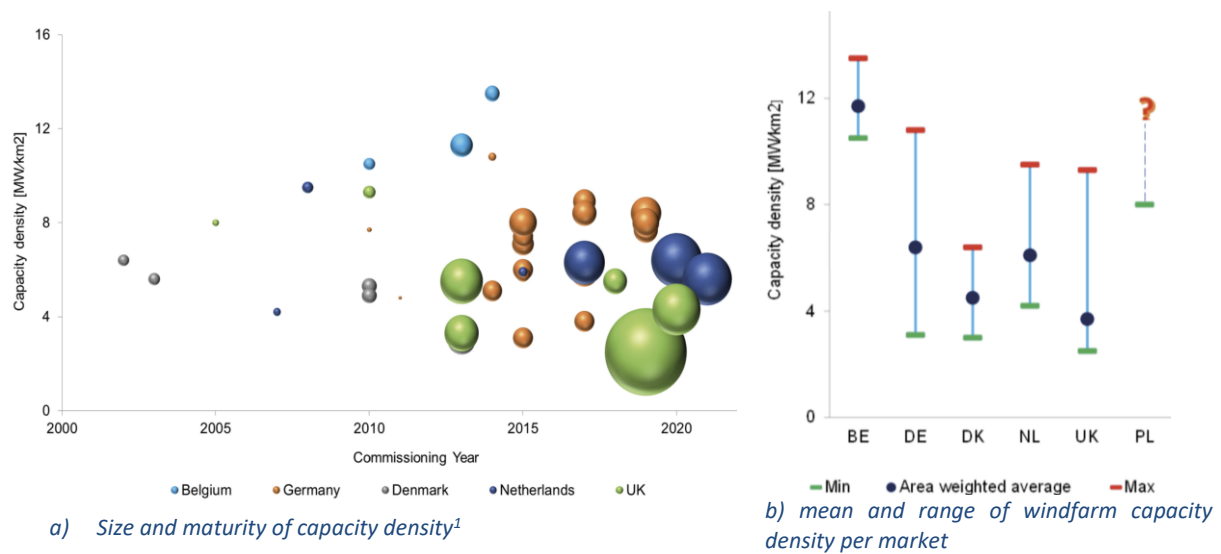
Figure 3.1 Capacity Density estimates in Europe [9]

Different studies have analyzed and reported the optimum derived capacity density as per the offshore location in North Sea. The Deutsche Wind Guard GmbH analysis states the corrected capacity densities of realized offshore wind farms in the North Sea region to be around 6 MW/km^2. The Energy Center Netherlands (ECN) conducted a study and determined that the optimal capacity density for a 15 MW wind turbine (WT) is 5.06 MW/km^2. Separate research by Müller derived a mean capacity density of 5 MW/km², and several other studies suggested a range between 4.9 and 5.9 MW/km^2 for both 13 MW and 15 MW turbines [6]. Research on the Princess Elisabeth Zone identified an optimum value of 7.5 MW/km^2. Looking ahead to 2030, the ECN (part of TNO) estimated a projected optimal wind farm power density of 3.6 MW/km^2 [5].

3.3 Prospective development in the wind industry

The capacity density of a wind farm is intrinsically tied to the megawatt capacity, which, in turn, relies on the specifications and rating of the wind turbines. The offshore wind industry is showing a noticeable inclination towards setting up bigger wind turbines that have a higher capacity. Figure 3.2 and Figure 3.3 shows the trend in turbine size for offshore wind energy production. In 2022, the average rated capacity of the turbines ordered amounted to 12.2 MW, 50% more than the average turbine connected to the grid, but the industry is moving towards installing even larger turbines with capacity exceeding 12MW. The most powerful turbines ordered in 2022 were 14MW by Siemens Gamesa in the UK [4]. This forms the basis for the selection of a turbine for the master's thesis.

The trend in recent years clearly shows a decline in specific power with the latest ordered turbine having 350 - 360 W/m^2 (refer to Figure 3.4) [4]. Generally, turbines with high specific power need higher average wind speed to reach the same capacity factor as compared to low specific power turbines. A more constant source of electricity would be required in the coming years to rely completely on renewables, and this could be achieved by an increase in rotor area, which will further result in reduction of specific power. The anticipated specific power is expected to come down to 325 - 332 W/m^2 by 2050 [6].

---

[1] Size of sphere represents the plant size in MW
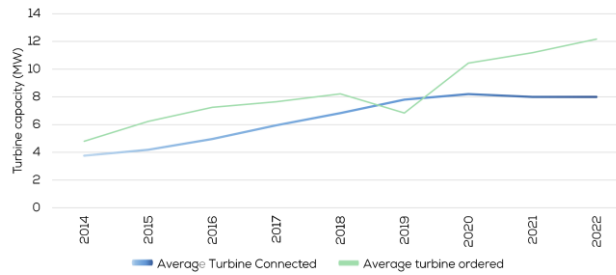
Figure 3.2 Yearly average of newly- installed offshore wind turbine rated capacity (MW)[4]
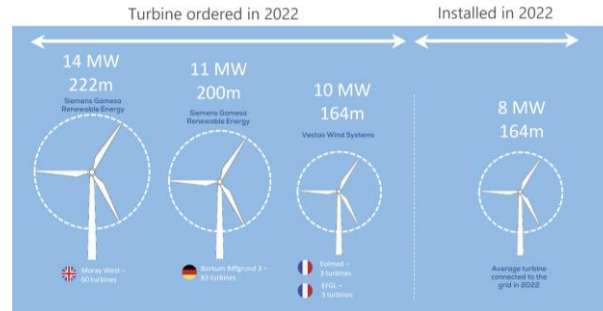
Figure 3.3 Offshore wind turbines trend in Europe [4]
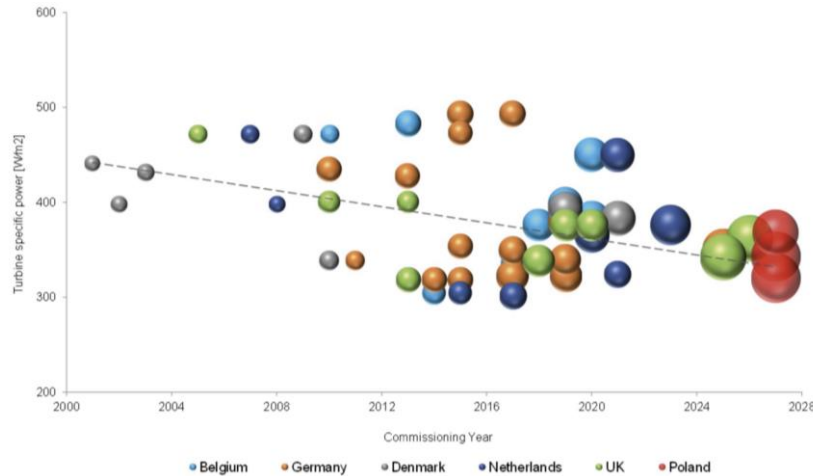
Figure 3.4 Trend in turbine specific power[1]

The analysis also shows 79% of all the wind turbines in offshore wind (including North Sea, Irish sea, Baltic Sea, Atlantic Ocean, and Mediterranean Sea) use monopiles (refer to Figure 3.6). Most operational offshore wind farms in Europe are below 50m deep waters but their distance to shore has increased over time (refer to Figure 3.5) [9]. Based on the historical analysis and future estimates for turbine rating, specific power, substructure and distance to shore consideration, the framework of this thesis is established.
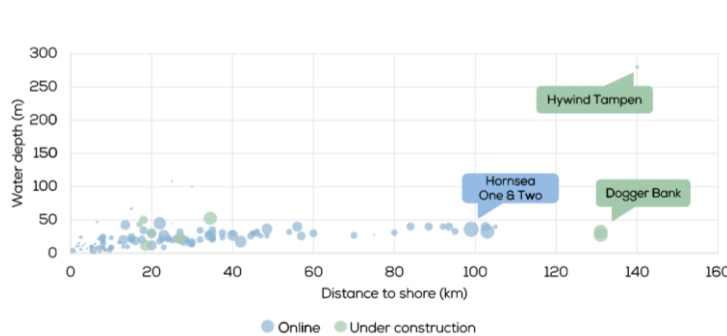
Figure 3.5 Water depth and shore locations of wind turbines installed till date[1] [4]
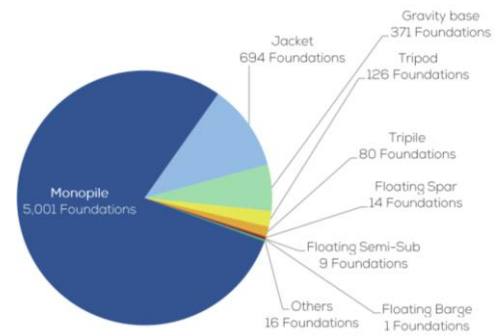
Figure 3.6 Types of substructures for wind turbines installed [4]

3.4 Site identification and assessment

This subsection addresses the preliminary work conducted as part of the master's research project with implementation of several Python[TM] modules. Firstly, a site with favorable wind resource was identified, followed by a comprehensive analysis of the wind data at the site. Additionally, an

extensive study was undertaken to examine various wake models in detail (refer to Energy Research project under the appendix).

For the assessment, wind speeds and wind directions with a temporal resolution of one hour measured at 10m and 100m above sea level were gathered for an offshore location in the North Sea. By utilizing Windpro[TM], wind speed predictions were generated for the specified hub height of 160m.

3.4.1 Wind resource analysis at the perspective site

Understanding the wind patterns and characteristics is crucial for determining the potential energy available at the site and planning the design of a wind farm. Analyzing wind speed and direction data helps optimize the arrangement of turbines to maximize energy capture and minimize wake effects. Wind velocity and direction can be effectively visualized using a windrose diagram, which is a polar plot divided into sectors of equal size. The circular representation of the wind rose visually illustrates the wind direction, with the length of each "spoke" indicating the frequency of wind from that direction. This graphical representation allows for a clear depiction of how the wind is distributed across different directions at the candidate site. The wind rose plot provides valuable information on the distribution of frequency, velocity, and energy in various directions, offering insights into the wind characteristics at the site [10].

Figure 3.7 displays a polar diagram created to represent windrose plot using in Python[TM]. The diagram is divided into 16 sectors, each spanning an angle of 22.5°. The highest prevailing wind direction (WD) originated from the south-west (SW) with an azimuth range of 225° ± 22.5°, accounting for 9.4% of the total occurrences. However, the strongest winds with most energy content are observed to originate from the south-southwest (SSW) direction with the wind speed of 28.6m/s. These findings align quite closely with the overall rose curve representing cumulative wind data from 1990 to 2021, which displays a wind prevalence of 10.2% along SW and a maximum recorded wind speed of 35.3 m/s (see Fig. 1).

While the dominant wind directions in both the windrose plot and the cumulative data are SW (Zone of west-southwest to south-southwest), it is worth noting that the strongest winds are observed to originate from the south-southwest (SSW) direction.

a)   Year 2021   *b) Average of cumulative data, Year 1990-2021*
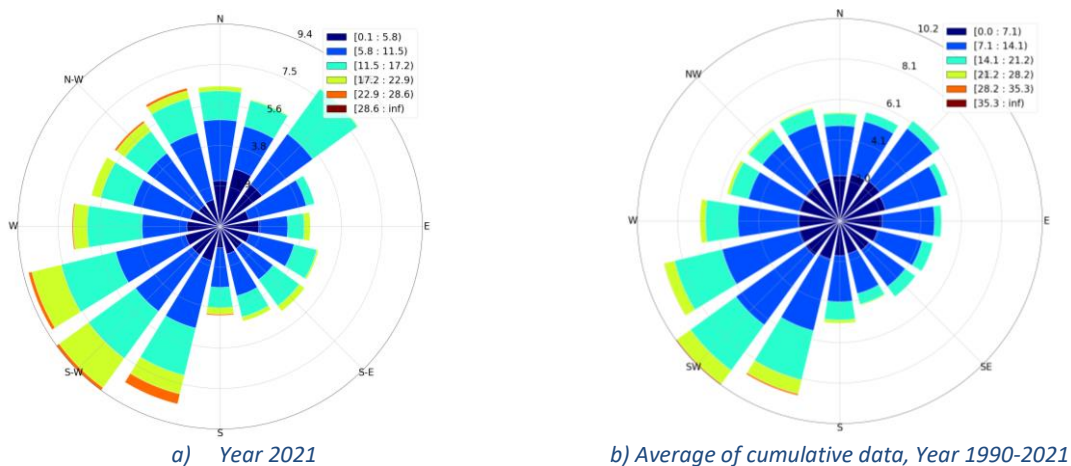
Figure 3.7 Wind rose at height 160m for the selected site

Further, the wind velocity distribution (both frequency and cumulative velocity distribution) can be effectively represented using standard statistical functions such as Weibull distribution. The Weibull distribution is recognized as a special case of the Pierson class III distribution, with probability density and cumulative density functions characterizing the variation in wind velocity [10]. The probability

distribution function quantifies the fraction of time during which the wind flows at a particular wind speed, as denoted by:

$$f(V) = \frac{k}{c}\left(\frac{V}{c}\right)^{k-1} e^{(-V/c)^k} \tag{3.4}$$

where k is the Weibull shape factor, c is the scale factor and V is the wind speed [10],[11]. The cumulative distribution represents the integration of the probability distribution function and signifies the percentage of time during which the wind speed is equal to or less than a specific value, denoted as V_0 [10],[11]. The relation is mathematically expressed as the integral of probability density functions using the following equation:

$$F(V \leq V_0) = \int_0^\alpha f(V) = 1 - e^{(-V/c)^k} \tag{3.5}$$

The statistical distribution of wind speeds varies across different locations worldwide due to factors such as local climatic conditions and the characteristics of the landscape and surface. These variations in the Weibull distribution encompass both the shape and mean value of the distribution.

a)   Weibull Probability distribution   b)   Weibull cumulative distribution
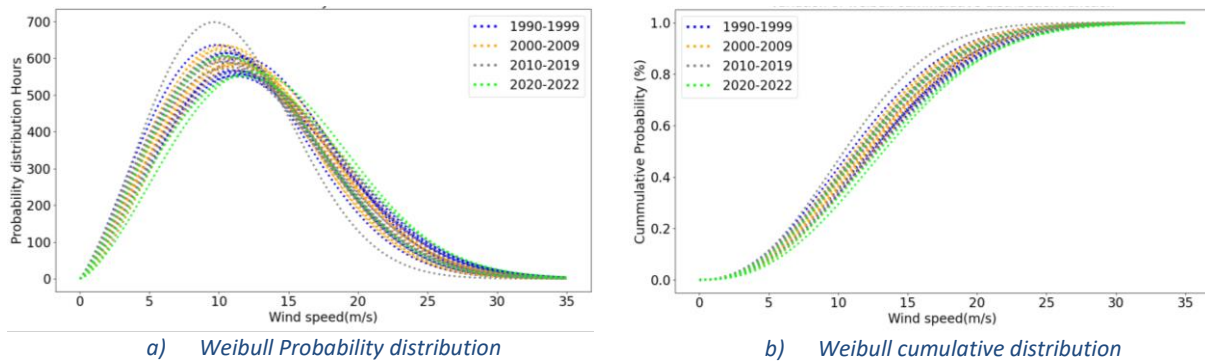
Figure 3.8 Weibull distribution for the years 1990 to 2022
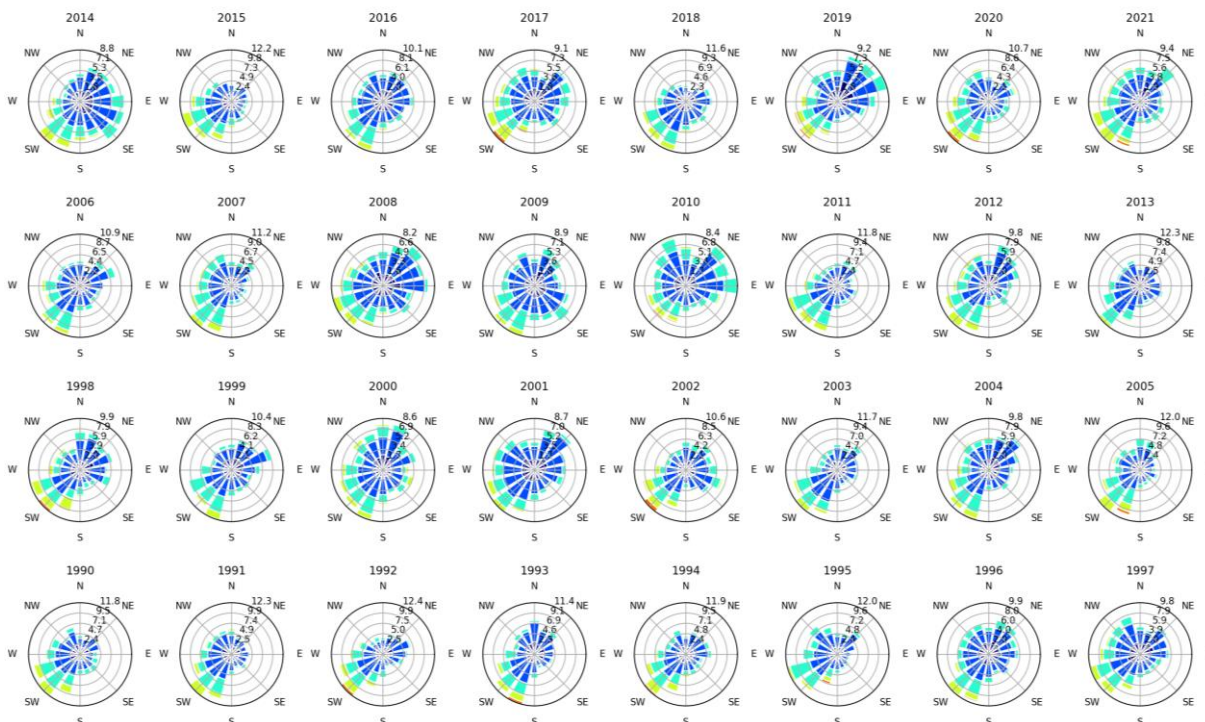
Figure 3.9 Wind rose for each year between 1990-2021

The variation of Weibull probability and cumulative distribution function for the year 1990-2021 are shown under Figure 3.8. These results can be correlated with the windrose plot depicting the same time frame (refer to the Figure 3.9). As seen from both the plots, year 2010 stood out as an anomaly with a significant dominance of wind from the east (E), followed by north-northwest (NNW). The corresponding values for the Weibull shape factor, scale factor, and probability density function were observed as 2.37, 12.16m/s, and 7.87%, respectively (refer to peak grey curve in Figure 3.8).

To account for the variations in the Weibull shape and scale factors across different years, an average value over the 32-year period was computed for further analysis (see subsection 3.4.2). The resulting Weibull shape factor, k exhibited a mean value of 2.28 (ranging from 2.15 to 2.45), while the scale factor c had a mean value of 13.91 m/s (ranging from 12.16 to 15.41 m/s). The peak probability distribution of the new Weibull distribution indicated a probability of 6.76%, corresponding to approximately 592.30 hours per year with wind velocities equal to or below 10.8 m/s, and an associated energy production of 8.88 GWh.
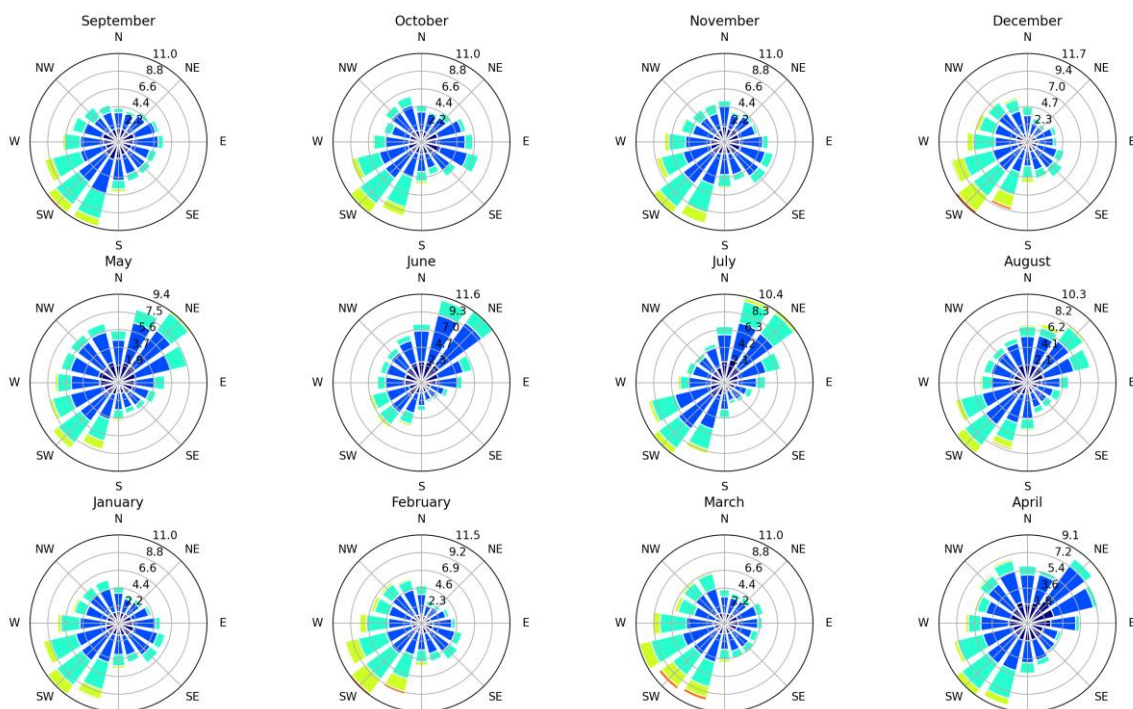
Figure 3.10 Wind rose for different months
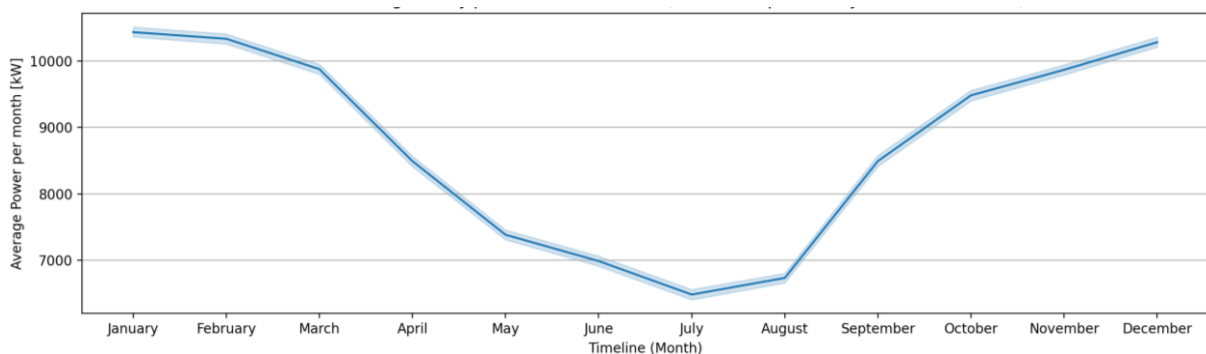
Figure 3.11 Predicted average hourly production for each month within the span of 32 years

The windrose Figure 3.10 illustrates a variation in wind speed and direction during January to December months and the corresponding wind power levels depicted in a graph (refer to Figure 3.11). Power is calculated from the formula under subsection 3.4.2 below. The results indicate that wind patterns vary by season and that average energy production is noticeably lower from May to August. The average wind power is highest during winter and lowest during the summer. Additionally, the highest prevailing wind direction shifts from southwest (SW) to northeast (NE) from April to June and then transitions back to southwest (SW) from June to August.

3.4.2 Selection of wind turbine

According to the literature study performed, a bottom fixed National Renewable Energy Laboratory (NREL) turbine with 15MW rating was selected to deploy on the selected site. Monopile, with a rotor diameter of 240m and a hub height of 160m seems realistic for after 2030 [12],[13]. The operational characteristics and performance curves of the selected turbine, suited to match specific wind conditions at the site, are presented in the accompanying table and figures (refer to Table 1, Figure 3.12 and Figure 3.13).

Table 1 Wind turbine characteristics

Parameters	Units	Abbreviation	
Turbine Type and Foundation	-	-	Fixed bottom; Monopile
Wind Turbine Nominal Power	MW	WTP	15
Rotor Diameter	m	D	240
Hub Height. MSL	m	H	$(40 + 0.5D)$ = 160
Rotor power density or Specific Power	W/m^2	RPD	332
Cut in speed	m/s	V_I	3.0
Rated speed	m/s	V_R	10.6
Cut-out speed	m/s	V_C	25.0
Velocity power proportionality	-	n	2.83
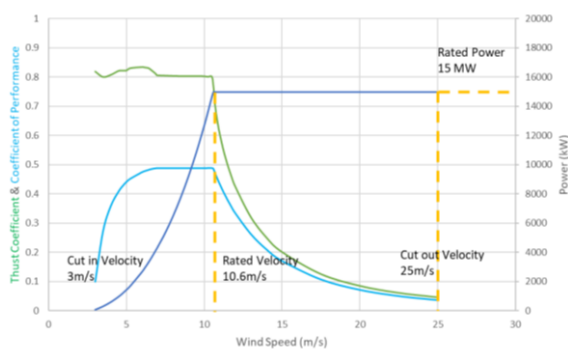
Figure 3.12 Figure. Power curve, Coefficient of thrust and performance
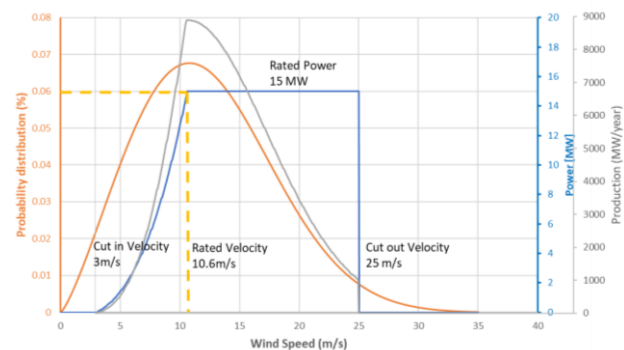
Figure 3.13 Power curve, Weibull curve and theoretical annual production

Figure 3.13 presents the probability distribution, power curve and the gross annual energy production as a product of these two factors. The representation of AEP is based on installation of a single turbine and probability distribution derived from the average values of k and c over a 32-year period. The gross AEP (E_t) of a wind turbine can be calculated using various numerical methods, such as the Newton Raphson method, by applying the equation provided:
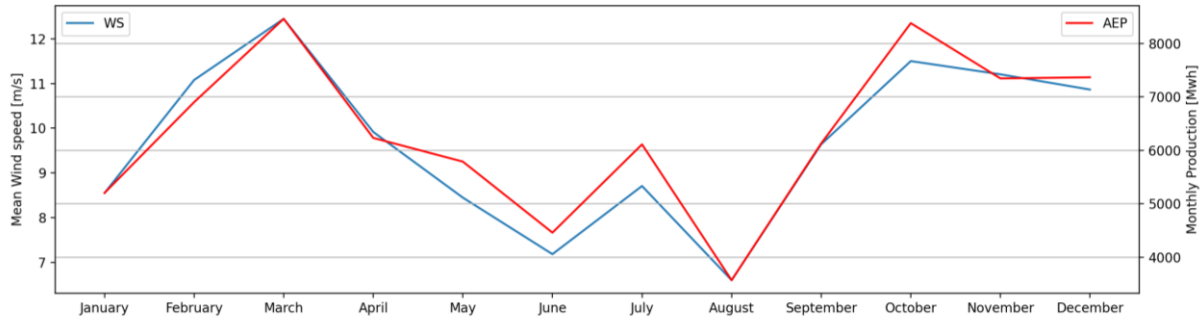
Figure 3.14 Predicted monthly energy production for the year 2021
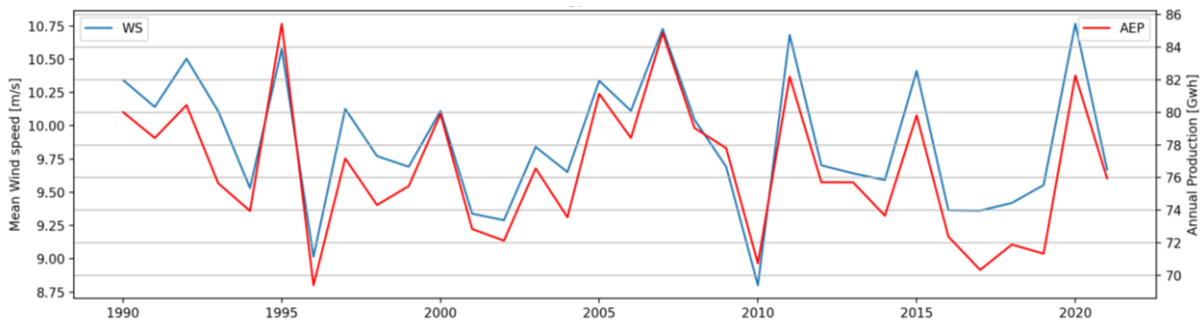
Figure 3.15 Predicted annual energy production for years between 1990-2021

$$E_t = \left[\int_{V_I}^{V_R} P(V) \cdot f(V) + P_R \int_{V_R}^{V_C} f(V) \right] \cdot 8760 \qquad (3.6)$$

$$P(V) \text{ or } P_v = P_R \left[\frac{V^n - V_I^n}{V_R^n - V_I^n} \right] \qquad (3.7)$$

where V_I, V_R, and V_C, are cut-in rated, and cut-out wind speed respectively. P_R is the rated power and $P(V)$ can be obtained by finding velocity power proportionality n using curve fitting and the Power-velocity values of 15MW NREL WT.

Figure 3.14 and Figure 3.15 shows how wind correlates with energy production. The wind speed and energy are not consistent with respect to month or the year. Figure 3.14 shows monthly analysis for the year 2021 based on mean wind speed (ranging between 6.5 to 12.5m/s) and energy production. Another analysis based on the 32-year span shows the fluctuation in average wind falls in between 8.75 - 10.75 m/s. The data shown for the year 2022 is incomplete (only available till July 2021) and hence not be taken into account (refer to Figure 3.15).

3.4.3 Time series analysis of wind

The analysis of meteorological data using time series is of great significance in the field of wind energy as it helps in determining the climate of a particular region, predicting extreme weather events, and understanding atmospheric phenomena for modeling purposes [14]. Figure 3.16 displays the relationship between energy production and wind variation across three regions based on hourly data. When the wind speed falls below the cut-in speed (Region 1) or exceeds the cut-out speed (Region 2), the turbine ceases operation, resulting in zero energy production. Conversely, when the wind speed lies between the cut-in and rated velocities (Region 3), energy production follows eq. (3.6). Furthermore, if the wind speed falls within the range of rated and cut-out velocities (Region 4), the turbine operates at its maximum rating of 15 MW.
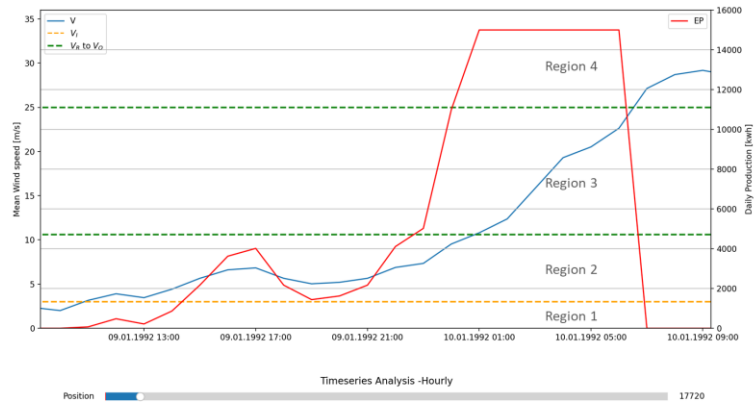
Figure 3.16 Timeseries analysis on hourly basis for wind data during 1990-2021
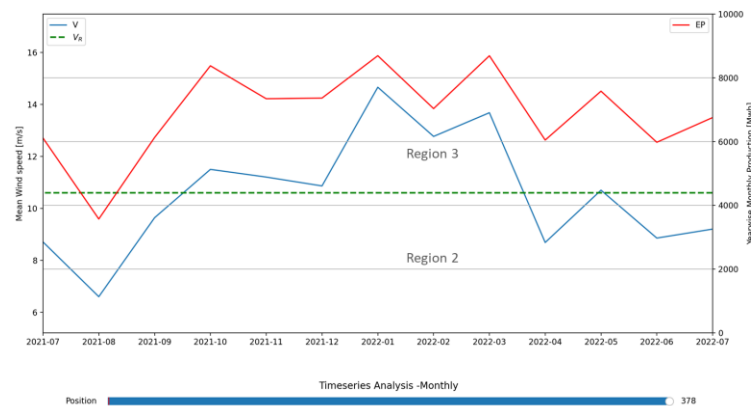
Figure 3.17 Timeseries analysis considering monthly average for wind data during 1990-2021

To observe the relationship more clearly, a time-series plot between monthly average production and wind speed is depicted in the accompanying figure (Figure 3.17). The analysis reveals that the average wind speed for all the months during the last year fell within Region 2 or Region 3, thereby indicating a good amount of energy production. Additionally, throughout this period, the average wind speed remains consistently above 7m/s which serves as an indicator that the chosen wind turbine is well-suited for the site.

3.4.4 Wind farm modelling with PyWake models

The average power loss due to WT wakes in the case of large offshore wind farms is approximately 10 to 20 % of the AEP and therefore the need for a suitable wake model assists in wind farm planning as well as estimating the revenue it will generate. To evaluate the wake losses within a windfarm, several pre-defined models from PyWake are implemented in this master's thesis.

PyWake is an open-source software, developed by DTU (Technical university of Denmark) that excels in evaluating wind farm flow fields, power production, and Annual Energy Production (AEP) based on a given wind farm layout. One notable aspect of PyWake is its efficient use of vectorization and numerical libraries, resulting in faster execution times. The wake models implemented including - Original Jensen Model (NOJ), Local Jensen (NOJLocal), TurbOpark (also referred to as Turbo Jensen; TurboNOJ), BastankhahGaussian (BP), IEA37SimpleBastankhahGaussian (IEA37SBG), TurboGaussian, Fuga, FugaBlockage) have gained wide adoption in both industry and academia.

This study incorporates the aforementioned wake models for simulation and analysis purposes, facilitating informed decision-making and wind farm layout optimization. Detailed information regarding the theory behind the various wake models implemented in this work can be found in the Energy Research project under the appendix.

4. Economics of Wind Energy and Valuation Theory

Careful analysis and modeling of the financial aspects are crucial for making informed decisions in wind farm planning, ensuring long-term viability, and attracting investors. Wind farms require significant upfront investments for the construction of turbines, infrastructure, and grid connections, as well as ongoing operational and maintenance costs. Proper financial planning is essential to ensure the project can generate adequate revenue to cover these expenses and deliver a satisfactory return on investment. This chapter delves into the economic framework, such as profitability assessment involving the time value of money and discounting future cash flows. Furthermore, it discusses securing financing and investments through revenue streams derived from power purchase agreements.

4.1 Project life cycle – offshore wind

The project life cycle for offshore wind could be broadly subdivided into four main phases as shown in the Figure 4.1.

Development and consent:

The scope of development and consent encompasses mainly project management and tasks that lead up to a financial decision or the point where firm orders are placed to initiate wind farm construction. This includes activities necessary to obtain planning consents, such as environmental impact assessments, and activities that define the design and engineering aspects of the project [16].
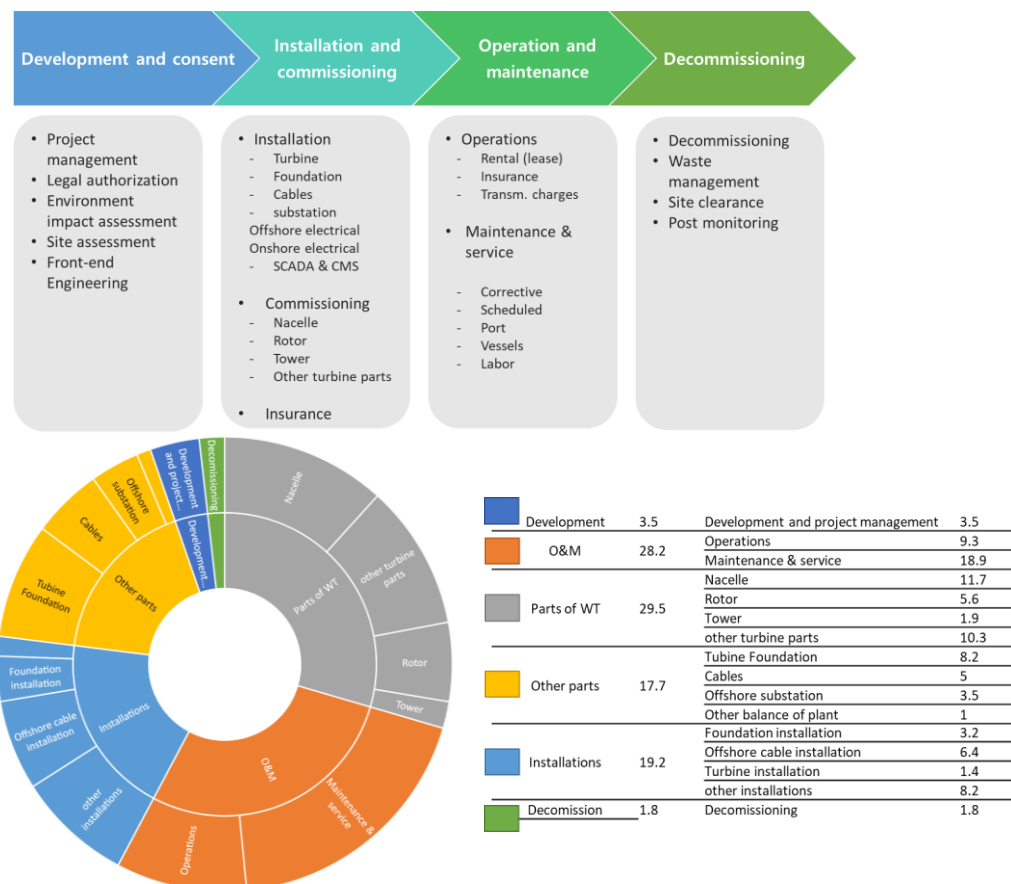
Figure 4.1 Wind farm costs (Percentage distribution) from BVG associates [15]

Installation and commissioning:

This phase involves installation and commissioning of the wind turbines and the infrastructure (balance of plant) required to deliver electricity from source to grid. The process begins by transporting the necessary components from the nearest port to the construction site. All activities are considered complete on the wind farm construction works completion date, at which point the assets are transferred to the operations teams [16].

Operation and Maintenance:

The operation and maintenance phase begins once the developed assets are transferred to the operations team. Operation, maintenance, and service (O&M) involve the collective functions that support the ongoing operation of wind turbines, balance of plant, and transmission assets throughout the lifespan of the wind farm. In the operational phase, the primary objective is guarantee safe operations, sustain the physical condition of wind farm assets, and maximize electricity generation [16].

Decommissioning:

After the operating life of the offshore wind asset has ended, the decommissioning phase involves the removal, safe abandonment, and safe disposal of offshore infrastructure [16].

The cost involved in each of the four phases falls in the category of either capital expenditures (CapEx) or operating expenses (OpEx), which are discussed in more detail in the following subsections.

4.1.1 CapEx

Capital expenditures (CapEx) are monetary resources that companies utilize to obtain, enhance, and uphold tangible assets such as real estate, facilities, infrastructure, technology, or machinery. CapEx is commonly employed for new projects or investments. These expenditures are initial investments aimed at expanding a company's operations or generating future economic benefits [17].

CapEx in offshore wind projects could be broadly subdivided into the following categories [15]:

1) Turbines and Foundations: The cost of procuring and installing wind turbines and their foundations, which are essential components of offshore wind projects, constitutes a significant portion of CapEx. This includes the purchase or lease of wind turbines, as well as the construction and installation of foundations such as monopiles, jackets, or floating platforms.

2) Subsea Cables and Grid Connection: The expenses associated with laying and connecting subsea cables to transmit electricity from the offshore wind farm to the onshore grid are another important CapEx component. This includes the cost of manufacturing, installing, and maintaining subsea cables, as well as constructing the necessary grid connection infrastructure onshore.

3) Offshore Substation: Building and installing an offshore substation, which serves as a hub for collecting, transforming, and transmitting electricity from multiple wind turbines, is also a significant CapEx item in offshore wind projects. This includes the construction of the substation's foundation, topside structure, and associated electrical equipment.

4) Installation and Commissioning: The cost of installing and commissioning offshore wind turbines, including the transportation of components to the project site, assembly, and testing, is another significant CapEx component. This includes specialized vessels, equipment, and labor for the offshore installation process.

5) Project Development and Management: Expenses related to project development and management, such as engineering and design, permitting, environmental assessments,

project management, and other associated costs, are also part of the CapEx for offshore wind projects.

4.1.2 OpEx

Operating expenses (OpEx) are the expenditures that a company faces in the course of its regular operational activities, which are the essential tasks that need to be carried out on a daily basis to run the business and generate income [17].

In the context of offshore wind farms, OpEx typically refers to the costs associated with the ongoing operation and maintenance of the installed and commissioned offshore wind farm. These costs include various expenses incurred during the operational phase of the offshore wind farm, such as routine maintenance, inspections, repairs, and replacements of components like turbines, foundations, and subsea cables. Personnel and labor costs related to operations and maintenance tasks, vessel and equipment costs for offshore operations, insurance and warranties for risk management, monitoring and control system costs for data collection and performance monitoring, grid connection costs for connecting to the onshore electrical grid, environmental and regulatory compliance costs, and administration and overhead costs are also included in OpEx [15].

Efficient management of OpEx is crucial for the overall economic performance of offshore wind farms, as it can significantly impact operational efficiency and profitability throughout the project's lifetime. Strategies for effective OpEx management may include preventive and predictive maintenance, optimized logistics and supply chain management, asset management, performance monitoring, and data-driven decision-making, among others.

Optimizing OpEx is an important consideration in the overall economic performance of offshore wind farms, as it can significantly impact the operational efficiency and profitability of the project over its lifetime. Effective OpEx management involves strategies such as preventive and predictive maintenance, efficient logistics and supply chain management, asset management, performance monitoring, and data-driven decision-making, among others [18].

4.2 Financial terms involved in economics of wind

The sections below provide an overview of some financial terms related to offshore wind economics that would be helpful in comprehending the work presented in this thesis.

4.2.1 Incentives for wind energy production (Purchase power agreement or Strike price)

Contracts for Difference (CfD) are a policy mechanism used to promote the deployment of renewable energy projects, particularly in countries with liberalized electricity markets. The mechanism provides a guaranteed price for renewable electricity producers, which reduces the financial risks associated with developing and operating renewable energy projects [19].

The Contract for Difference (CfD) is an agreement between a company that generates low-carbon electricity and the government (For example. Low Carbon Contracts Company, a government-owned company in the UK). The purpose of CfDs is to guarantee that low-carbon electricity generators receive a predetermined fixed price for the energy they produce throughout the contract period, known as the strike price. While generators still earn revenue by selling their electricity through the market, the CfD provides an additional payment to make up for any shortfall when the market reference price is lower than the strike price. The Low Carbon Contracts Company calculates and pays this top-up amount. If the market reference price is higher than the strike price, the generator must reimburse the difference to the company [20].
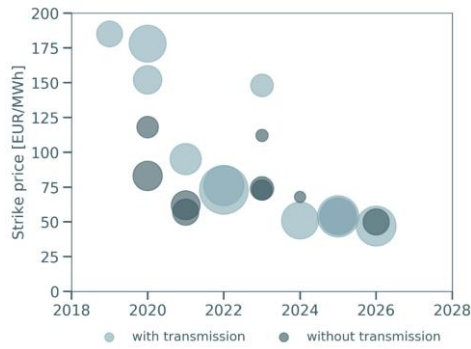
Figure 4.2 Strike price values for offshore wind in recent auction [21]
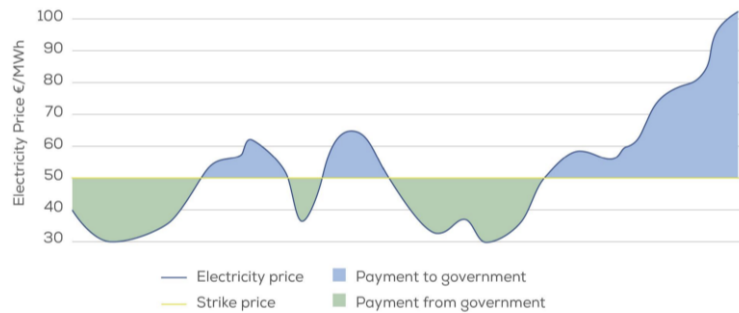
Figure 4.3 Revenue stabilization from two-sided Contract for Difference [22],[23]

Based on the recent auctions for offshore wind projects in Europe, a downward trend in the offshore wind farm costs is observed. Figure 4.2 displays the strike price for projects that will be launched within the next 7 years in the UK, Germany, the Netherlands, and France. After 2022, the socialized transmission costs for projects may reach 50-70 €/MWh, which is less than half the strike price of some projects that were (or planned to be) commissioned in 2020 [21]. Figure 4.3 illustrates an example of revenue stabilization with a two-sided CfD, wherein the generator sells electricity in the market based on a strike price. If the electricity prices fall below the guaranteed price, the generator receives the difference; otherwise, generators are required to pay back the difference [22],[23].

According to a Norwegian research study conducted on Equinor's Dogger Bank, the world's largest offshore wind farm, an analysis revealed that the project is deemed unprofitable, with an anticipated net present value of -£970m. This unfavorable outcome can be attributed to the significant decrease in the strike price award, resulting from aggressive bidding. A drastic reduction occurred from £114.39/MWh in the 2015 CfD auction to the 2019 Dogger Bank award of £39.650/MWh for phase A and £41.611/MWh for phases B and C [24].

While the popularity of CfDs has grown in recent years, it is difficult to predict whether they will fade with time. Several factors may affect the use of CfDs in the future such as changing energy policies, technological advancements, market competition, climate change goals etc. Overall, while the future of CfDs is uncertain, they have proven to be an effective policy mechanism in promoting renewable energy deployment in many countries. As the energy landscape evolves, it is likely that the role of CfDs and other policy mechanisms will continue to evolve as well [25].

4.2.2 Weighted average capital cost of (WACC)

The cost of capital refers to the minimum return a company needs to justify a capital budgeting project, like financing the construction of a new wind farm. It is a term commonly used by analysts and investors to assess if a decision is financially viable. Investors may also use it to evaluate the potential return and risks of an investment in relation to its cost [17]. This cost of capital (r in the NPV eq. 4.14) is most commonly calculated using the Weighted Average Cost of Capital (WACC) method [26]. The WACC method considers the costs associated with both debt and equity capital components and can be represented as follows [27]:

$$WACC = W_d \cdot r_d \cdot (1 - T) \ + \ W_e \cdot r_e \qquad (\%) \quad (4.1)$$

where W_d, W_e is the target proportions of debt and equity. r_d and r_e refer to the cost of debt and equity. T stands for the marginal tax rate and $r_d \cdot (1 - T)$ is the cost of debt after-tax.

The reason for using the word 'target' for debt and equity proportions in the WACC formula is because every firm has an ideal combination of debt and equity known as its optimal capital structure, which results in the highest possible stock price. A company that aims to maximize its value will determine its optimal capital structure, set it as a target, and then raise new capital in a way that maintains the actual capital structure close to the target over time [27].

Cost of debt

The expense incurred by a company for borrowing money, known as the cost of debt, is determined by the interest rate on its debt. It's important to note that this cost is calculated after taking into consideration the tax deductibility of interest expenses, which means it is based on the amount of debt paid after taxes [17],[28].

There are multiple methods to compute a company's cost of debt, depending on the available information. One approach involves using the formula:

$$Cost\ of\ debt\ = (risk-free\ rate\ of\ return\ +\ credit\ spread) \cdot (1 - tax\ rate) \qquad (€) \quad (4.2)$$

The risk-free rate of return is the hypothetical rate of return on a zero-risk investment, typically associated with government bonds such as U.S. Treasury bonds. The credit spread is governed by the amount of the company's borrowings and its credit rating. This formula is advantageous as it considers economic fluctuations, as well as company-specific factors such as debt usage and credit rating. If a company has higher debt levels or a lower credit rating, its credit spread will be greater, resulting in a higher cost of debt [17].

Alternatively, a company may choose to calculate the after-tax cost of debt by summing up the total interest paid on each of its debts throughout the year. This interest rate includes both the risk-free rate of return and the credit spread, as lenders consider both factors when determining the initial interest rate for a company's debts, as mentioned in the formula mentioned above.

Cost of equity

The Capital Asset Pricing Model (CAPM) is the most widely used method for calculating the cost of equity r_e. It is defined as follows [27]:

$$r_e = r_{RF} + (RP_M) \cdot \beta \qquad (€) \quad (4.3)$$

where
$$RP_M = r_M - r_{RF} \qquad (€) \quad (4.4)$$

Here r_{RF}, risk-free rate is typically calculated using the yield of government bonds such as a 10-year treasury bond or a short-term Treasury bill rate. β is the Beta coefficient of the company's stock, which serves as an indicator of its risk compared to the overall market. RP_M is the expected market risk premium, which is the difference between the return that investors demand to hold an average stock and the risk-free rate.

The beta value is a numerical measure that indicates the level of volatility associated with investing in a particular project or company, relative to a market or index. A beta of 1.0 theoretically suggests that the investment carries the same risk as the market. A beta below 1.0 indicates lower risk compared to the market, while a beta above 1.0 suggests higher risk and high volatility of the stock. The CAPM utilizes the beta parameter to anticipate higher returns from investments with higher beta values. In other words, beta is a key parameter in the CAPM that enables risk-adjusted returns on investments [28],[29].

Cost of capital vs discount rate

The cost of capital (or WACC) is the lowest acceptable return on an investment, while the discount rate is used to determine the present value of future cash flows from an investment and evaluate its profitability. These terms are similar and often mistaken for each other [17]. In this project, the terms WACC and nominal discount (or interest) rates are used interchangeably for simplicity proposes.

4.2.3 Inflation

Inflation refers to an increase in prices, resulting in a decrease in purchasing power over time. The decline in purchasing power can be measured by the average price increase of a selected category of goods and services over a certain period. This increase in prices is typically expressed as a percentage, indicating that the same amount of currency can buy fewer goods or services compared to earlier periods [17].

Figure 4.4 shows the historical trend of inflation (%) in Norway and the European Union for the past 20 years. The trend shows fluctuation in values between $0.45 - 5.76\%$ with a mean value of close to 2.5% for the past ten years [30]. The average inflation rate in Norway is forecasted to continuously decrease between 2023 and 2028 and is estimated to amount to two percent by 2028 [31].
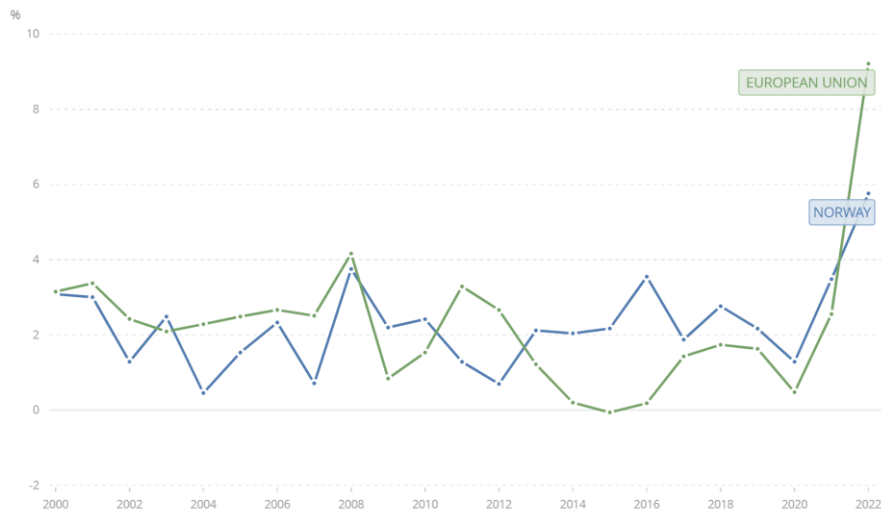
Figure 4.4 Historical inflation percentage of Norway and European Union [30]

4.2.4 Real interest rate

A real discount rate is used to calculate the present value of future cash flows from an investment after taking inflation into account. The relationship between real discount rate r, nominal discount rate R and inflation i is described by the Fisher Equation [32]:

$$r = \frac{(1 + R)}{(1 + i)} - 1 \qquad\qquad (\%) \quad (4.5)$$

4.2.5 Annuity and Capital recovery factor

An annuity refers to a series of identical cash flows, C that are distributed periodically at consistent intervals for n number of years [29]. If the cashflows in a project could be assumed as constant and spread at regular intervals, then annuity and capital recovery factor could be used to simplify the NPV calculations.

From the NPV equation (refer to NPV eq. 4.14 in section 4.4 for more details):

$$NPV = \sum_{t=0}^{n} \frac{C}{(1+r)^t} \qquad\qquad (\text{€}) \quad (4.6)$$

Since cashflows (C) for an annuity is constant:

$$NPV_{annuity} = C \sum_{t=0}^{n} \frac{1}{(1+r)^t} \qquad\qquad (\text{€}) \quad (4.7)$$

$$NPV_{annuity} = C \cdot \frac{1}{(1+r)} \sum_{t=0}^{n-1} \frac{1}{(1+r)^t} \qquad\qquad (\text{€}) \quad (4.8)$$

By using the equation for sum of a geometric series:

$$NPV_{annuity} = C \cdot \frac{1}{(1+r)} \left(\frac{1 - (1+r)^{-n}}{1 - (1+r)^{-1}} \right) \qquad\qquad (\text{€}) \quad (4.9)$$

$$NPV_{annuity} = C \cdot \left(\frac{1 - (1+r)^{-n}}{r} \right) \qquad\qquad (\text{€}) \quad (4.10)$$

$$NPV_{annuity} = C \cdot \left(\frac{(1+r)^n - 1}{r(1+r)^n} \right) \qquad\qquad (\text{€}) \quad (4.11)$$

$$NPV_{annuity} = \frac{C}{CRF} \qquad\qquad (\text{€}) \quad (4.12)$$

The capital recovery factor (CRF), calculated using an interest rate r, is the ratio of a fixed annuity to the present value of receiving that annuity over a specific time period [33]. It is basically an inverse of annuity a and is denoted as:

$$CRF = \frac{r(1+r)^n}{(1+r)^n - 1} \qquad\qquad (\text{y}^{-1}) \quad (4.13)$$

where n is the number of annuities received.

4.3 Levelized cost of energy (LCOE)

The Levelized Cost of Energy (LCOE), or Levelized Energy Cost (LEC), is a measure of the costs involved in producing energy, typically electricity, for a particular system. It provides a comprehensive assessment of all the costs related to the energy generation system over its lifetime, including the initial investment, ongoing maintenance, fuel costs, and capital expenses [34]. The LCOE of an energy producing system is calculated by summing up all cash outflows (both CapEx and OpEx) divided by the total energy generated over an assumed lifetime. [34]

LCOE serves as a metric to assess and compare alternative methods of energy production. Moreover, it could also be used as a minimum selling price at which energy must be sold in order for an energy generation project to break even.

When conducting a comparison of LCOEs for various systems, it is crucial to establish the scope of the 'system' and determine the costs that should be incorporated. For instance, it should be decided whether transmission lines and distribution systems should be considered as part of the overall cost. Similarly, it should be determined if R&D, tax, and environmental impact studies should be included. Furthermore, there is the question of whether the expenses incurred due to government subsidies should be factored into the calculated LCOE. Another crucial consideration is the determination of the value of the discount rate r. The selection of r can significantly influence the decision-making process for or against an option, so it must be carefully assessed. The discount rate is influenced by the cost of capital, which includes the balance between debt-financing and equity-financing, as well as an evaluation of the financial risk [33s].

Lastly, the LCOE should not be the sole metric used for evaluating a project's viability, and it should not be relied upon blindly. What ultimately matters is the LCOE values and the projected revenue streams generated by developers at financial close, which takes into account all the costs, revenues, and detailed financial planning. In reality, the LCOE is not a measure of the required tariff, as a more in-depth cash flow approach, which considers factors such as taxation, subsidies, and other incentives, is necessary for renewable energy product developers to assess the profitability of real-world projects. [7],[33] This, however, is dependent on the individual circumstances and the market and is beyond the scope of this project.

Figure 4.5 shows the LCOE estimates predicted for the future according to a BVG associates [21]. The study conducted for Norwegian industry shows that by 2030, the LCOE estimates for Norwegian are expected to fall up to 63 €/MWh and it could drop up to 35 €/MWh by 2050. However, these estimates are volatile and driven by several other uncertainties like inflation or geopolitical situation.

Literature estimates of LCOE from different studies within the North Sea and European offshore wind indicate that LCOE may vary from one country to another. The LCOE values from the 21 different scenarios and seven different capacity densities using 15 MW for the study implemented over the Princess Elisabeth zone shows a range between 52.7 and 53.2 €/MWh and 7.5 MW/km^2 as the optimal capacity density [7]. A similar study conducted by ECN demonstrates an LCOE of 62.5 €/MWh (with an optimal capacity density of 5.06 MW/km^2 and turbine spacing of 7.16D) [35]. A study carried out by Deutsche Windguard GmbH derived the optimal capacity density of 5.4 ± 0.5 MW/km^2 with the projected competitive price of LCOE around 65 €/MWh by 2030. The presented estimates in the study are based on 13 MW and 15 MW wind turbine spacings of 9D x 6D [6]. Another study with NSWPH (North Sea Wind Power Hub Consortium) states the LCOE could vary between 33 and 45 €/MWh for a capacity density of 3.6 MW/km^2 (15 MW of 67 turbines). It concludes the analysis based on the attractive offshore locations falling under the zones of Norway, the UK, the Netherlands, and the North Sea EEZs (exclusive economic zone) of Denmark and Germany [5].
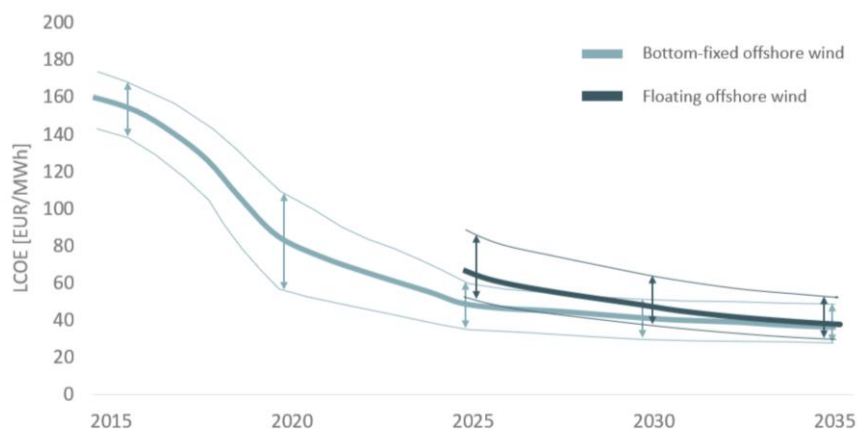
Figure 4.5 Projection for LCOE of offshore wind energy [21]

4.4 Net present value (NPV)

The Net Present Value (NPV) represents the present value of all projected cash flows, both positive and negative, throughout the entire lifespan of an investment after being discounted to the present time [32]. It can be represented by the equation below:

$$NPV = C_0 + \frac{C_1}{(1+r)^1} + \frac{C_2}{(1+r)^2} + \frac{C_3}{(1+r)^3} \cdots + \frac{C_n}{(1+r)^n} \qquad (€) \qquad (4.14)$$

$$NPV = \sum_{t=0}^{n} \frac{C_t}{(1+r)^t} \qquad (€) \qquad (4.15)$$

Here C_t is the expected net cash flow at time t, r is the discount rate and n is the operational life of the project. Cash outflows such as CapEx and OpEx are negative cashflows, while cash inflows are positive which are mainly the revenue generated from selling goods & services, which have been adjusted to reflect taxes, depreciation, and salvage values [27].

The purpose of performing an NPV analysis is to assess the value of an investment, project, or set of cash flows [32]. If the calculated NPV is positive, it indicates that the investment is financially viable and should be pursued. Conversely, if the NPV is negative, it suggests that the investment may not be profitable and should be avoided.

4.5 Internal rate of return (IRR)

The internal rate of return (IRR) is defined as the discount rate that forces the project's NPV to equal zero [27]. In other words, IRR could be explained as the expected compound annual rate of return that will be earned on a project or investment. Put another way, the initial amount of money invested at the start will be equivalent to the current value of the expected future cash returns from that investment [27]. The equation can be represented as:

$$NPV = C_0 + \frac{C_1}{(1+IRR)^1} + \frac{C_2}{(1+IRR)^2} + \frac{C_3}{(1+IRR)^3} \cdots + \frac{C_n}{(1+IRR)^n} = 0 \qquad (€) \qquad (4.16)$$

$$NPV = \sum_{t=0}^{n} \frac{C_t}{(1+IRR)^t} = 0 \qquad (€) \qquad (4.17)$$

Although both NPV and IRR methods are used in conjunction as decision gates for a potential investment, the NPV method is considered more reliable in many aspects. Even though the IRR is commonly understood by corporate executives and widely used in the industry to determine the potential rate of return for a project, it can sometimes conflict with the NPV method, especially when evaluating mutually exclusive projects. Hence, it's crucial to comprehend the IRR, its relationship with NPV, and the instances where choosing a project with a lower IRR might be preferable over an alternative project with a higher IRR [27].

'Independent projects' are those where the cash flows associated with their acceptance or rejection are not influenced by the acceptance or rejection of any other projects, while 'Mutually Exclusive projects' are those where only one could be accepted for a set of projects.

When assessing an independent project with conventional cash flows, both the NPV and IRR criteria consistently result in the same decision of acceptance or rejection. If the NPV indicates acceptance,

the IRR will also indicate acceptance. However, for mutually exclusive projects, there could be a conflict between the decision based on NPV and IRR.

There are two primary reasons for conflicts between NPV vs IRR seen for mutually exclusive projects [27]:

1. Variations in timing: where one project generates cash flows predominantly in the initial stages while the other project generates cash flows later on.

2. Differences in project size or scale: where one project requires a larger investment compared to the other.

Also, there could be scenarios where multiple IRRs exist, in that case decisions are made based on the NPV rule. Nevertheless, the IRR method retains its value as a valuable tool. The IRR calculates the average return of an investment throughout its lifespan and provides insights into how sensitive the NPV is to errors in estimating the cost of capital. Hence, understanding the IRR can be advantageous, but solely relying on it for investment decisions can be risky [29].

4.6 Economic parameters from literature survey

After performing a thorough literature survey on several published case studies of offshore wind farm development, the values for each parameter have been summarized in the Table 2. This will serve as a foundation for the economic analysis presented in this work.

Table 2 Summary of case studies [7],[5],[15],[35]

Parameter	Unit	Princess Elisabeth zone	BVG Associates	ECN Studies	NSWPH Consortium
Wind turbine rating	MW	15	10	15	15
Capacity Density range	MW/km2	6.2 to 12.5	-	4 to 10	3.6
Optimal Capacity density	MW/km^2	7.5	-	5.06	3.6
Additional losses	%	7.2% loss (Higher end 12.6 to 19.5%)	-	7.07-10.44%	45 to 150 km/kW (DC and AC transmission)
CapEx based on lifetime	M€/MW	2.56	2.7 (excl. Decom) to 3.08(incl. Decom)	2.26 to 2.27^2	1.90
Decommissioning in CapEx	-	yes	yes	Not specified	No
OpEx	k€/MW/y	58.74	86.64	121.10 to 125	45-47
Operating expenditure based on lifetime	k€/MW	833.69	1144.56	1721.12 to 1776.55	900-940
TotEx/MW	M€/MW	3.38 to 3.54	3.85(excl. Decom) to 4.22(incl. Decom)	3.98 to 4.05	-
depreciation period / number of annuities	years	25	27	20	30
Nominal discount rate	%	7.03	6.00	-	4.4
Inflation rate	%	2.00	-	-	1.5
Interest rate or real discount rate	%	4.93	6.00	3.50	2.9
Annuity	years	14.19	13.21	14.21	20
LCOE	€/MWh	52.7 to 53.2	-	62.5	33 to 45

---

^{2} The decommissioning costs (including turbine, foundation, cable, and substation) are marginal and range between 376k€/MW. Although they are not included in the CapEx for ECN extrapolation, the additional cost is included in the sensitivity for CapEx. Refer section 6.4, 6.5 and 6.6 for detail.

5. Methodology
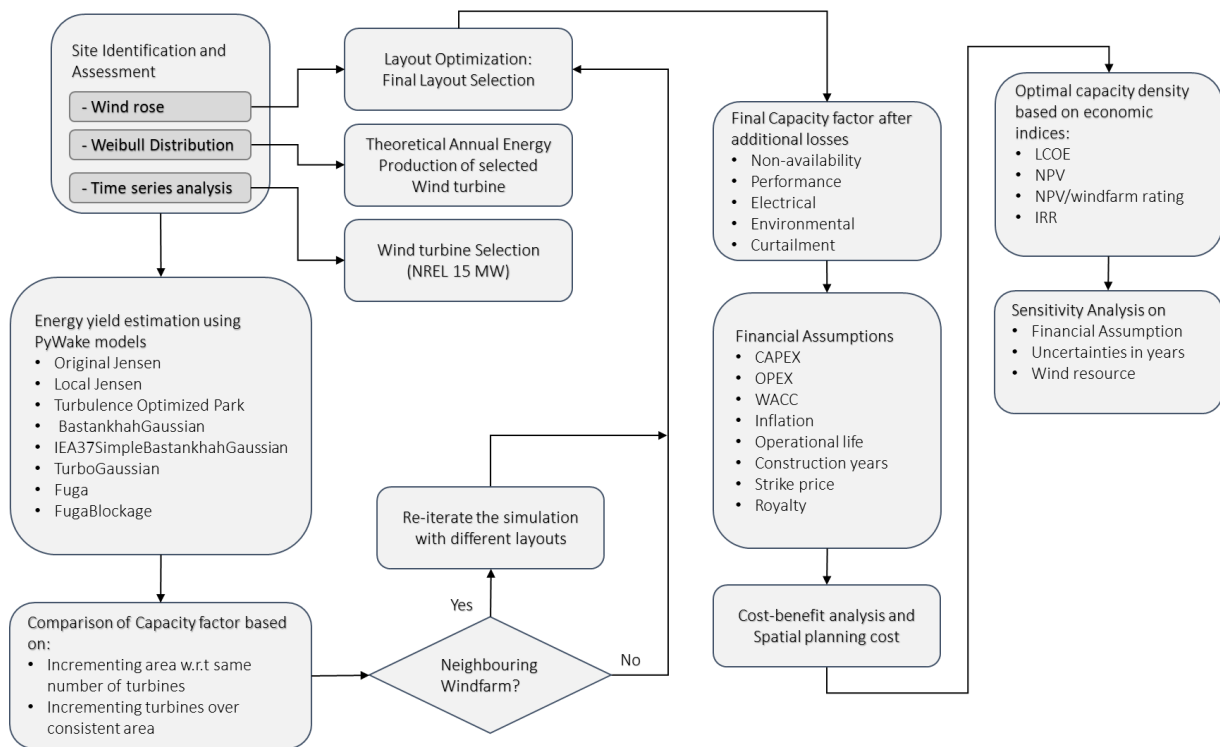
Figure 5.1 Flowchart of procedure for identifying optimal capacity density[3]

Figure 5.1 describes the overall procedure followed in this research to arrive at a suggestion. Optimal capacity density of a wind farm relies on several factors, including wind resources at the site, the type of turbines used, the terrain (in the case of onshore wind farms), and other environmental considerations. To determine the optimal capacity density of a wind farm, the necessary steps involved are as follows:

1) Site assessment: The primary step is to evaluate the proposed site for the wind farm and obtain the optimal layout of wind turbines. The assessment should include an analysis of the wind resource potential, including wind speed and direction measurements, using windrose, Weibull distribution and time-series analysis.

2) Turbine selection: The next step is selection of wind turbine type and rating with specified technical data such as power curve and thrust coefficient. Different turbine types have varying performance characteristics and efficiencies, which can influence the optimal capacity density of the wind farm.

3) Energy yield estimation: An energy yield estimation can be made using PyWake simulation to compute the anticipated yearly energy output of the wind farm using the wind speed data and chosen turbine specifications. Several companies use their in-house wake simulation tools and software that incorporate wake models with different empirical constants, superposition methods, and other coded characteristics which is proprietary to them.

4) Layout optimization: Following the assessment of the energy yield, an optimization analysis can be conducted to identify the best configuration or layout for the turbines in order to maximize energy production while minimizing wake losses and other turbine interactions.

5) Capacity density scenarios: Different capacity density scenarios can be achieved in the chosen marine area and with a comparable arrangement by installing a range of turbines.

---

[3] The selected location has no neighbouring windfarm and spatial planning cost is not included in the present work.

6) Cost-benefit and sensitivity analysis: Using different scenarios of capacity density and estimated energy generation, a cost-benefit analysis can be used to determine whether the wind farm is financially viable. The capital expenditures for installing the turbines, ongoing operational expenses, and revenue from selling the generated electricity should all be taken into account in this study.

7) Spatial planning risk assessment: To evaluate the potential environmental impact of the wind farm, including the impact on wildlife and the visual landscape, an environmental impact assessment should be carried out. Risk formulas are developed by conducting a societal cost-benefit analysis, where the risks associated with each user function are identified in consultation with the corresponding stakeholders [5]. However, this is not included within the scope of this work due to data limitations.

5.1 Basic assumptions

The selected site is anticipated to have an average water depth of 35m to ensure monopiles can be employed and onshore grid connections points that are able to accommodate the connected capacity [4],[7]. For this study, the discount rate is set equal to the nominal WACC, which is 6% [36]. The WACC has been determined from the company's annual report (financial statements and other supplements), while the value for inflation is assumed based on the average value for the past ten years in Norway [37]. Operational time for the wind turbines is considered around 27 years as an average value and the number is assumed based on different wind farm studies (Refer section 4.6). Other factors have been determined on the characteristics of North Sea area reported under the study based on Princess Elisabeth Zone [7]. Table 3 lists the basic parameters considered in this project.

Table 3 Overview of basic parameters considered for calculations

Description	
Operational Life	27 years
Average water depth	35m
Soil conditions	Sand clay
Entire zone Area	290km2
Distance to shore from the closest platform	40km
Substructure and foundation	Monopile
Array cable voltage	66kV
Array cable size	300 / 800 mm2
Foundation installation	Floating vessel
Array cable installation	Cable vessel
Turbine Installation	Jack-up vessel
WACC	6 %
inflation	2.5%

5.2 Layout planning of selected offshore wind farm

Designing and optimizing the layout of a wind farm is a complex process that involves numerous iterations. Wake effects occur when the wind passing through a wind turbine is disrupted, causing a

decrease in wind speed and generating turbulence. These effects can considerably impact the performance of turbines located downstream, but they can be reduced with careful placement within the permitted area. A better layout can minimize the consequences of higher turbine interaction effects, reduce structural loads, extend the project's lifetime, and eventually lower the LCOE. This section explains the work carried out in optimizing the layout and arriving at the capacity factor corresponding to various capacity densities.

5.2.1 Initial selection and Modification of Layout

Once the wind resource and area designated for the wind farm have been evaluated turbine placement can be optimized by exploring different layouts. The primary objective is to position them in a way that maximizes wind energy capture and minimizes wake losses by taking into account crucial factors such as wind speed, wind direction, and turbulence. The proposed site experiences a predominant wind direction from the southwest (as reported in subsection 3.4.1), leading to selection of three different layouts: rectangular, hexagonal, and trapezoidal (as portrayed in the Figure 5.2). The work involves manual turbine placement without assistance from any tool or layout optimization software and hence, involves less complex shapes for analysis. Additionally, two alternative orientations of the hexagonal layout were considered to assess whether the capacity factor would improve, but no significant difference could be observed. Figure 5.2 illustrates the sequence of conceptual framework for developing the final version. Table 12 in the appendix shows the wind distribution divided into 12 sectors which is used to perform the PyWake simulation, with an average wind speed of approximately 10 m/s at the given site.

a) Rectangular Layout

b) Polygon Layout - I (Orientation of Hexagonal Layout at -30°)

c) Polygon Layout - II (Orientation of Hexagonal Layout at -15°)

d) Hexagonal Layout

e) Trapezoidal Layout
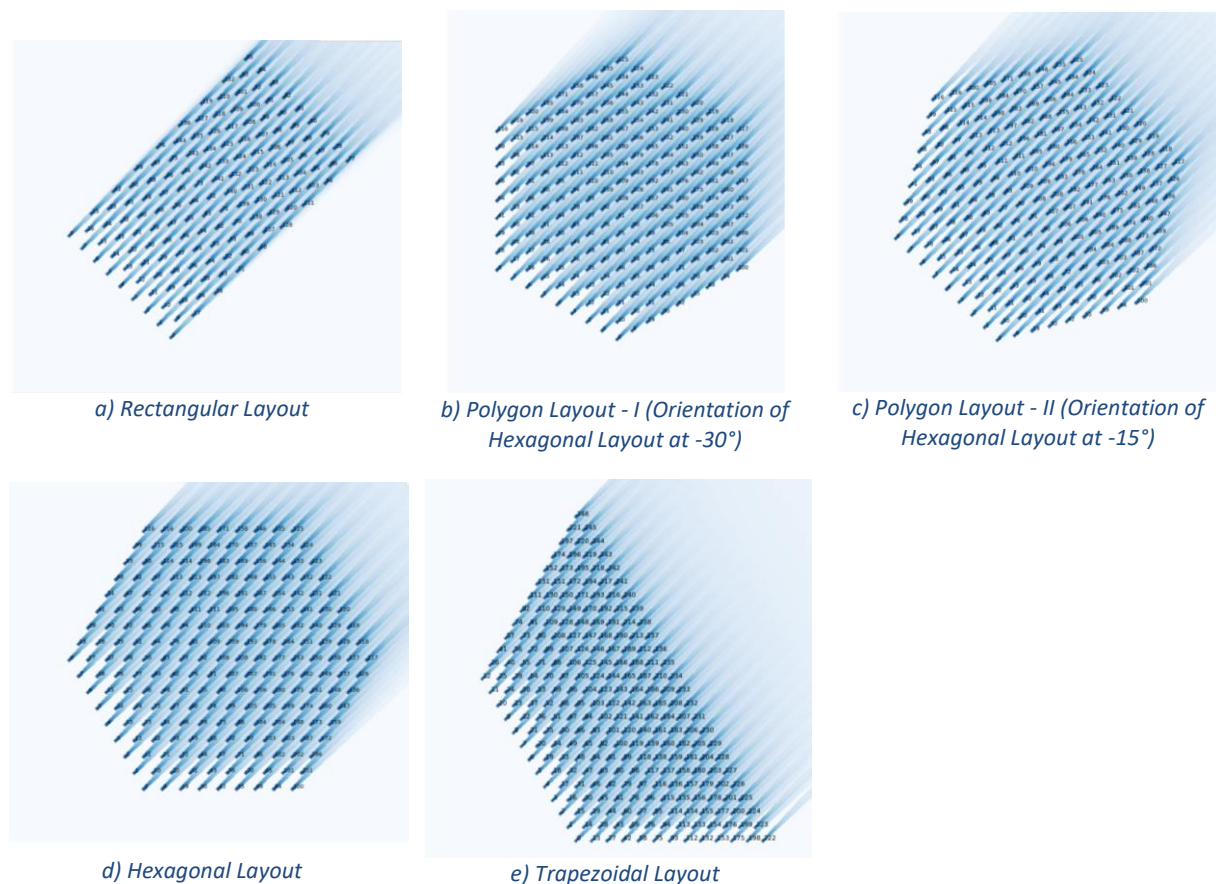
Figure 5.2 Layout designs

5.2.2 Placement of turbines in the selected Layout

To maintain the confidentiality of the actual wind resource location, a dummy site near the Dudgeon wind farm was chosen to evaluate various layouts and conduct PyWake simulations. Figure 5.3 illustrates the outputs of wake modeling for 11 different scenarios using 15 MW wind turbines arranged in the selected shape. The label on the right of each simulated scenario indicates the wind field output using the Jensen model for a free-stream wind and direction (225°), illustrating the wake impacts on downstream wind turbines.

The scenarios were developed using a square grid spacing concept (i.e., uniform row and column spacing) within the selected area of 290 km² (actual value: 287 km²) and based on a minimum turbine spacing of 5D. The inter-turbine spacing can be calculated using the following equation:

$$S = \frac{1}{D \cdot n} \sqrt{\frac{4A}{3\sqrt{3}}} \qquad (D) \quad (5.1)$$

where S, A, D are the turbine spacing, sea area (in m²), rotor diameter respectively and n is the minimum no. of divisions for creating grids within the layout. The relationship between n and no. of turbines T can be obtained by the equation below:

$$T = n \cdot (n+1) + \frac{(n+1) \cdot (n+2)}{2} \qquad ; n \in [2,12] \qquad (5.2)$$

Although the work investigates the outcome based on a wide range of capacity densities, the target zone for this study is practically between 2.64 and 9.10 MW/ km². It is common practice for wind farm developers to maximize yield and asset life by spacing turbines as far apart as possible while remaining within the practical limit of 12D to 15D, which equates to a capacity density of 2.64 km² for the preferred layout. The higher limit of 9.10 MW/ km² is established on the grounds of reduction in capacity factor with overplanting, as explained in subsection 5.3.3. Similar to the steps performed in trapezoidal layout, Figure 9.1 in the appendix includes flow map for hexagonal layout and simulation results are depicted in the following subsection.
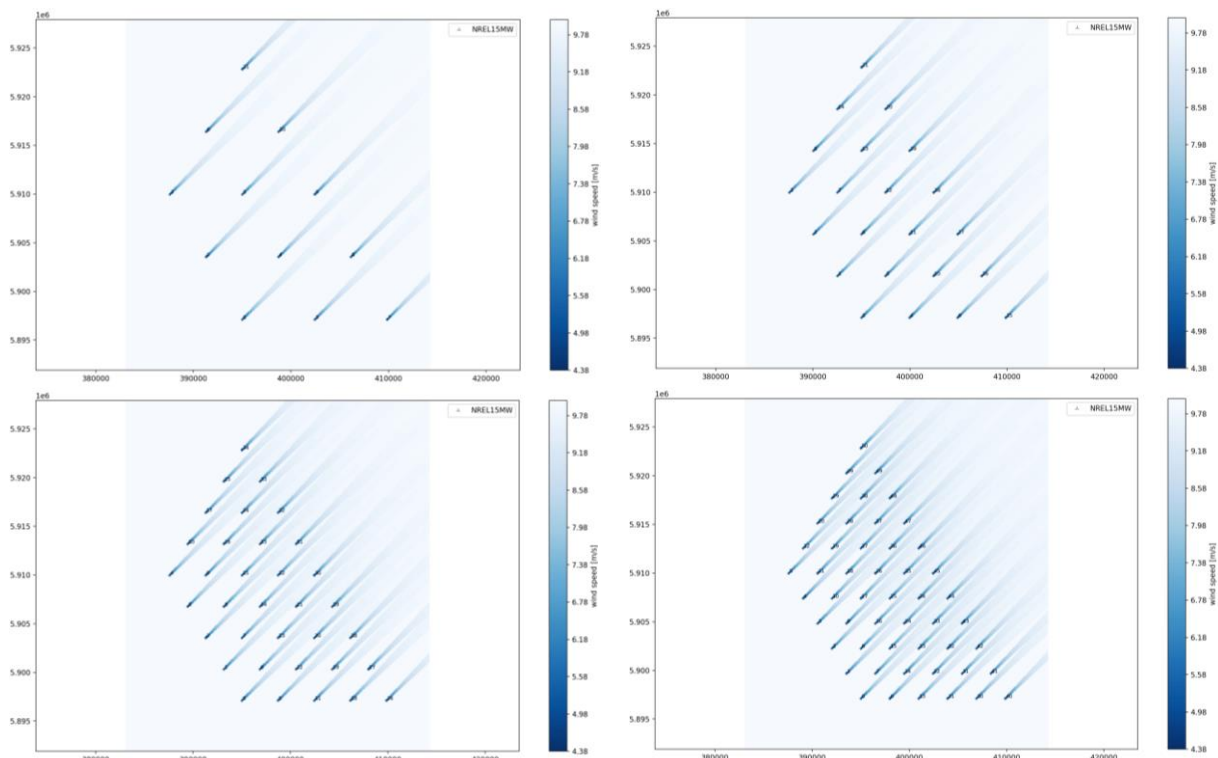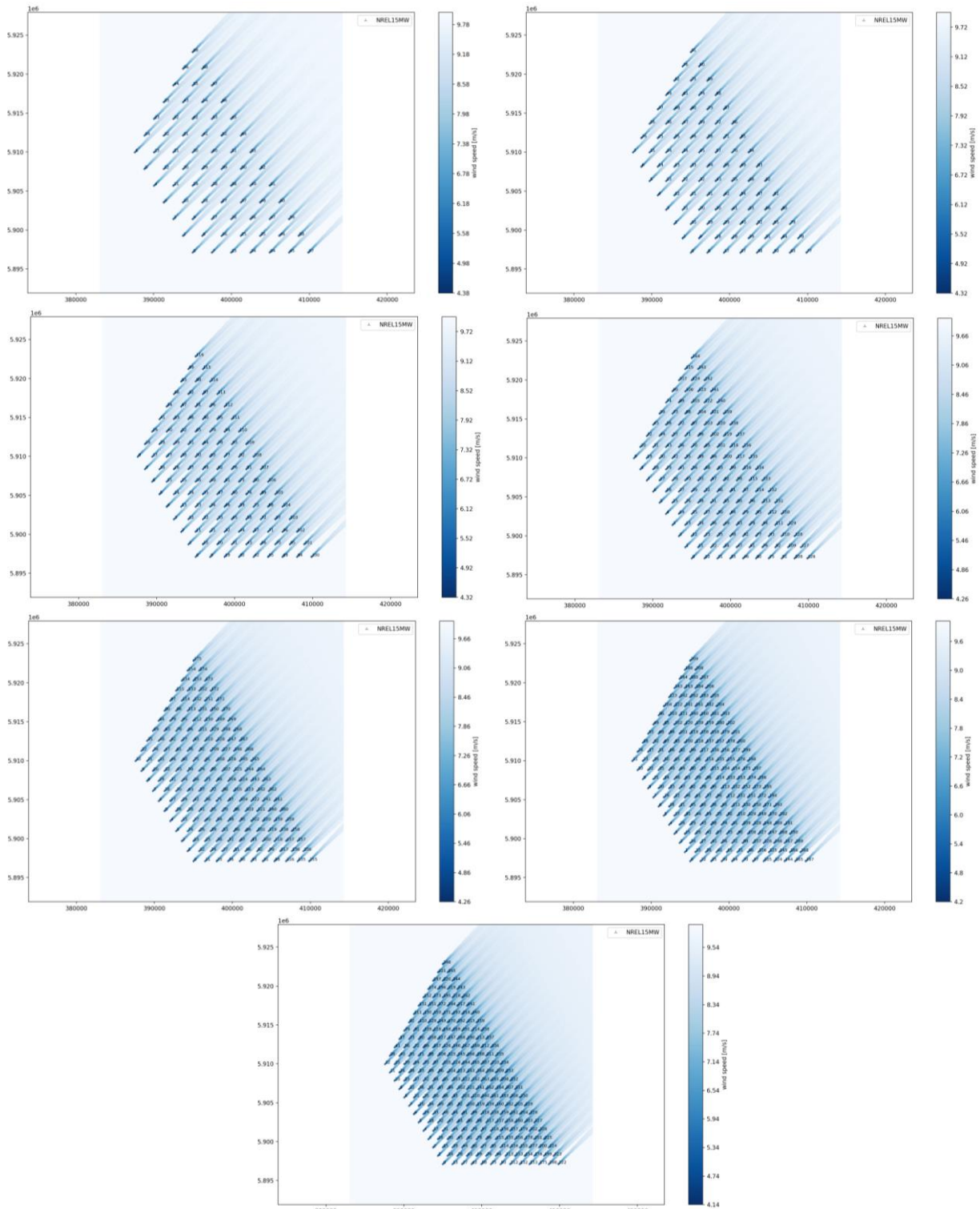
Figure 5.3 Different capacity density scenarios with Trapezoidal layout[4]

5.2.3 Comparison of capacity factors based on selected layout

Figure 5.4 showcases a capacity factor comparison for three layouts (Hexagonal, Trapezoidal, and Dudgeon wind farm) based on resizing the area and windfarm capacity (i.e., populating turbines within a designated area). The graph from Dudgeon represents results based on the positioning of

---

[4] Distance of smallest side of the Trapezoidal layout is 14.85km.

15MW wind turbines in the pre-defined layout and expanding the area by repositioning the turbines further apart (refer to Energy Research project under the appendix). Results include PyWake simulation using the industry-recognized wake models, TurbOPark, and Fuga models as depicted and does not take into account any other type of losses apart from wake. The difference in capacity factor between expanding the area and overplanting turbines is quite apparent. The graph below confirms that wind farm efficiency drops when turbines are placed narrower, and the choice of layout significantly influences the capacity factor. Expanding the area or reducing plant size can have different effects on the expenditures, both CapEx and OpEx in terms of lease, number of turbines etc. This work emphasizes the change in capacity density relative to a fixed area and not otherwise.

a) TurbOPark Model   *b) Fuga Model*
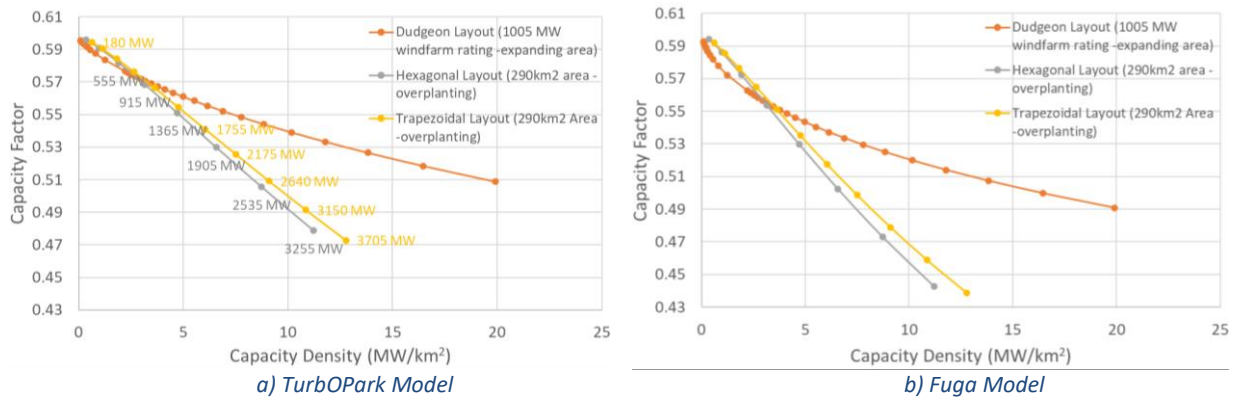
Figure 5.4 Capacity Factor Comparison based on industry-standard wake models[5]

5.3 Wake modelling and final yield

This section covers the wake analysis from different PyWake models, the surplus losses included in the final yield at various densities, and how these elements affect the actual efficiency or capacity factor of the windfarm [38].

5.3.1 Flowmap of PyWake models

Different wake models use different assumptions or mathematical equations to predict wake effects, and they can vary in accuracy and computational complexity. Some models may be more appropriate than others depending on the wind farm layout, turbine type, atmospheric conditions, and other factors. The variety of wake models implemented in this work estimates a spectrum of wake effects and the resulting power losses depending upon the superposition model, empirical constants and other coded characteristics. Figure 5.5 shows a flow map for several PyWake models, including Original Jensen, Local Jensen, TurbOpark, BastankhahGaussian, IEA37SimpleBastankhahGaussian, TurboGaussian, Fuga, and FugaBlockage at a capacity density of 4.76 MW/km^2. The PyWake code incorporates a heat map to visualize how different wake models affect wind and evaluate the net production. As seen on the label of figures, FugaBlockage and IEA37SimpleBastankhahgaussian simulate the highest and lowest energy production, respectively and are thus referred to as the conservative and optimistic wake models in the research. Significant differences can be observed between the turbines located in the innermost part of the layout (including the rear) and turbines located at its perimeter, the latter being subjected to higher wind speed more often, resulting in higher power extractions.

---

[5] 15MW Turbines were installed in the original Dudgeon layout. (Refer to Energy Research project in the appendix)
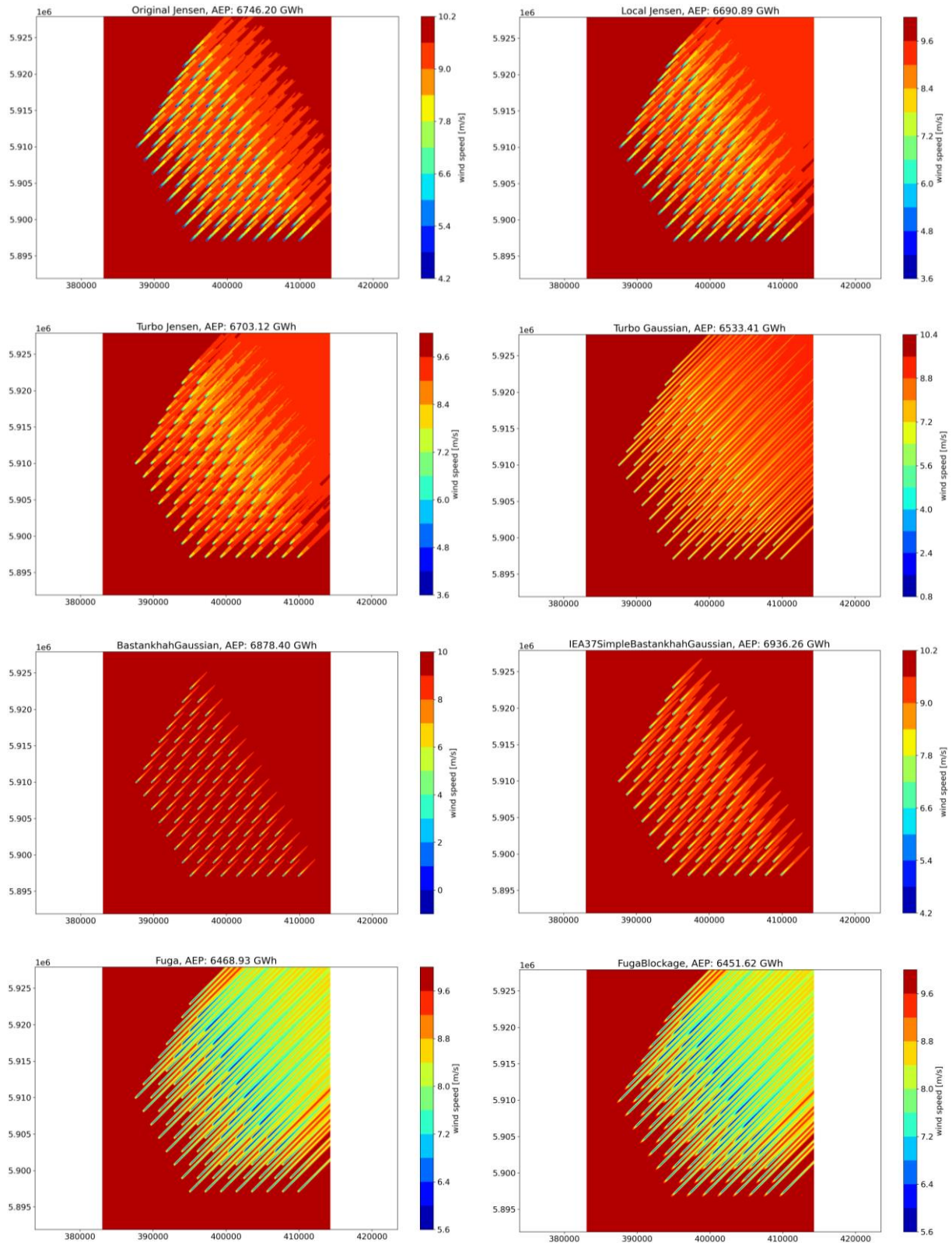
Figure 5.5 PyWake simulation[6] using different wake models with capacity density 4.76 MW/km[2]

Figure 5.6 shows the wind direction with maximum production and the probability distribution of energy production according to the wind speed for the case with 92 turbines. The maximum production is from wind coming in the direction of 225±25° with approx. 10 to 11m/s.

---

[6] The PyWake simulation only accounts for wake losses.

a) Energy production vs wind direction

b) Energy production vs wind speed
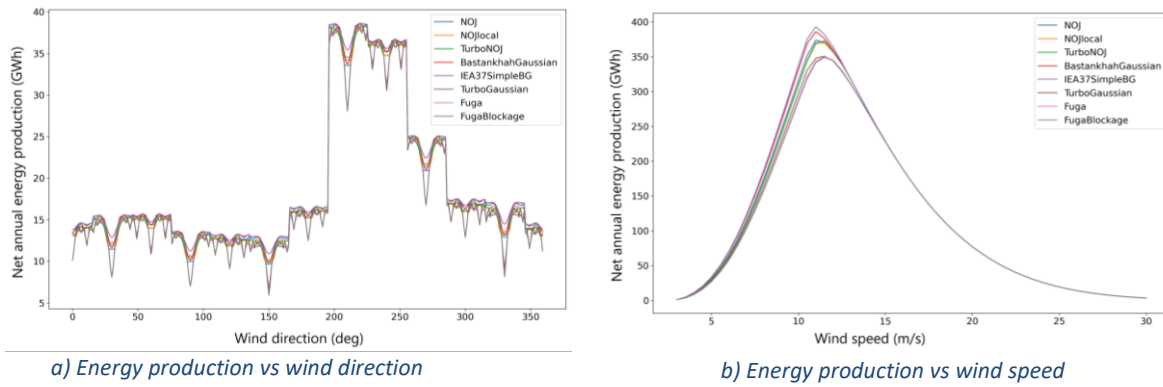
Figure 5.6 Energy production with wind speed and direction for capacity density of 4.76 MW/km²

5.3.2 Annual energy production (AEP) and wake losses

Figure 5.7 and Figure 5.8 provides findings on the energy yield and wakes for different densities anticipated from the Trapezoidal layout at the perspective site. Figure 5.8 demonstrates a correlation between turbine spacing, capacity density, and wind farm wake losses. AEP_{net} represented in the figure only accounts for wake losses here. As the number of turbines increases, the AEP_{net} (net annual energy production) also increases. However, the ratio of AEP_{net} to wind farm power decreases, indicating an overall increase in the percentage of wake losses (refer to Figure 5.7). When turbines are placed closer together at a spacing of 5.16D, there is substantial variance in wake loss predictions, ranging from 10.26% to 28.98%. Some models may underestimate wake losses, while others may overestimate them. It raises the uncertainty in AEP prediction and accentuates the need to verify a more accurate wake model. However, the gap narrows at lower capacity densities; for instance, when the turbines are apart at a spacing of 12.37D, the range of predicted wake losses is between 1.97% and 5.46%.

AEP_{net} per Windfarm for higher capacity density could be improved by a formal layout optimization and design which can lead to a reduction in wake loss estimates.
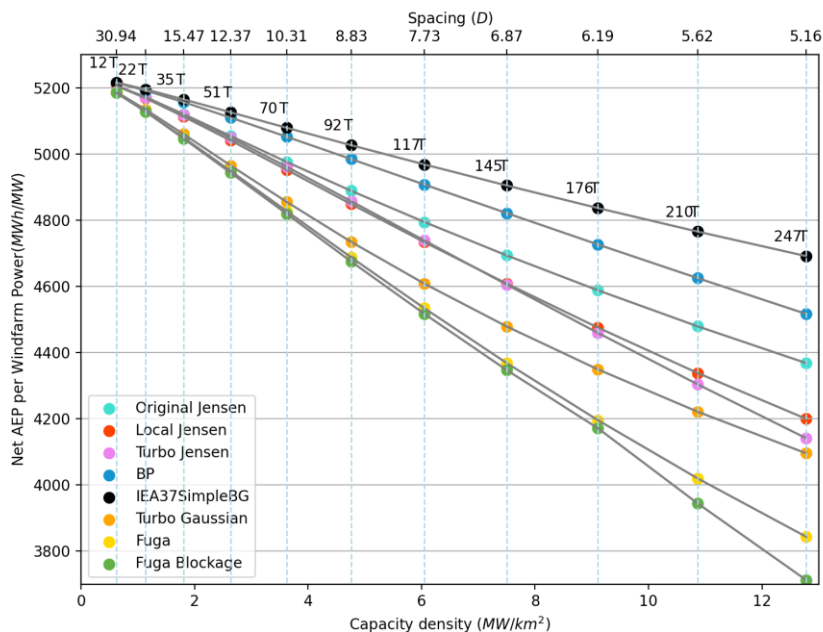
Figure 5.7 AEP_net /WFP vs Capacity density
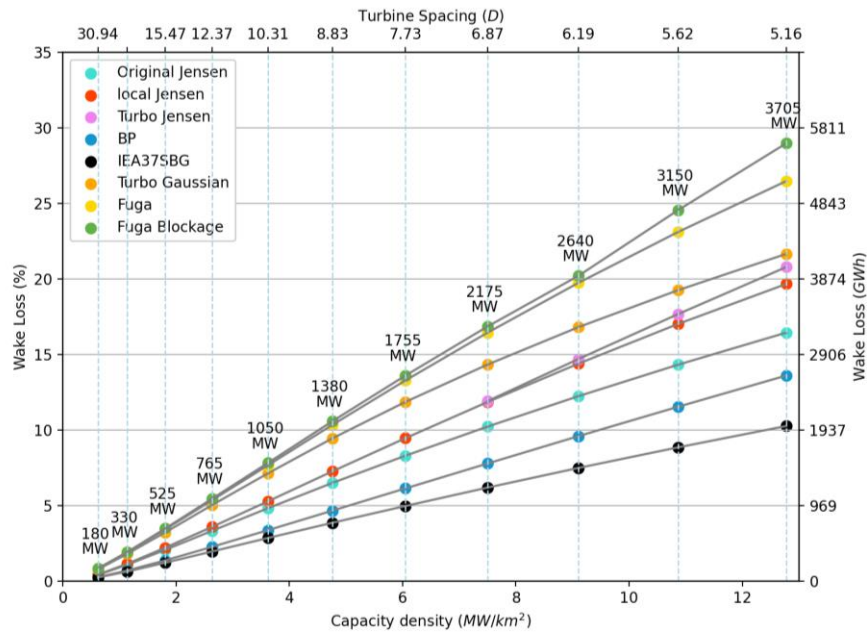
Figure 5.8 Wake loss vs Capacity density

A limitation encountered during this study is while performing simulation with over 100 turbines using the FugaBlockage model. Due to the memory constraints and execution time needed for each run, the capacity factor values for FugaBlockage values could not be simulated for data points beyond 200 turbines, where the memory requirement exceeded 32 GB, and the computation time exceeded 6 hours (reported time was 22051 seconds for the case with 145 turbines). Therefore, the AEP_{net} and wake losses were extrapolated using a linear relationship. To address this issue, many researchers have turned to cloud computing as a solution to solve such heavy simulation problems. The power of cloud computing allows use of multiple computing resources simultaneously, which can drastically decrease the time required to perform simulations.

5.3.3 Net capacity factor after additional losses

Table 4 Energy production losses per type

Additional losses	Depending on the scenario (%)
Unavailability losses	3.6
- Turbine	3.0
- BOP	0.3
- Grid	0.3
Performance losses	0.6
- Non-standard wind conditions	0.3
- Turbine control limitation	0.3
Electrical losses	2.5
Environmental losses	0.5
- Performance degradation due to icing	0.0
-Shutdown due to icing	0.0
-High and low temperature	0.0
- Other types of Performance degradation	0.5
Curtailment losses	0.0
Total losses	Average 7.2
	12.6 to 19.5 depending on scenario

Table 13 contains the capacity factor simulated from PyWake with respect to a variation in wind resource ranging from -30% to 10%. This is used further for performing the sensitivity analysis. The simulation from PyWake does not account for any other type of losses. Losses, such as mechanical, electrical, environmental, etc. affect the ultimate supply of energy and impair a wind farm's total efficiency. The energy production losses taken into account are industry standards relevant to the project and are estimated as mentioned in the Table 4.
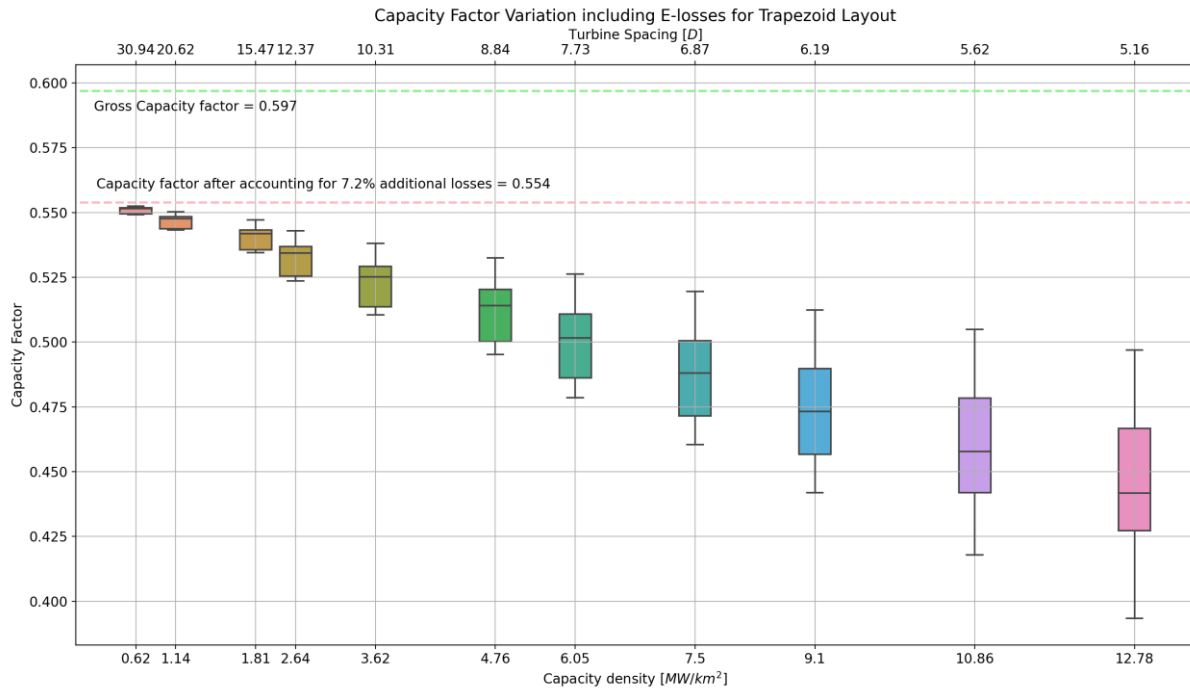
Figure 5.9 Box plot for net capacity factor variation using Trapezoidal layout

Figure 5.9 displays the box plot for net capacity factor including both wake losses and an additional 7.2% loss attributed to wind unavailability, performance, transmission, environmental, and curtailment. The gross capacity factor for a 15 MW wind turbine is 0.597, but the highest achievable capacity factor is 0.554 when accounting for the extra losses. The wake losses increase with the number of turbines and reduce the overall capacity factor. Turbine spacing beyond 12.37D has minimal impact on the capacity factor. On the contrary, turbine spacing below 6.19D reduces the mean capacity factor below 0.475. The variation in capacity factor is significantly high for higher capacity densities. For instance, the conservative wake model predicts a wake loss value above 20% (as reflected under Figure 5.8) when the turbines are placed closer (S<6.19D), which is unrecommended.

5.4 Cost model assumptions and sensitivities reference scenarios

The cost model utilized in this research is derived from ECN studies conducted on three distinct wind farms, each with a 15MW WT and rated at 4, 7, and 10 MW/km^2. The windfarm model of ECN includes semi engineering model for predicting the capital and Operating cost [35]. The fitting is carried out with a linear or quadratic curve, whichever provides the most accurate fit (refer to Figure 5.10 for detail). The overnight capital cost comprises of various components, including the costs of turbine, array string cable, installation, and other related balance parts. The cost of the hardware[7] for

---

[7] NSPH consortium reports the cost of 15MW wind turbine 14M€ and cost of substructure ranges between 5.1M€ to 10M€ depending on water depth between range 5 to 55m [5].

a 15MW WT is 19.552M€. Additionally, the cost of other balance parts for a 15MW WT is 272.5 M€/ MW/km^2. To determine the total cost in M€, one can simply multiply the capacity density by the balance part cost.
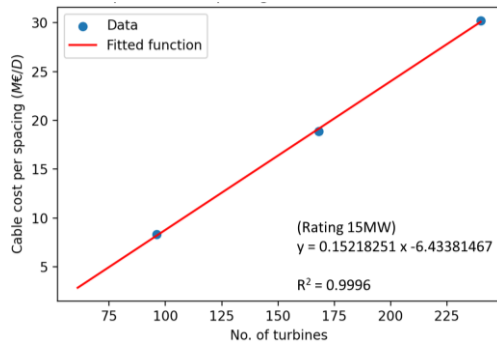
a) *Linear Regression: Cable cost per turbine spacing vs no. of wind turbines*
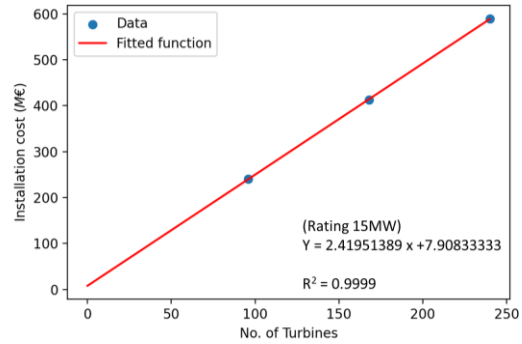
b) *Linear Regression: Installation cost vs no. of wind turbines*
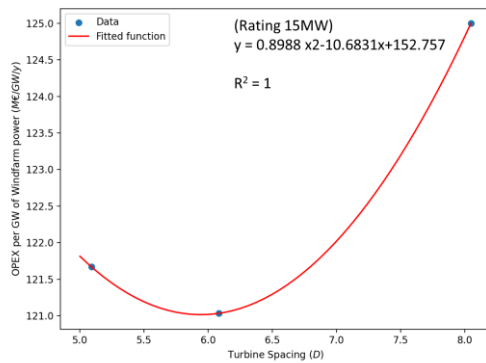
c) *Polynomial Regression: OpEx per windfarm power vs turbine spacing.*
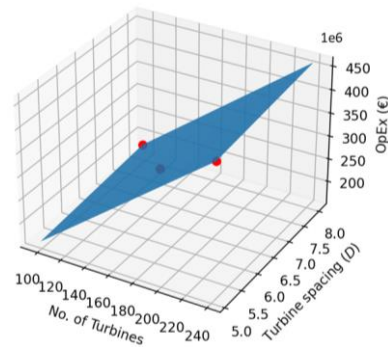
d) *Multiple linear Regression: OpEx w.r.t no. of turbines and turbine spacing*

Figure 5.10 ECN cost extrapolation using regression methods[8]

Cable cost (in M€) can be calculated using linear regression as shown in the equations below:

$$y = \frac{(152.183x) - 6433.814}{1000} \qquad (M€/D) \quad (5.3)$$

$$Cable\ cost = y \cdot S \qquad (M€) \quad (5.4)$$

where y is the cable cost per spacing, x is the no. of turbines and S is the turbine spacing. The eq. (5.3) is only valid for Turbine no.>69 (in 290km^2 area). The minimum cable cost for a wind farm is assumed 40M€ [5]. (Refer to Figure 5.10 a))

Similar to array string cable cost, installation cost (in M€) can be determined from the following equation:

$$y = (2.420x + 7.908) \qquad (M€) \quad (5.5)$$

where y is the installation cost, x is the no. of turbines. (Refer to Figure 5.10 b))

---

[8] ECN studies indicate the land lease increases with higher capacity densities for the same area. Due to insufficient data this is not included in the OpEx [35]

For OpEx (in M€/y) calculation trial methods included– polynomial (refer to Figure 5.10 c)), multiple linear (refer to Figure 5.10 d)) with independent variables such as no. of turbines, turbine spacing, and a relation was established as represented:

$$y = 0.89882x^2 - 10.6831x + 152.757 \qquad (M€/GW/y) \quad (5.6)$$

$$OpEx = \frac{y \cdot WFP}{1000} \qquad (M€/y) \quad (5.7)$$

where y is operating cost per windfarm spacing (M€/ GW/y) and x is the turbine spacing. (Refer to Figure 5.10 c))

5.5 Fixed and variable parameters

Table 5 Overview of scenarios with capacity densities, expenditures and energy production[9]

No. Of Turbines	Plant size	Capacity Density	Turbine Spacing		Construction years	CapEx	OpEx	AEP$_{net,min}$	AEP$_{net,max}$
-	MW	MW/km^2	D	km	y	M€	M€/y	GWh/y	GWh/y
247	3705	12.78	5.16	1.24	6	9,064	450	12,767	16,130
210	3150	10.86	5.62	1.35	5	7,714	381	11,532	13,930
176	2640	9.10	6.19	1.48	4	6,472	319	10,221	11,849
145	2175	7.50	6.87	1.65	4	5,337	264	8,774	9,899
117	1755	6.05	7.73	1.86	3	4,309	217	7,356	8,091
92	1380	4.76	8.84	2.12	2	3,388	177	5,987	6,437
70	1050	3.62	10.31	2.47	2	2,572	145	4,696	4,949
51	765	2.64	12.37	2.97	1	1,884	121	3,509	3,639
35	525	1.81	15.47	3.71	1	1,308	106	2,458	2,516
22	330	1.14	20.62	4.95	1	840	103	1,570	1,591
12	180	0.62	30.94	7.42	0	480	122	866	871

Table 5 displays eleven scenarios for which the economic indices are evaluated, and a comparative analysis is performed. An extensive study has been conducted to demonstrate the sensitivity of some uncertain input parameters and their immediate influence on the resulting optimal capacity density. The fixed parameters are the general characteristics of the offshore wind farm that are already set. It includes AEP$_{net}$ corresponding to the capacity density and turbine spacing according to the baseline setting in this study. On the other hand, the variable parameters are those that introduce uncertainty and are outside the control of the project, such as government policies, weather conditions, technical limitations and expenses projected for the future. Sensitivity analysis in this project encompasses these variable parameters in two ways:

- Relative changes in percentage of - Wind resource, CapEx and Opex
- A revision in the value of - Additional losses, Operational life, Nominal discount rate, Inflation rate, Strike price and Royalty

The overall cost extrapolated from the ECN studies might seem high compared to presently reported cost results and this is because the ECNs cost model is developed with a nominal power 5-8 MW [35].

---

[9] The realistic target zone for the selected scenario is between 2.64 and 9.10 MW/km^2. Below 2.64 MW/km^2, the capacity density and the corresponding expenditures extrapolated are hypothetical.

However, a sensitivity analysis by tuning OpEx and CapEx parameters is performed in the results to accommodate the variation. The construction years presented in the table are estimated based on literature, assuming a rate of 0.6 MW/day for the time required [39].

5.6 Financial metric

$-CapEx$ $-OpEx$ $-OpEx$ $-OpEx$
            $+Revenue$ $+Revenue$ $+Revenue$

0th Year 1st Year 2nd Year 3rd Year 4th Year   .... n_o Year
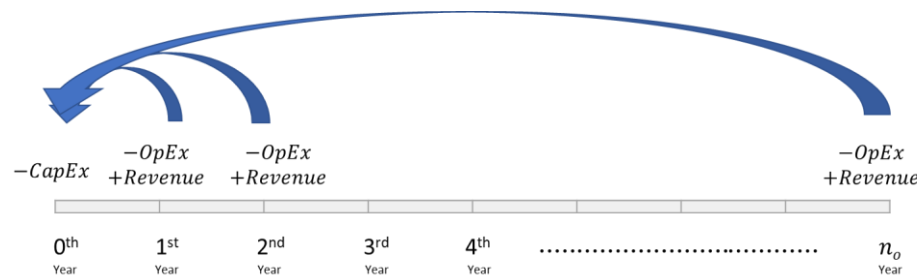
Figure 5.11 NPV using simple method

n_c = 2 years
n_o = 27 years

$\dfrac{-CapEx}{n_c+1}$ $\dfrac{-CapEx}{n_c+1}$ $\dfrac{-CapEx}{n_c+1}$

0th Year 1st Year 2nd Year 3rd Year 4th Year   .... n_c+n_o Year

                               $-OpEx$ $-OpEx$ $-OpEx$
                                 $+Revenue$ $+Revenue$ $+Revenue$
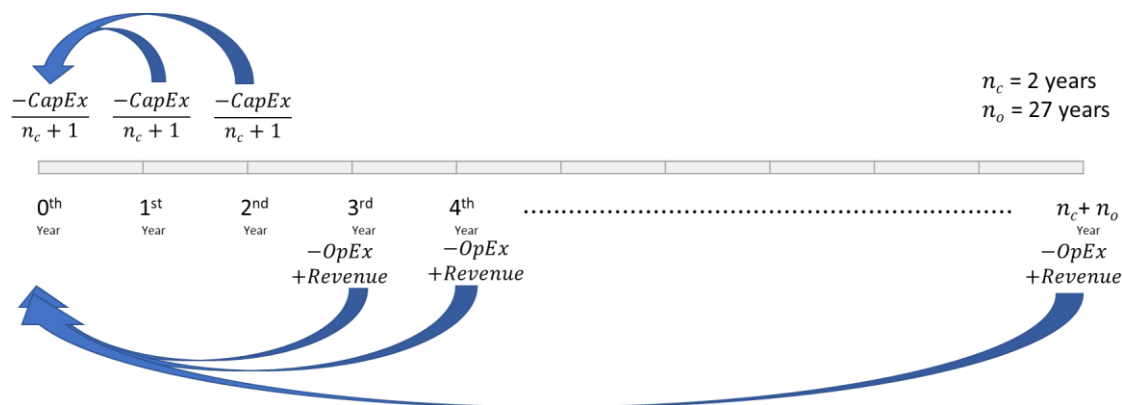
Figure 5.12 NPV using advanced method (for a scenario with construction years n_c = 2)

The financial metric calculations for LCOE, NPV, and IRR follow two different methods in this thesis. The first method is a simple formula that assumes investment for CapEx as a lump sum amount after complete installation and operating expenses start from the following year until the final operation date. Although this approach is commonly used in many studies, it is not an accurate reflection of reality. On the other hand, the advanced method follows a more sophisticated approach and distributes CapEx equally based on the number of construction years. Figure 5.11 and Figure 5.12 represent the cash flow for a reference scenario with 1380 MW plant size using both the methods.

A simple calculator is developed within the scope of this thesis that evaluates the financial viability of a wind energy project, taking into account various factors such as capital costs, performance, and O&M. However, it is important to note that this doesn't include factors such as financing issues, future replacement costs, degradation costs, and etc. which would need to be included for a more complex analysis [33]. The equations used in developing the sensitivity tool are mentioned below, where CapEx, OpEx, and AEP are considered in €, €/y, and MWh, respectively.

LCOE Calculation

$$LCOE_{simple\ method} = \frac{\frac{CapEx}{a} + OpEx}{AEP_{net}} \qquad (€/MWh) \qquad (5.8)$$

where

$$a = \frac{1}{(1+r)} + \frac{1}{(1+r)^2} + \ldots\ldots + \frac{1}{(1+r)^{n_o}} = \frac{1-(1+r)^{-n_o}}{r} \qquad (y) \qquad (5.9)$$

$$r = \frac{(1+R)}{(1+i)} - 1 \qquad (\%) \qquad (5.10)$$

$$AEP_{net} = WFP \cdot (CF \cdot \eta) \cdot 8760 \qquad (MWh) \qquad (5.11)$$

$$\eta = (1 - Additional\ losses) \qquad \% \qquad (5.12)$$

Here a refers to annuity based on operational years, r is the real interest rate, and n_o refers to the number of operating years. AEP_{net} is the annual energy production including all the losses. WFP refers to wind farm power, CF is the capacity factor based on wake losses and η accounts for the reduced efficiency due to additional losses.

$$LCOE_{advanced\ method} = \frac{\{CapEx \cdot (1+a_c)\} + (OpEx \cdot a_o)}{AEP_{net} \cdot a_o} \qquad (€/MWh) \qquad (5.13)$$

where $a_o = (a_{c+o} - a_c)$

$$a_o = \frac{(1+r)^{-n_c} - (1+r)^{-(n_c+n_o)}}{r} \qquad (y) \qquad (5.14)$$

$$a_c = \frac{1}{(1+r)} + \frac{1}{(1+r)^2} + \cdots\ldots\ldots + \frac{1}{(1+r)^{n_c}} = \frac{1-(1+r)^{-n_c}}{r} \qquad (y) \qquad (5.15)$$

$$a_{c+o} = \frac{1}{(1+r)} + \frac{1}{(1+r)^2} + \cdots\ldots\ldots + \frac{1}{(1+r)^{n_c+n_o}}$$
$$= \frac{1-(1+r)^{-(n_c+n_o)}}{r} \qquad (y) \qquad (5.16)$$

Here a_o, a_c refers to annuity based on construction and operational years. n_c, n_o refers to the construction and operational years.

NPV Calculation

$$NPV_{simple\ method} = -TotEx_{simple\ method} + Revenue_{simple\ method} \qquad (€) \qquad (5.17)$$

where $TotEx_{simple\ method} = [CapEx + (OpEx \cdot a)] \qquad (€) \qquad (5.18)$

$$Revenue_{simple\ method} = AEP_{net} \cdot (1 - Royalty) \cdot Strike\ price \cdot a \qquad (€) \quad (5.19)$$

$$NPV_{advanced\ method} = -TotEx_{advanced\ method} + Revenue_{advanced\ method} \qquad (€) \quad (5.20)$$

where $TotEx_{advanced\ method} = [\{CapEx \cdot (1 + a_c)\} + (OpEx \cdot a_o)]$ $\qquad (€) \quad (5.21)$

$$Revenue_{advanced\ method} = AEP_{net} \cdot (1 - Royalty) \cdot Strike\ price \cdot a_o \qquad (€) \quad (5.22)$$

TotEx refers to the total expenditure or the net present value of cash outflow, i.e., CapEx and OpEx.

IRR Calculation

$$NPV_{simple\ method} = -\left[CapEx + \left(OpEx \cdot \frac{1 - (1 + IRR)^{-n_o}}{IRR}\right)\right] +$$

$$\left[AEP_{net} \cdot (1 - Royalty) \cdot Strike\ price \cdot \frac{1 - (1 + IRR)^{-n_o}}{IRR}\right] = 0 \qquad (\%) \quad (5.23)$$

$$NPV_{advanced\ method}$$
$$= -\left[\left\{CapEx \cdot \left(1 + \frac{1 - (1 + IRR)^{-n_c}}{IRR}\right)\right\}\right.$$
$$+ \left\{OpEx \cdot \left(\frac{(1 + IRR)^{-n_c} - (1 + IRR)^{-(n_c+n_o)}}{IRR}\right)\right\}\right]$$
$$+ \left[AEP_{net} \cdot (1 - Royalty) \cdot Strike\ price\right.$$
$$\left.\cdot \left(\frac{(1 + IRR)^{-n_c} - (1 + IRR)^{-(n_c+n_o)}}{IRR}\right)\right] = 0 \qquad (\%) \quad (5.24)$$

5.7 Assumptions

Aspects mentioned below were not included in the work due to their data needs and complexity to the scope of thesis.

1) Cost model assumptions with CapEx and OpEx:
    - The preliminary values were extrapolated from ECN research to obtain the results for eleven scenarios and the extrapolated parameters were adjusted to a value from other sources (BVG Associates and Princess Elisabeth Zone) as a case study [7],[15].
    - Costs pertaining to decommissioning, blade degradation, wind hysteresis, increase in number of substations, export cable to shore, land lease, project delays and permitting were not accounted for separately. However, this is reflected in the sensitivity analysis as an increase in CapEx or OpEx percentages.

2) Mega wind project for larger plant size: CapEx is allocated based on the construction years for advanced calculations. However, construction for windfarms with higher capacity densities often takes place in phases, resulting in a difference in AEP for the windfarm, which in turn impacts the LCOE and NPV. To simplify the analysis, it is assumed that the wind farm

would start producing power only when all turbines are installed, regardless of the project's size.

3) Spatial planning costs or adaptation costs: This work does not include regularity frameworks and spatial planning risk mitigation, such as fishing areas, shipping lanes, helicopter zones, and other constraints. The cost of spatial planning or adaptation of co-utilization is determined by the cost of the user function adapting to the new offshore wind farm or the cost of the offshore wind farm adjusting to the user function's pre-existence in the sea.

4) Turbine Spacing constraints: Spacing requirements for substations have not been taken into account for higher capacity densities. For example, the maximum available area for a 3705MW plant size is 1km², excluding the space covered by rotor sweep.

5) Electricity pricing in revenue: A constant value for the strike price is selected to generate revenue and compute profitability. However, it would be more relevant to consider the electricity price without considering any government scheme or include a capture factor to evaluate the economic feasibility of a wind farm. Moreover, the duration for CfD is often set to a period of 15 years and is subject to changes after the contract ends, which has not been taken into account.

6) Cash flow valuation:
   - Interest is compounded annually.
   - The nominal discount rate or WACC increases each year due to the debt and equity capital components, leading to small variations in NPV over long periods. This is not projected in the calculations.

7) Layout Identification: The capacity factor for larger wind farm ratings could be enhanced with a better optimized layout, but only a limited number of basic layouts were evaluated for this report.

8) Inter OSW-wake loss factor: Wake interactions due to neighboring are a critical subject but were not applicable in the wind farm currently selected.

9) Wind resource variation: While this work includes sensitivity to wind speed, it does not consider sensitivity with respect to wind direction.

6. Results

6.1 Influence in economic Indices with baseline setting
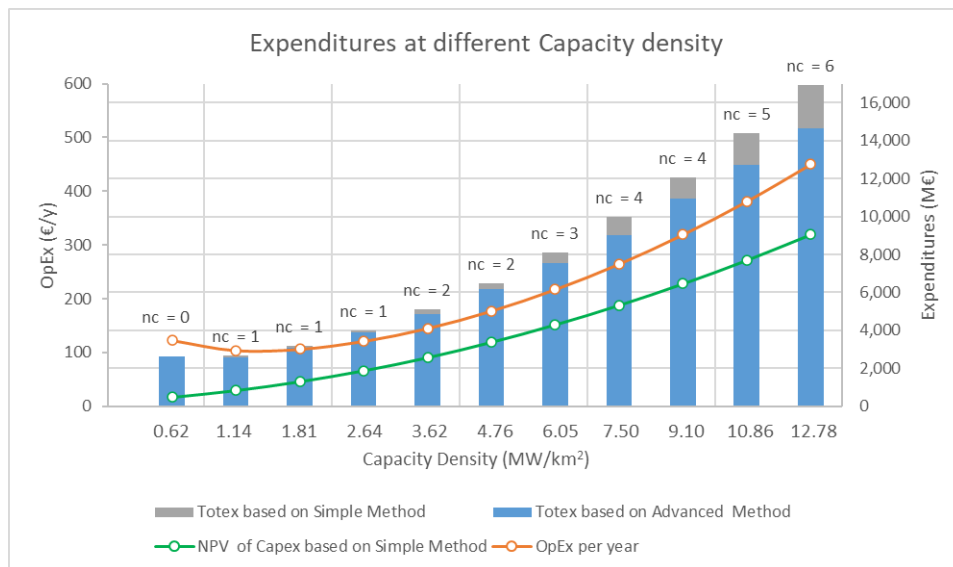
Figure 6.1 Expenditures at baseline setting

Figure 6.1 represents CapEx, OpEx, and TotEx as a function of capacity density. The advanced method presents a more realistic way to calculate results as it takes into account the number of construction years (referred to as 'nc' in the plots) over which the capital investment splits. Since the value of money decreases over time, higher capacity densities for the advanced method result in a lower TotEx. Although the TotEx calculated using the advanced method is low, the annuity of operating years is also less, which is why the method calculates a higher value of LCOE than the simple approach.

Table 6 Baseline setting

Parameter	Symbol	Unit	Value
Additional Losses (non-availability, performance, electrical, environmental, and curtailment losses)	-	%	7.20
Economic Lifetime / operational life	n_o	years or y	27
Nominal discount rate (WACC)	R	%	6.00
inflation rate	i	%	2.50
OpEx Increment/Deduction	-	%	0
CapEx Increment/Deduction	-	%	0
Wind resource Increment/Decrement	-	%	0
Strike Price	-	€/MWh	70
Royalty	-	%	1.00
Uncertainty in Construction years due to bad weather at North Sea	-	%	0
interest rate or real discount rate	r	%	3.41
Annuity (Simple method)	a	years or y	17.46
Capital recovery factor	CRF	-	0.057

Table 6 represents the values for input parameters considered at the baseline setting. The current inflation (2023) is higher than the value accounted in the baseline setting, the reported average rate

was around 5.76% during 2022 in Norway. Several offshore windfarm developers delayed their final investment decisions due to inflation, electricity prices and market uncertainty all across Europe. The 2.5% inflation is an approximated average in the last 10 years [37],[30],[31].

The economic indices are greatly influenced by the capacity density (CD) of the windfarm. The objective of comparative analysis (depicted under Figure 6.2 and Figure 6.3) between different scenarios is to obtain an optimal value of capacity density. The optimal point is the minimum point in the LCOE plot and the maximum point of value in the NPV and IRR plot. The general observation reported with the baseline setting shows that on incrementing the number of turbines based on the chosen area, the LCOE dramatically drops up to a certain value, showing a dip, after which the curve rises upward, suggesting an increase in the cost of energy. The NPV and IRR that take the revenue component into account exhibit the opposite pattern. It is evident in the graphs that for all the economic indices, the divergence between minima and maxima increases as the capacity density increases. Key observations with greater emphasis on the realistic computation using the advance method (refer to Figure 6.3 and Table 7) are described below:

The LCOE for simplistic calculation (refer to Figure 6.2 a)) suggests a range of value between 57 – 62 €/MWh with the optimal point as 4.76 and 6.05 MW/km^2 predicted by the conservative and optimistic wake model respectively. However, a more realistic calculation (refer to Figure 6.3 a)) shows the LCOE could lie between 59 – 63 €/MWh with an optimal CD at 4.76 MW/km^2 irrespective of the wake model. The conservative wake model predicts almost 7.5% higher LCOE than the optimistic wake model at the predicted optimal capacity density of 4.76 and this increase is exclusively due to stronger wake effects (which amount to 7% difference). On comparing the wake models, FugaBlockage predicts a shallow dip at 3.62 with LCOE of 63 €/MWh, close to the model's minimum estimate. Similar findings can be made for other models with low-capacity factors. Contrary to this, IEA37SBG displays a steep decline from 3.62 to 4.76 MW/km^2, followed by a shallow upward increase at CD 6.05 with LCOE of 59 €/MWh, nearly close to the model's optimal LCOE. Figure 6.3 e) represent the LCOE curve with respect to turbine spacing displaying the optimal CD at 8.84D.

For the selected strike price of 70 €/MWh, NPV displays a bell curve for conservative wake models (FugaBlockage and Fuga) and a plateau curve for the optimistic wake model (refer to Figure 6.2 b) and Figure 6.3 b)). The strike price is established based on the optimistic assumption with the current scenario, achieving an overall profit for a wide range of capacity densities. The maximum NPV estimated by different wake models for the realistic calculation (refer to Figure 6.3 b)) ranges between 599 – 1596 M€ with capacity densities spanning in the wide range of 4.76 to 9.10 MW/km^2. The same result in optimal capacity density broadens up to 12.78 MW/km^2 when analyzed using simple method (refer to Figure 6.2 b)). It's Interesting to observe that going a step higher or lower w.r.t. optimal CD, in the case of optimistic wake model, causes the NPV to decline by 5% (84 M€) and 10% (165 M€), respectively. Although the monetary value of the decline is virtually the same when choosing the conservative wake model, the relative decline is a little higher, i.e., 14% (86 M€) and 24% (144 M€) on moving a step higher or lower w.r.t CD. The industry-standard wake models, Fuga and TurbOpark forecasts a negative value beyond the capacity density of 7.5 and 10.68 MW/km2, respectively.

The IRR graph exhibits a skewed curve with a maximum value range of 4.80 - 5.88 % at optimal capacity densities of 3.62 and 4.76 MW/km^2 (refer to Figure 6.2 c) and Figure 6.3 c)). Compared to the advanced approach, simple method approximates a higher NPV worth (especially with overplanting) and hence a higher internal rate of return equivalent to 5.25 - 6.52% with optimal CD between 4.76 and 6.05 MW/km^2. Since IRR is the interest rate at which NPV becomes zero, it follows a similar trend as NPV. On examining the variation with respect to the conservative wake model, an increase in capacity density to 4.76 MW/km^2 has an insignificant shift in the IRR% (4.800% to 4.798%) which implies that optimal capacity density can be taken as 4.76 MW/km^2 (refer to Figure 6.3 c)).

Further, in the case of the optimistic wake model, increasing or decreasing capacity density to a level up/down can reduce IRR by up to 0.27%. Uncaptured in the graph, IRR projection from various models approaches a negative value with a range of (-8.82 to -9.97%) for the capacity density of 1.14 MW/km². In terms of Profitability, IRR falls below the actual interest rate at capacity densities lower than 2.64 MW/km² and over 7.5 MW/km², this bulge is relatively narrow for a lower strike price (discussed under IRR sensitivity subsection 6.6.2) which suggests that the ideal NPV value is strongly influenced by the agreed-upon strike price. However, all models, with the exception of Fuga and FugaBlockage, continue to favorably evaluate better IRR up to the capacity density of 9.1 MW/km². Furthermore, wake models -Jensen, IEA37Bastankhahgaussian, and Bastankhahgaussian produce IRR above the real interest rate under all the circumstances of capacity densities exceeding 2.64 MW/km². NPV/windfarm rating follows a close pattern to IRR (refer to Figure 6.3 d)).

Overall, it seems the choice of capacity density can be seen as a strategic economic decision. Choosing a relatively high capacity density of around 9.10 MW/km² results in a larger spread of NPV (-100M€ to 1600 M€) at a lower IRR. On the other hand, choosing a more common capacity density around 4.76 MW/km² results in the lowest LCOE, highest IRR and smaller spread in NPV (600 to 1100 M€). It also illustrates that developers using optimistic wake models might be more inclined to higher capacity densities if they are optimizing for NPV. However, it is essential to consider the impact of wake-induced turbulence on the operational lifespan of wind turbines. A sensitivity analysis utilizing the turbine's economic life reveals that if it reduces below 22 years, the IEA37Bastankhahgaussian model indicates a shift in the optimal capacity density for NPV from 9.10 to 6.05 MW/km². (Refer section 6.5).

The Figure 9.2 in appendix shows the sensitivity analysis tool prepared for the research to perform a detailed study on how the optimal point is affected. The results are discussed in the next subsections.

Table 7 Results at baseline setting

Parameters	Units	Advanced Calculation				Simple Calculation			
		TurbO Park	Fuga	FugaBl ockage	IEA37S BG	TurbO Park	Fuga	FugaBl ockage	IEA37S BG
LCOE$_{Min}$	€/MWh	60.80	63.00	63.17	58.75	59.72	61.88	62.05	57.38
CD$_{@LCOE Min}$	MW/km²	4.76	4.76	4.76	4.76	4.76	4.76	4.76	6.05
S$_{@LCOE Min}$	D	8.84	8.84	8.84	8.84	8.84	8.84	8.84	7.73
CapEx/WFP	M€/MW	2.46	2.46	2.46	2.46	2.46	2.46	2.46	2.46
OpEx/WFP	k€/MW/y	128.55	128.55	128.55	128.55	128.55	128.55	128.55	123.90
AEP	GWh/y	6220	6220	6220	6220	6220	6003	5987	8091
Initial Capital Cost	€/kW	2455	2455	2455	2455	2455	2455	2455	2456
Annual Operating Cost	€/MWh	28.52	28.52	28.52	28.52	28.52	29.55	29.63	26.87
IRR$_{Max}$	%	5.37	4.84	4.80	5.88	5.89	5.29	5.25	6.52
CD$_{@IRR Max}$	MW/km²	4.76	4.76	3.62	4.76	4.76	4.76	3.62	6.05
NPV$_{Max}$	M€	908	618	599	1596	1283	827	794	2587
CD$_{@NPV Max}$	MW/km²	6.05	4.76	4.76	9.10	7.50	6.05	6.05	12.78
NPV/WFP$_{Max}$	M€/GW	626	447	434	803	754	563	549	959
CD$_{@NPV/WFP Max}$	MW/km²	4.76	4.76	4.76	4.76	4.76	4.76	4.76	6.05
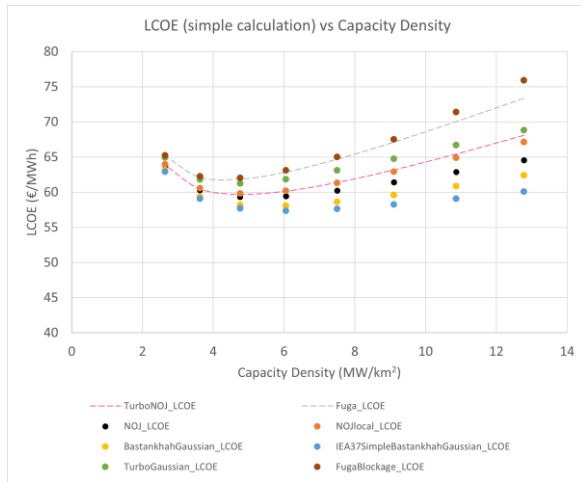
a) *LCOE vs Capacity Density*
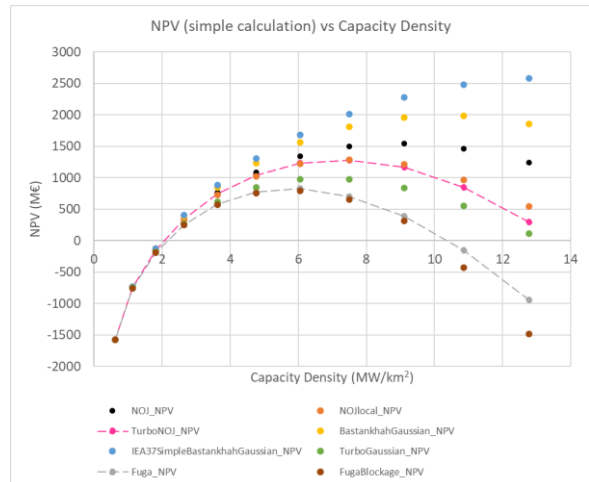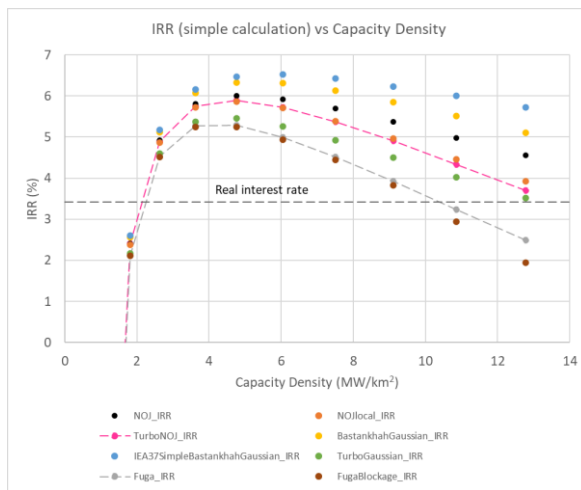
b) *NPV vs Capacity Density*

c) *IRR vs Capacity Density*
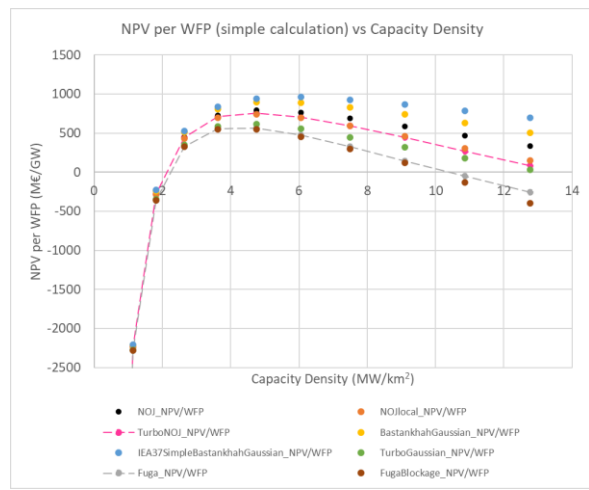
d) *NPV per WFP vs Capacity Density*
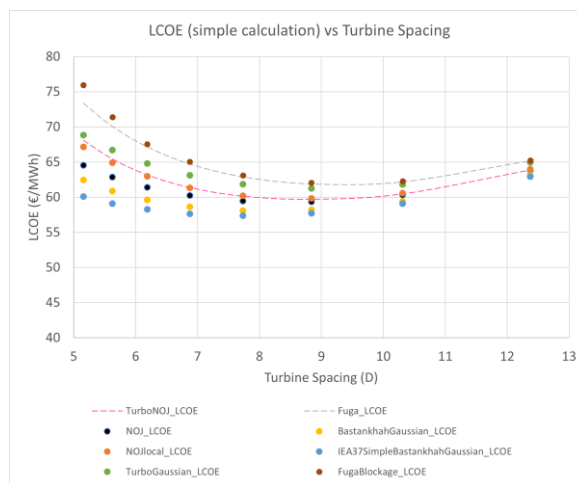
e) *LCOE vs Turbine Spacing*

Figure 6.2 Plots of various economic indices using simple calculations at baseline setting[10]

---

[10] The LCOE model in the simple method is based on the methodology used by National Renewable Energy Laboratory (NREL) [33]
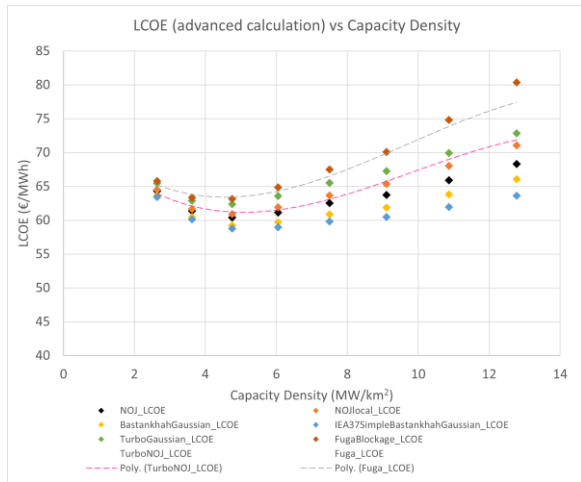
a)   *LCOE vs Capacity Density*
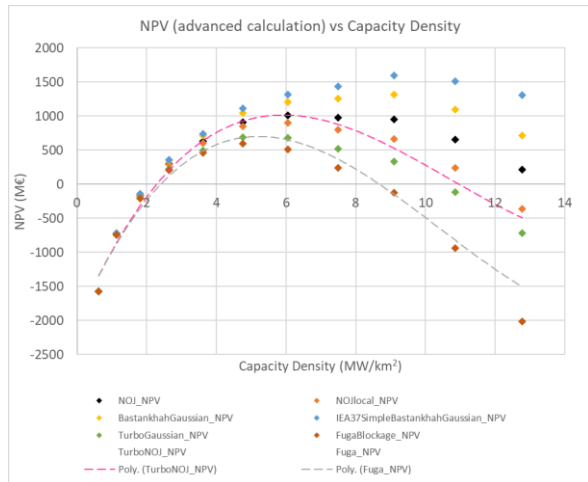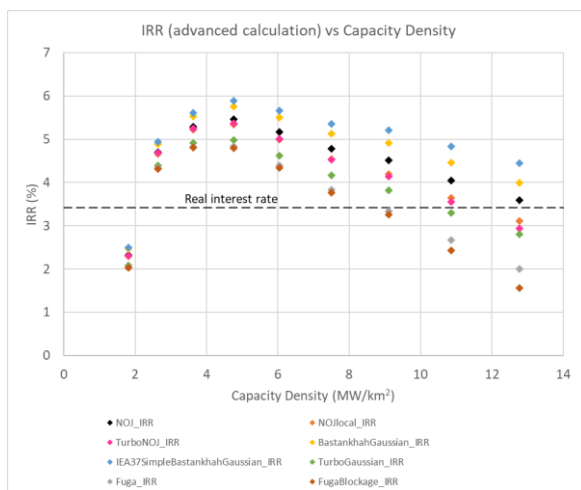
b)   *NPV vs Capacity Density*

c)   *IRR vs Capacity Density*
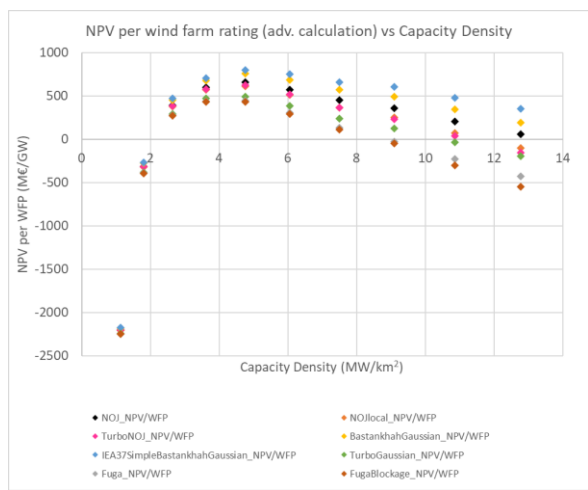
d)   *NPV per WFP vs Capacity Density*
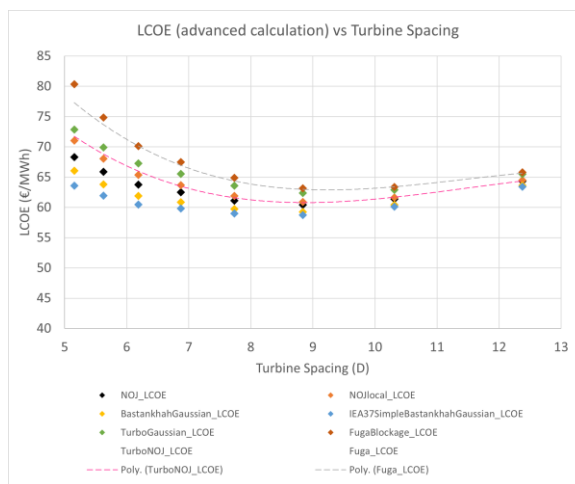
e)   *LCOE vs Turbine Spacing*

Figure 6.3 Plots of various economic indices considering realistic calculations at baseline setting[11]

---

[11] The LCOE model in the simple method is based on the methodology used by International Renewable energy Agency (IRENA) [43]

6.2 Influence in economic Indices using the strike price variation

6.2.1 UK Strike price 2015 CfD auction
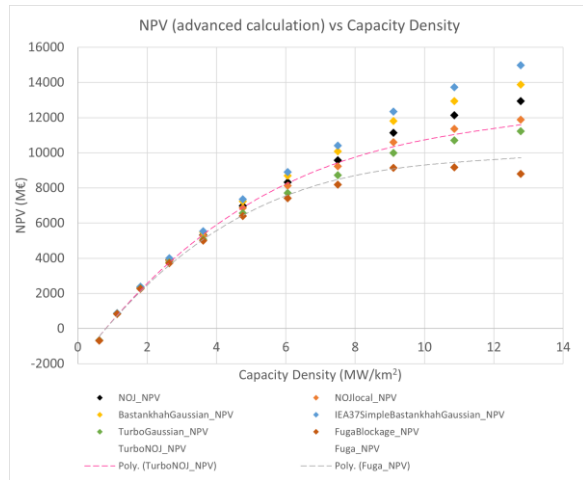
a) NPV vs Capacity Density (advanced method)
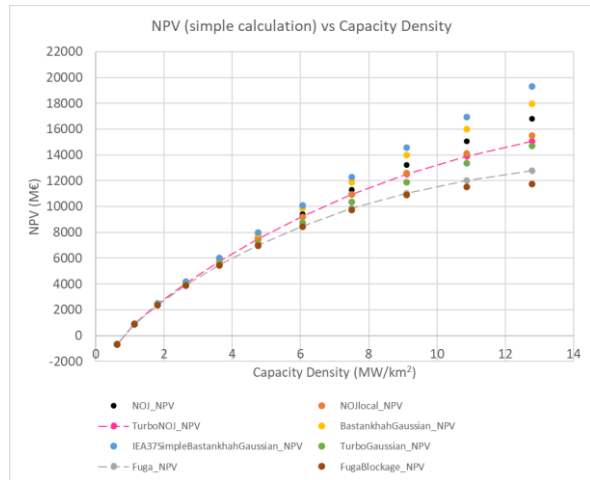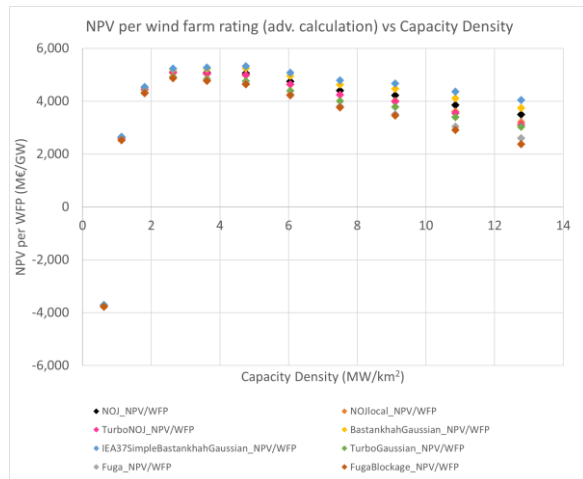
b) NPV vs Capacity Density (simple method)

c) NPV per WFP vs Capacity Density (advanced method)
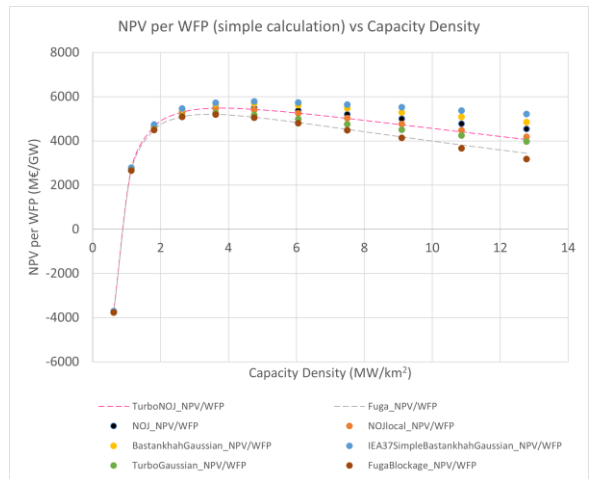
d) NPV per WFP vs Capacity Density (simple method)
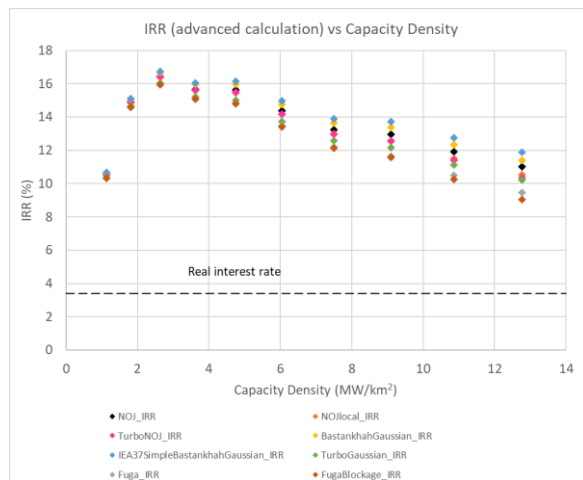
e) IRR vs Capacity Density (advanced method)
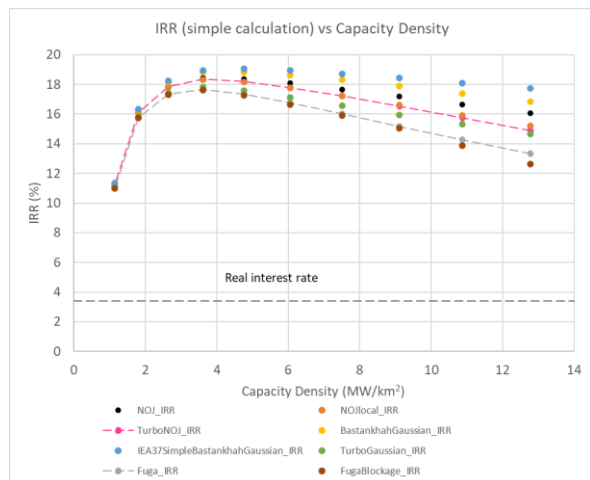
f) IRR vs Capacity Density (simple method)

Figure 6.4 Plots of various economic indices using advanced and simplified method at strike price 130 €/MWh

Figure 6.4 and Table 8 show NPV, NPV/WFP and IRR for the strike price Setting = 130 €/MWh, while keeping the rest of the parameters constant. With higher strike prices, the optimal capacity density decreases to a value of 2.64 MW/km^2 when optimizing the IRR and acts opposite for NPV [24]. However, the curve shows that the internal rate of the return exceeds the real interest rate irrespective of the capacity density selected. In situations like these, a company might opt for a project that has a lower IRR because the bigger project, despite having a lower IRR, is expected to generate greater cash flows or net present value (NPV)

Table 8 Results at strike price of 130 €/MWh

Parameters	Units	Advanced Calculation				Simple Calculation			
		TurbO Park	Fuga	FugaBl ockage	IEA37S BG	TurbO Park	Fuga	FugaBl ockage	IEA37S BG
IRR$_{Max}$	%	16.41	15.97	15.95	16.74	18.35	17.67	17.63	19.04
CD$_{@IRR Max}$	MW/km^2	2.64	2.64	2.64	2.64	3.62	3.62	3.62	4.76
NPV$_{Max}$	M€	11511	9633	9169	14985	15064	12766	11756	19313
CD$_{@NPV Max}$	MW/km^2	12.78	12.78	10.86	12.78	12.78	12.78	12.78	12.78
NPV/WFP$_{Max}$	M€/GW	5085	4883	4872	5326	5482	5203	5186	5780
CD$_{@NPV/WFP Max}$	MW/km^2	2.64	2.64	2.64	4.76	3.62	3.62	3.62	4.76

6.2.2 2019 Dogger Bank award

Figure 6.5 and Table 9 show NPV, NPV/WFP and IRR results for the strike price of 45 €/MWh, while keeping the rest of the parameters constant. When a lower strike price is considered, the optimal capacity density while maximizing for IRR and NPV/WFP increases for some of the models. However, the computed IRR remains below the real interest rate, regardless of the selected capacity density. When optimizing for NPV, the results show a lower value of capacity density, raging between 1.81 and 2.64 MW/km^2, would yield relatively lower losses. The negative NPV and IRR are because the assumed strike price is below the LCOE estimate which lies in the range of 58-63 €/MWh. However, the report uses publicly available generic information for some of the key inputs, so the actual project economics would probably look a bit different [24].
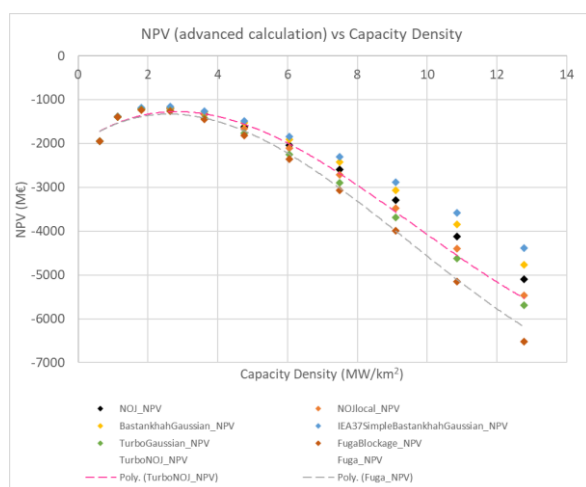
a) NPV vs Capacity Density (advanced method)   *b) NPV vs Capacity Density (simple method)*
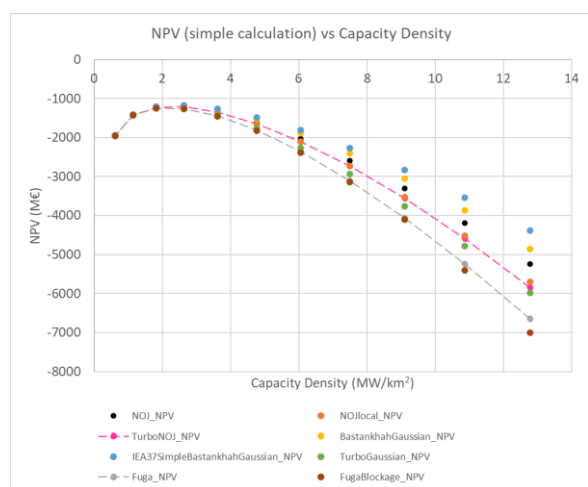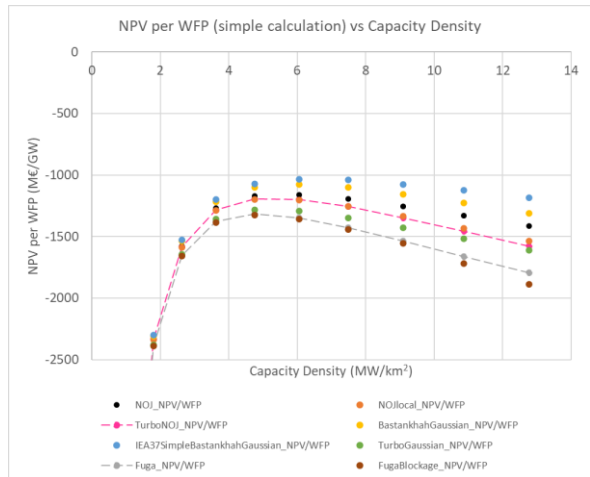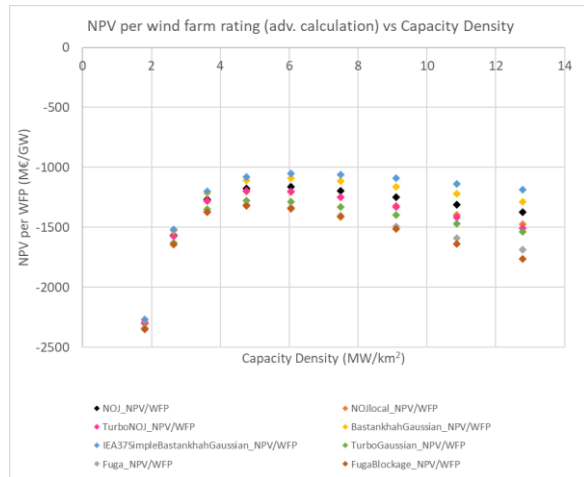
c) NPV per WFP vs Capacity Density (advanced method)

d) NPV per WFP vs Capacity Density (simple method)
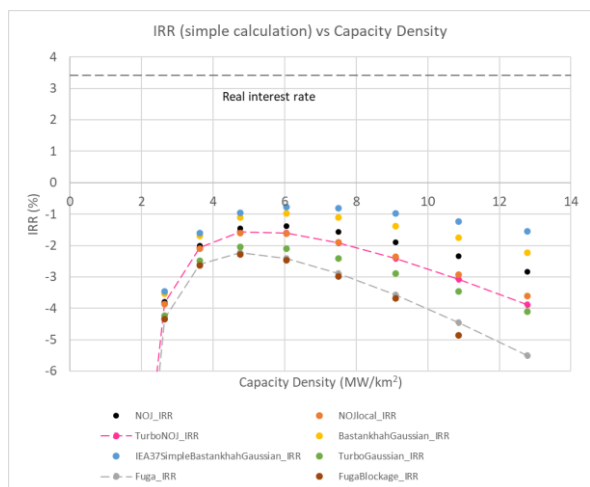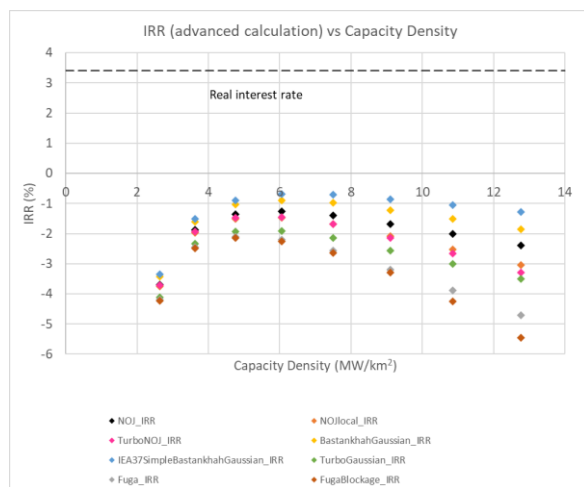
e) IRR vs Capacity Density (advanced method)

f) IRR vs Capacity Density (simple method)

Figure 6.5 Plots of various economic indices using advanced and simplified method at strike price 45 €/MWh

Table 9 Results at strike price of 45 €/MWh

Parameters	Units	Advanced Calculation				Simple Calculation			
		TurbO Park	Fuga	FugaBl ockage	IEA37S BG	TurbO Park	Fuga	FugaBl ockage	IEA37S BG
IRR_{Max}	%	-1.46	-2.10	-2.15	-0.70	-1.57	-2.24	-2.29	-0.77
$CD_{@IRR\ Max}$	MW/km^2	6.05	4.76	4.76	6.05	4.76	4.76	4.76	6.05
NPV_{Max}	M€	-1201	-1232	-1233	-1160	-1210	-1252	-1253	-1167
$CD_{@NPV\ Max}$	MW/km^2	2.64	1.81	1.81	2.64	2.64	1.81	1.81	2.64
NPV/WFP_{Max}	M€/GW	-1195	-1310	-1318	-1050	-1194	-1316	-1325	-1033
$CD_{@NPV/WFP\ Max}$	MW/km^2	4.76	4.76	4.76	6.05	4.76	4.76	4.76	6.05

6.3 LCOE distribution using the CapEx and OpEx for Princess Elisabeth zone

The variables used in the standard scenario are calibrated to the one of the LCOE studies related to Princess Elisabeth zone [7]. In order to quantify a comparable amount of expenditures, the setting is kept at CapEx of +10% and OpEx of -55% for the eleven chosen capacity densities while rest of the parameters are held constant. The attempt is to keep the CapEx in the range of 2.55-2.7 M€/MW and OpEx close to 837 k€/MW. (Refer to Figure 6.6)
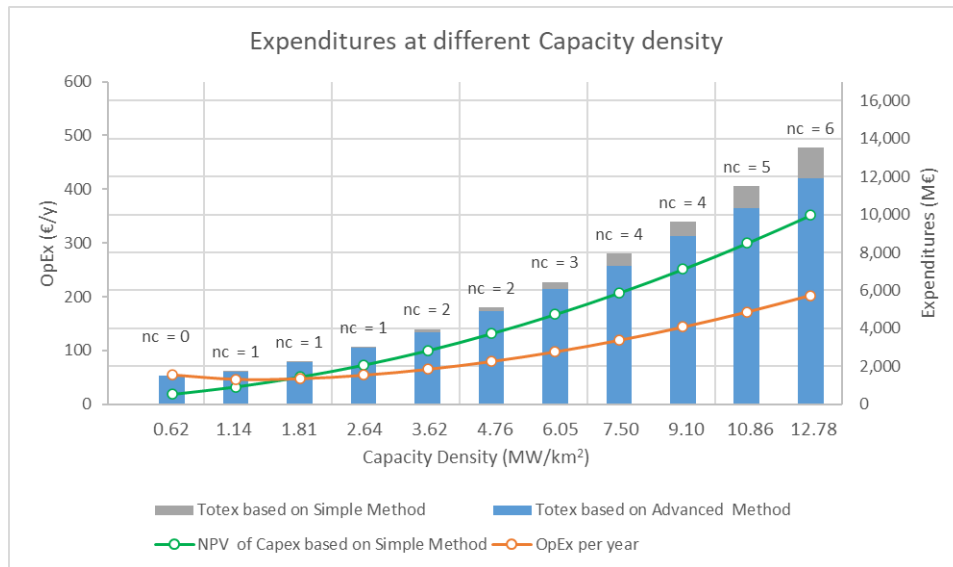
Figure 6.6 Expenditures tuned to Princess Elisabeth Zone

Essentially, OpEx has a huge effect on the economic indices – LCOE, NPV and IRR due to a considerable reduction in the total expenditure. With reduction in the TotEx, the negative part of the NPV reduces and hence the profitability of the project increases. This also means that the levelized cost or the minimum electricity price to earn a profitable business reduces and comes down to a value range of 47 – 50 €/MWh (refer to Table 10). In this case, a strike price as low as 50 €/MWh would give a positive NPV.
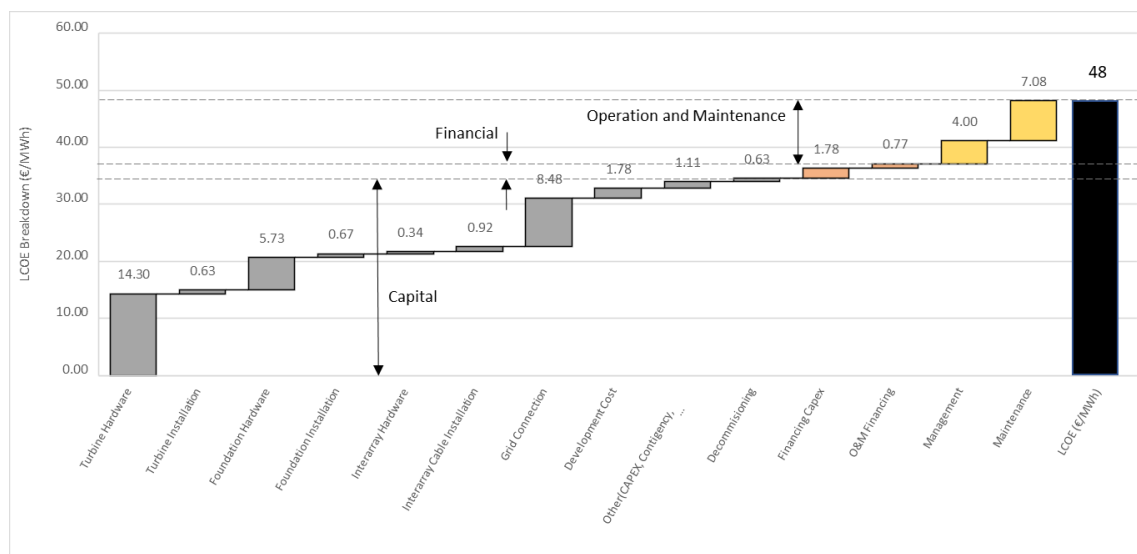
Figure 6.7 LCOE breakdown according to tuned parameters

Figure 6.7 represents the LCOE split in terms of detailed cost estimates for each sub-category of Capital and operating expenditures. The levers that drive the LCOE in terms of costs are turbine, foundation hardware, grid connection, maintenance, and management.

Table 10 Results with parameters (OpEx and CapEx) tuned to Princess Elisabeth Zone

Parameters	Units	Advanced Calculation				Simple Calculation			
		TurbO Park	Fuga	FugaBl ockage	IEA37S BG	TurbO Park	Fuga	FugaBl ockage	IEA37S BG
LCOE$_{Min}$	€/MWh	48.19	49.53	49.61	46.71	47.03	48.34	48.42	45.57
CD$_{@LCOE\ Min}$	MW/km^2	3.62	3.62	3.62	4.76	3.62	3.62	3.62	4.76
S$_{@LCOE\ Min}$	D	10.31	10.31	10.31	8.84	10.31	10.31	10.31	8.84
CapEx/WFP	M€/MW	2.69	2.69	2.69	2.70	2.69	2.69	2.69	2.70
OpEx/WFP	k€/MW/y	62.18	62.18	62.18	57.85	62.18	62.18	62.18	57.85
AEP	GWh/y	4834	4834	4834	6220	4834	4704	4696	6437
IRR$_{Max}$	%	5.37	4.84	4.80	5.88	5.89	5.29	5.25	6.52
CD$_{@IRR\ Max}$	MW/km^2	4.76	4.76	3.62	4.76	4.76	4.76	3.62	6.05
NPV$_{Max}$	M€	2697	2021	1991	4025	3739	2806	2734	6005
CD$_{@NPV\ Max}$	MW/km^2	9.10	6.05	6.05	12.78	10.86	9.10	9.10	12.78
NPV/WFP$_{Max}$	M€/GW	1614	1505	1499	1720	1790	1639	1630	1932
CD$_{@NPV/WFP\ Max}$	MW/km^2	2.64	2.64	2.64	4.76	3.62	3.62	3.62	4.76

6.4 Analysis I: LCOE sensitivity analysis
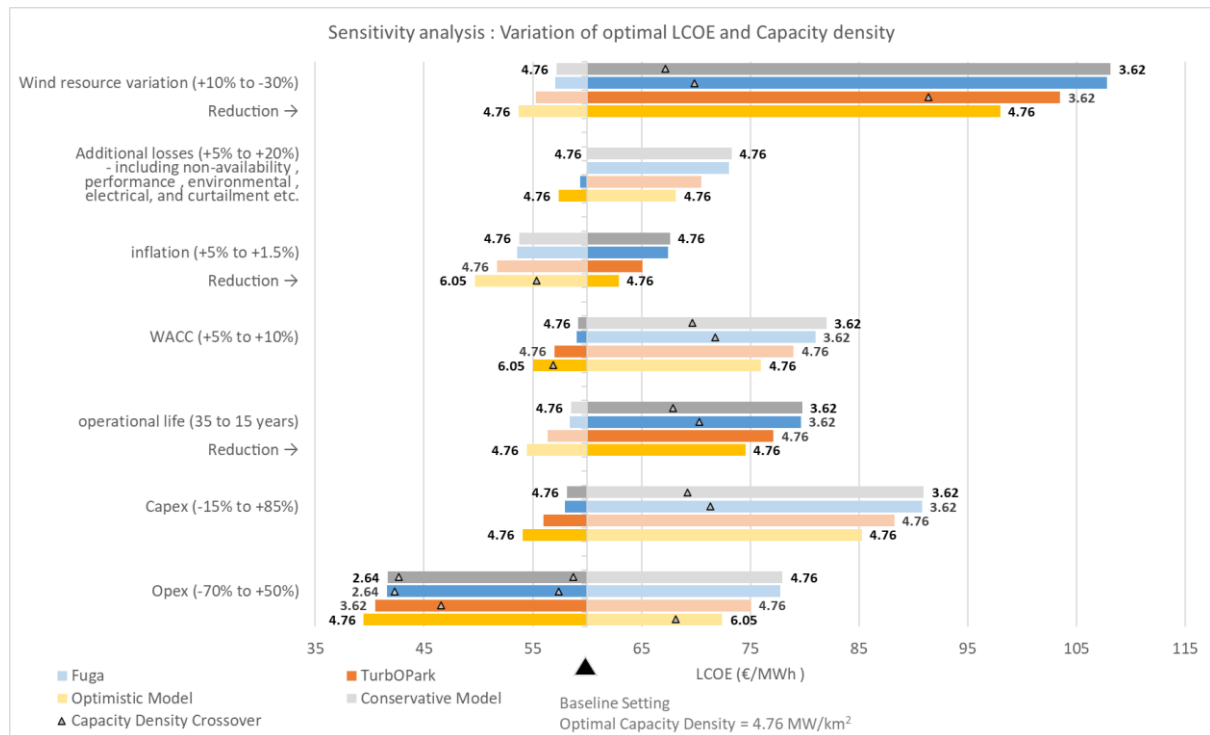
Figure 6.8 LCOE sensitivity analysis

The tornado plot under Figure 6.8 illustrates how the levelized cost of electricity responds to sensitivity analysis depending on several parameters. The purpose of the plot is to compare the relative impact of different variable parameters on the LCOE, rather than to determine the precise absolute value of LCOE. The numbers denoted in the graph show the optimal capacity density for the extreme case taken into consideration, and the markers indicate the transition between optimal points for the minimized LCOE value. For example, if the wind resource increases to 10%, the conservative wake model illustrates the minimized LCOE as 57 €/MWh, with the corresponding optimal capacity density of 4.76 MW/km². As the wind speed decreases by 5%, the optimal point shifts from 4.76 to 3.62 MW/km², and the LCOE value increases to 67 €/MWh. In other words, the effect of inter turbine spacing on capacity factor become more significant with decreasing wind speed. The details of the graph can be viewed under the table (refer to Table 14 in the appendix). The study is performed based on deviation from the nominal values. The variation in the independent variables (y-axis) has been derived from - realistic estimates of wind in the North Sea, transmission losses depending upon the use of technology, inflation during the present scenario in Norway, operational life on the service/equipment quality of the turbines, and costs based on data gathered from research papers [7],[5],[15],[35].

Enhancement in parameters like wind resources, inflation, and operational life typically decreases LCOE. On the contrary, parameters such as transmission losses, WACC, operational life, CapEx, and OpEx have a direct impact, resulting in an increase in LCOE w.r.t. the parameter. The graph specifically focuses primarily on the optimistic, conservative, and industry-standard wake models (TurbOPark and Fuga) to determine how the listed parameters influence the optimal point.

It is evident from the graph that OpEx has the maximum weightage in terms of driving the optimum point of capacity density, and the reason is also due to the widespread range selected. On the other hand, additional losses excluding wake (such as non-availability, performance, electrical, environmental, and curtailment losses) have no effect on optimal capacity density, regardless of the variation (with a selected range between 5 and 20%). Similar to losses, inflation (from 1.5 to 5%) has no impact on the optimal point, with the exception of the optimistic wake model, where an increase of more than 3.4% causes the optimal point to change to a value of 6.05 MW/km². At 5% WACC, the same shift from 4.76 to 6.05 MW/km² for the optimistic wake model is apparently visible. However, this is precisely because of an overall decrease in the anticipated value of the real interest rate below 2.5%. The optimal point shifts from 4.76 to 6.05 MW/km² when the real interest rate, which has a direct proportionality with the WACC and an inverse correlation with inflation, decreases. Furthermore, a higher WACC value of over 7.5% leads to a drop in the optimal point to 3.62 MW/km² for Fuga and FugaBlockage models.

When wind resources are decreased (below -5% for Fuga, -8% for FugaBlockage, and -25% for the TurbOpark model), the overall capacity factor decreases, and the optimal point shifts from 4.76 to 3.62 MW/km². However, the optimal point in the case of the optimistic model is not affected by changes in the wind resource. CapEx and operational life reflect an optimal value of 4.76 MW/km² for IEA37SBG and TurbOPark irrespective of parametric changes in their value. Fuga and FugaBlockage reflects the same optimal CD at 15% reduction in CapEx or 35 years as operational life of the turbine. However, a decrease in operational life to 21 years and below or increase in CapEx above 18% results in optimal capacity density of 3.62 MW/km² for the conservative wake model. Similar observations are noted with Fuga model as well. LCOE correlation with OpEx is discussed further in the subsection below.

6.4.1 Correlation of LCOE with OpEx

Figure 6.9 a) illustrates the effect of variation on LCOE concerning changes in OpEx according to different wake models while Figure 6.9 b) depicts the coordinate location of optimal capacity density as a function of minimum LCOE for the selected change in OpEx. The coordinates represented in the

3D graph reflect the optimum CD on the x-axis, increment/decrement on the y-axis, and minimum LCOE on the z-axis only for optimistic and conservative wake models. The following observations can be made regarding the plot:

a) LCOE with increment in OpEx

b) Optimal Capacity Density
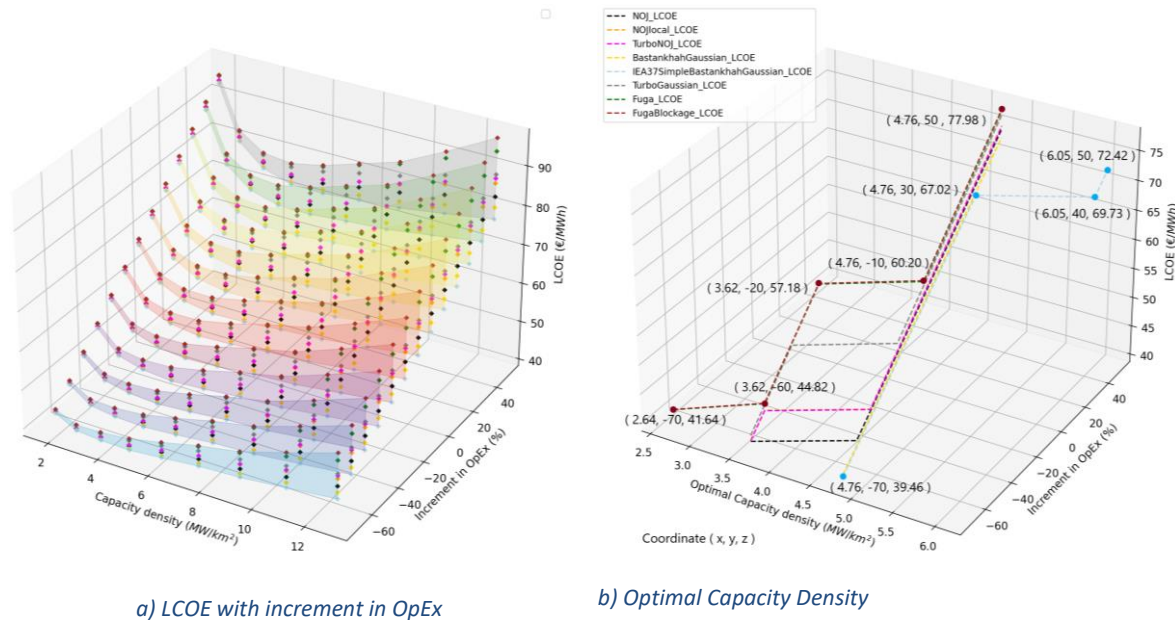
Figure 6.9 LCOE sensitivity with respect to OpEx

As LCOE and OpEx are directly proportional, cutting down OpEx also minimizes LCOE. The selection of OpEx range is largely based on the research papers and known sources [7],[15]. With the increase in OpEx and overplanting, the range between the maxima (optimistic wake model) and minima (conservative wake model) for LCOE increases. For the optimistic wake model, the optimal capacity density toggles from 4.76 to 6.05 MW/km^2 when the OpEx increases to or above 35%. However, within the range of -70% to 34%, the optimal point has barely any effect.

For the conservative wake model, the increment in OpEx values does not affect the optimal point until the OpEx increases 1.5 times. When the OpEx reduces below -15%, the optimal capacity density shifts to the left from the nominal value of 4.6 MW/km^2. At OpEx values falling in a range between -60% and 16%, the optimal value of capacity density is 3.62 MW/km^2, but as OpEx values decrease to -67%, the optimal value drops to 2.64 MW/km^2. The Fuga model follows a similar trend as the conservative wake model with optimal capacity density in the same range.

The TurbOpark model yields a result with an optimum capacity density of 4.76 MW/km^2 for 0.5 to 1.5 times the nominal value of OpEx. Reducing beyond -50%, the optimum value switches to 3.62 MW/km^2.

6.5 Analysis II: NPV sensitivity analysis

The NPV sensitivity conveys a wide range in the optimal capacity density as compared to the LCOE and IRR sensitivity analyses. It is more evident in optimistic wake model as compared to the conservative wake model. In contrast with LCOE, NPV rises when characteristics like the operational life of turbines, inflation, better wind resources, and strike prices improve. Increases in CapEx, OpEx, nominal WACC, or losses, on the other hand, have the reverse effect. Instead of representing the 3D plot for each independent variable, the values from the Table 15 (refer to the appendix) can be visualized using tornado plots for NPV sensitivity (refer to Figure 6.10) and optimal capacity density (refer to Figure 6.11). Both figures can be correlated to obtain the maximum NPV and corresponding

optimal capacity density concerning the amount of variation for the parameter in question. The labels in the Figure 6.11 present the percentage change or numeric value of the independent variable at which the ideal capacity density point shifts for the respective maximum value of NPV. The baseline is taken as the average of optimum NPV value between the optimistic and conservative wake model. The results reported in the NPV section are based on the maxima and many a times predict a single optimal value instead of providing a range of 'alternative' options. This is indicated in the text wherever possible.

The shift is very prominent in the case of NPV with changes in the strike price. Figure 6.11 represents capacity density as a function of strike price with resolution of 5 €/MWh and the labels with markers represent a range for input parameter which drives the optimal point. For example, a strike price between 65-70 €/MWh would result in an optimal CD of 4.76 MW/km^2 by the conservative wake model, i.e., FugaBlockage. At a strike price of 40 €/MWh, the optimal point can be as low as 1.81 (or alternatively 2.64 MW/km^2), and at a strike price of 70 €/MWh, the optimal point can be between 4.76 and 9.10 MW/km^2, depending on the wake model. NPV projected by all four models is indistinguishable for lower strike prices, but when the strike price increases to 100 €/MWh, the NPV estimated by the optimistic wake model is almost twice as high as the conservative wake model (refer to Table 15 under the appendix). It is worth noting that when a strike price of 60 €/MWh is assumed, which is close to the average LCOE, the NPV for the conservative wake model is negative, but the optimal capacity density lies close to the LCOE predicted optimal values (at the baseline setting). From the project management perspective, a strike price below 65 €/MWh could be unfavorable for a profitable business.
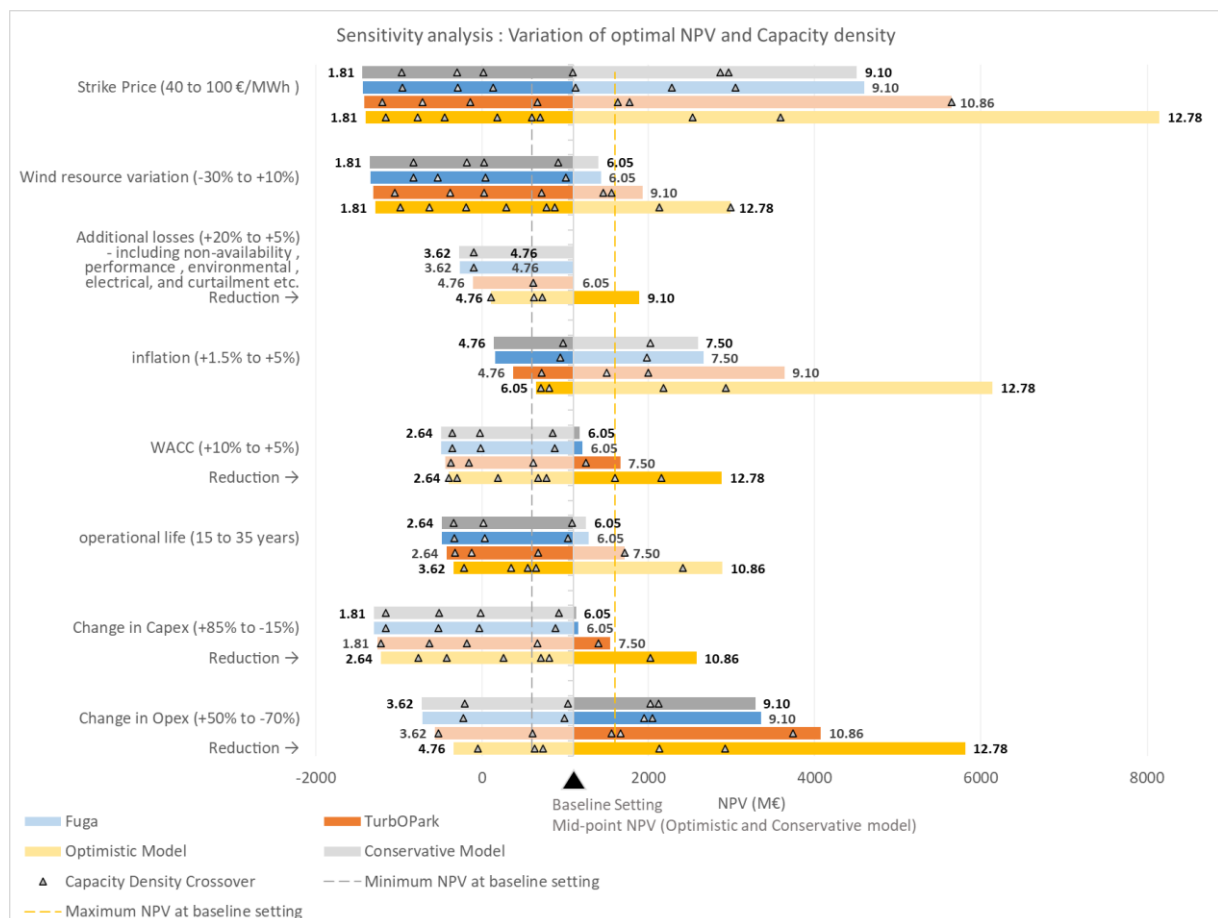
Figure 6.10 NPV sensitivity analysis
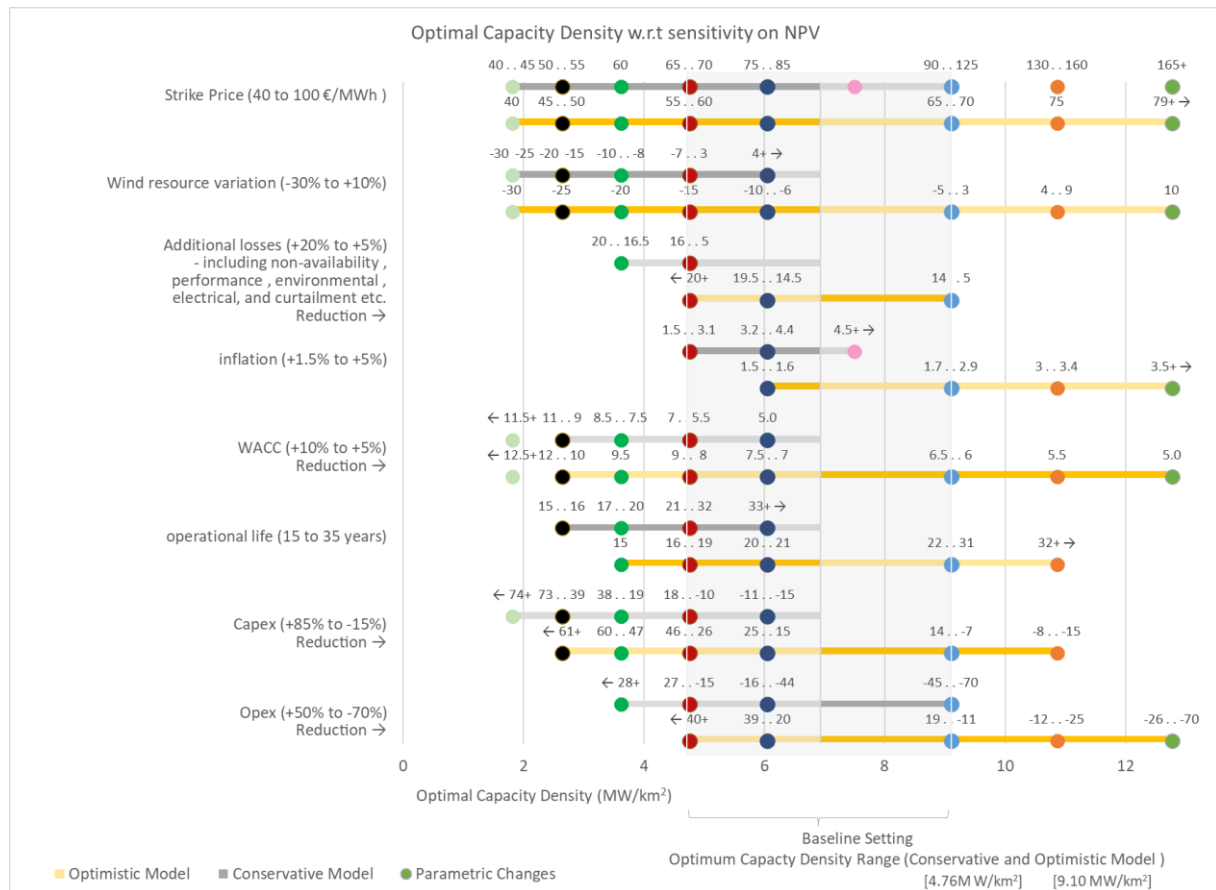
Figure 6.11 Optimal capacity density from NPV sensitivity analysis

Similarly, for the site with a mean wind speed of 7 m/s, while keeping the rest of the input parameters constant, the optimal capacity density might be as low as 1.81 MW/km^2 (or alternatively 2.64 MW/km^2). In some cases, with NPV sensitivity analysis, the crossover of optimal capacity density occurs from 9.1 to 6.05 MW/km^2 because of the NPV drop at 7.05 MW/km^2 (refer to Figure 6.10), and the double marker serves as a representation of them. In particular, the optimistic wake model never shows 7.5 MW/km^2 as the optimal point. For instance, in the case of wind resource variation, the change from 9.1 to 7.5 to 6.05 MW/km^2 occurs relatively quickly when the wind resource is reduced by -6%. The reason is that the same number of construction years apply, and hence the annuity used during construction and operation is the same, but the AEP$_{net}$ for a higher capacity density farm is significantly larger, boosting revenue and consequently the NPV. Another reason is that the results are reported based on the maxima, so the actual CD could be a range.

The percentage reduction in capacity factor caused by extra losses (such as non-availability, performance, environmental, electrical, and curtailment) points to an optimum value of 3.62 or 4.76 MW/km^2 for the highest anticipated loss (20%) and a range between 4.76 and 9.10 MW/km^2 for lower losses (5%). A deflation or increase in nominal WACC results in a lower value of the optimal CD. An exceptionally swift leap from CD 4.76 to 3.62 to 2.64 MW/km^2 occurs when WACC increases from 8 to 9.5% and finally to 10%. Overall, the real interest rate affects the economic index, and all the models forecast a negative NPV when it rises above 5.9%.

An increase in economic life leads to a higher NPV and capacity density. The optimistic wake model suggests a minimum operational life of 18 years, while the conservative wake model recommends a life above 20 years for net profitability (also referred as payback period) assuming an optimal capacity density of 4.76 MW/km^2. Moreover, an increase in CapEx above 18% and OpEx above 20% results in a negative NPV for all models.

6.6 Analysis III: IRR sensitivity analysis

The parameters that heavily influence the IRR sensitivity in terms of optimal capacity density are the strike price and the OpEx (as shown in Figure 6.12). Changes in capacity factors due to additional losses or wind variation also play a role in steering the optimal point. For the selected range of variation, strike price and wind availability show a wider range of prediction in IRR. The difference in IRR due to the strike price variation from 40 to 100 €/MWh predicted by the optimistic wake model is 14.08% (range of -2.60 to 11.48%) and 15.11% (range of -4.44 to 10.66%) by the conservative wake model. (refer to Figure 6.12 and Table 16 in the appendix) The variation in wind from -30% to 10% results into an IRR difference of 9.20% (range of -1.96 to 7.24%) and 10.61% (range of -4.32 to 6.29%) for the extreme circumstances. An IRR above the real interest rate of 3.41% (at baseline value) is desirable, provided WACC and inflation remains unchanged.

Variations in certain parameters such as CapEx, operational life, WACC, and inflation have no impact on optimal capacity density. The optimal point suggested by various models for all the uninfluential parameters is either 3.62 or 4.76 MW/km^2. Additional losses (including non-availability, performance, environmental, electrical, and curtailment) demonstrate similarity, except for the FugaBlockage model, which has a transition point when the losses exceed 7.5%. With the increase in nominal WACC, the optimal capacity density remains the same, and there is no change in the real IRR value, but the nominal IRR increases. Likewise, with an increase in inflation, there is no variation in the optimal capacity density or the real IRR, but the nominal IRR decreases. A decrease in anticipated wind speed (up to -30%) implies a higher optimal CD of 6.05 MW/km^2 for the optimistic wake model, whereas an increase in wind speed of 10% reduces the optimal point to the lowest value of 3.62 MW/km^2.
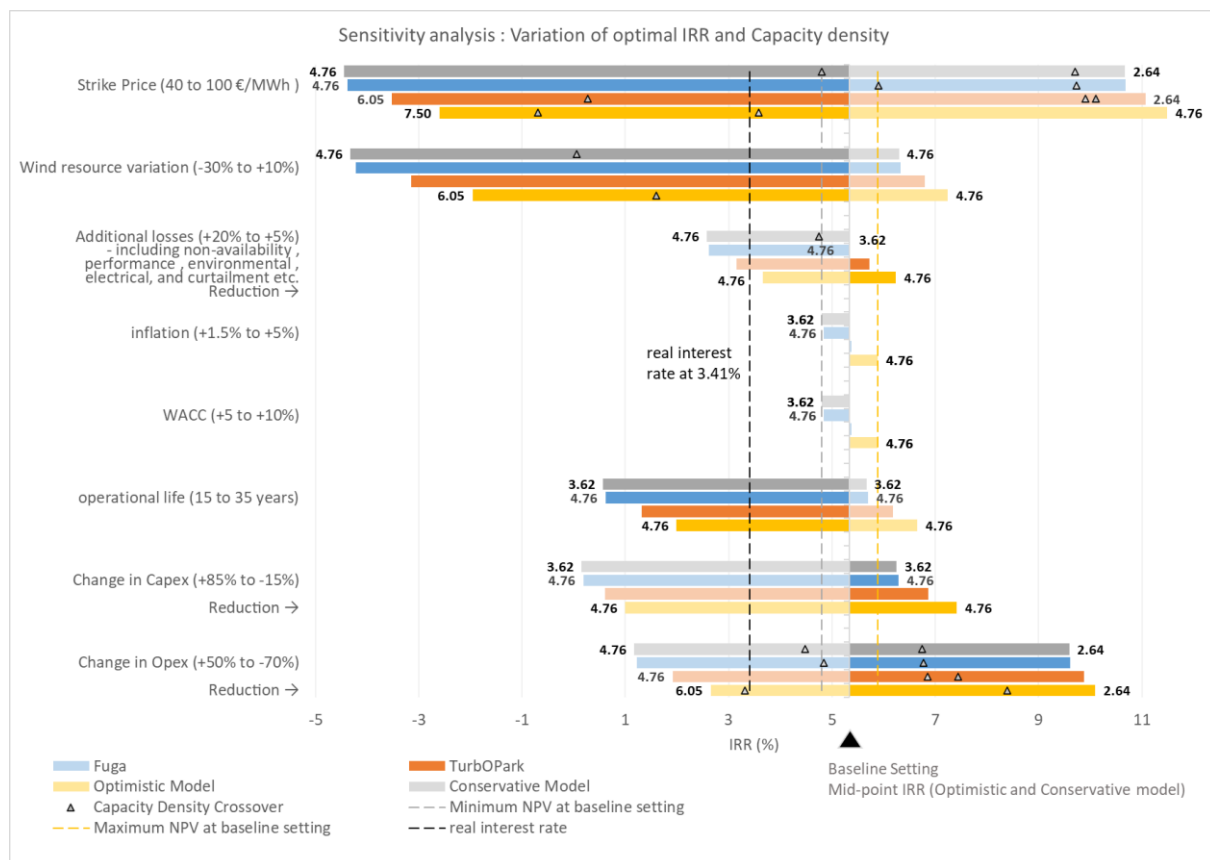
Figure 6.12 IRR sensitivity analysis

6.6.1 Correlation of IRR with OpEx

a) IRR with increment in OpEx

b) Optimal Capacity Density
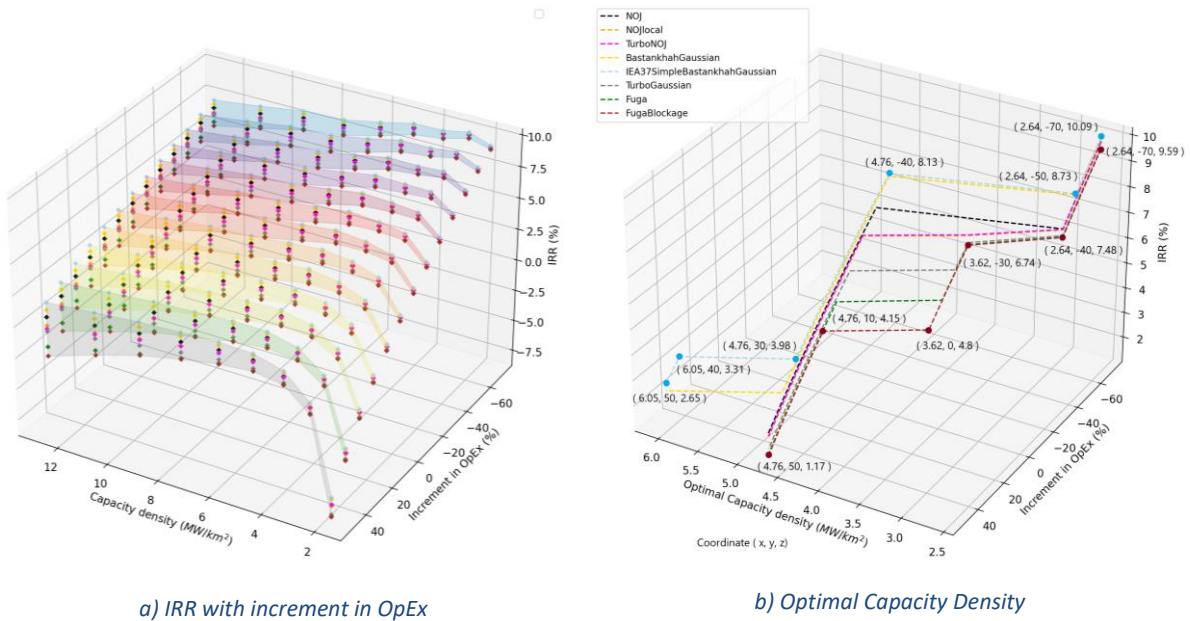
Figure 6.13 IRR sensitivity with respect to OpEx

A reduction in OpEx amounts to an increase in IRR and, at the same time, a reduction in optimal capacity density (refer to Figure 6.13 b)). If the OpEx increases, it results in a higher optimal CD. Higher capacity densities also result in an increase in the IRR gap between the optimistic and conservative wake models as OpEx rises (refer to Figure 6.13 a)). Thus, the uncertainty in the IRR projection rises as the optimal capacity density increases with increased OpEx. When the OpEx is increased above 20% for the conservative wake model and above 35% for the optimistic wake model, the IRR computed crosses below the real interest rate, which is undesirable (refer Figure 6.12).

6.6.2 Correlation of IRR with Strike price

a) IRR with increment in Strike price

b) Optimal CD
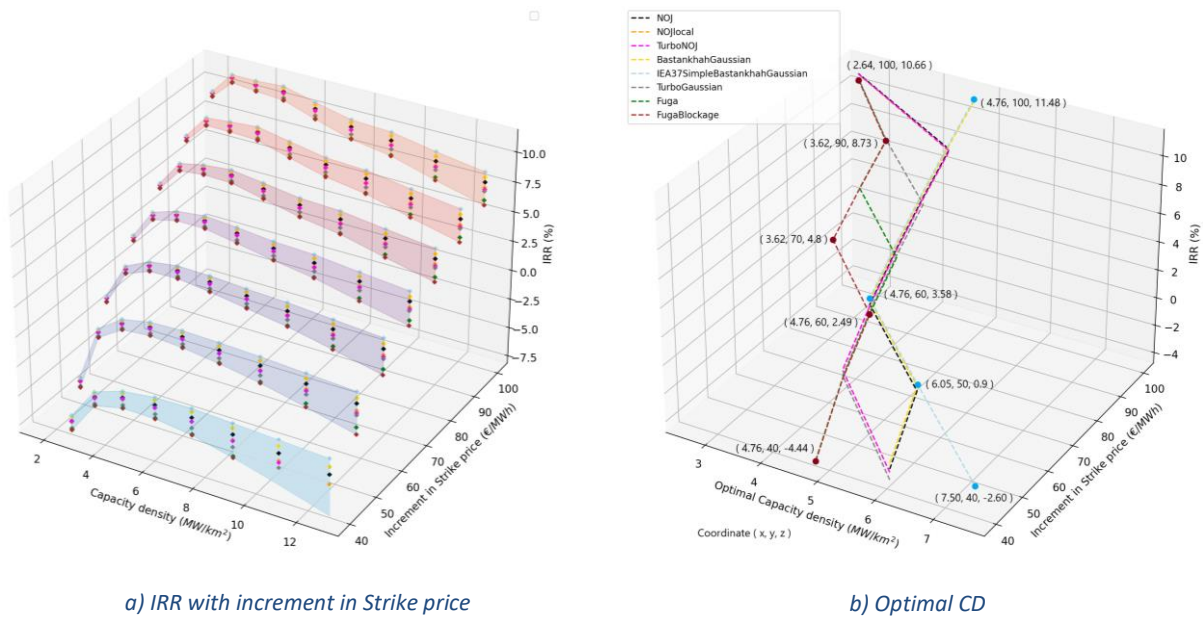
Figure 6.14 IRR Sensitivity with respect to strike price

Strike price has the highest influence in terms of economic index variability that involves the cash inflow into account. (Refer to Figure 6.12) With the baseline configuration, a strike price below 60 to 65 €/MWh results in an IRR lower than the real interest rate. It implies that the strike price decided upon should be above the minimal LCOE. The anticipated optimal capacity density (refer to Figure 6.14) in this scenario (with a strike price between 65 and 90 €/MWh) is 4.76 MW/km^2 according to the optimistic wake model and as low as 3.62 MW/km^2 for the conservative wake model. On agreeing to a lower strike price, around 50 €/MWh, the optimal point evaluated is 4.76 or 6.05 MW/km^2.

IRR predominantly increases with the strike price, while optimal capacity density, being a function of maximum IRR at the selected strike price, declines with an increase in the strike price. However, with lower strike prices and, subsequently, higher optimal capacity densities, the gap in IRR projections between the extreme models broadens. It raises the possibility that, since the optimal point for capacity density is high at lower strike prices, uncertainty in the IRR prediction increases too. IRR displays no solution in some circumstances since it is back computed from NPV, as seen in the graph for the capacity densities of 10.86 and 12.78 MW/km^2 at a strike price of 40 €/MWh.

7. Discussion

Table 11 Analysis Summary

Increase in Parameter	Wake model Type	LCOE value (€/MWh)	Capacity Density (MW/km²)	General observation from all the models	NPV value (M€)	Capacity Density (MW/km²)	General observation from all the models	Real IRR value (%)	Capacity Density (MW/km²)	General observation from all the models
Baseline Setting	Conservative	63.17	4.76		599.37	4.76		4.80	3.62	
	Optimistic	58.75	4.76		1596.03	9.10		5.88	4.76	
Strike price (70 to 100 €/MWh)	Conservative	-	-	-	Increase ↑ -1439 to 4507	Increase ↑ 1.81 to 9.10	CD → moves to right	Increase ↑ -4.44 to 10.66	Decrease ↓ 4.76 to 2.64	← CD moves to left
	Optimistic	-	-		Increase ↑ -1400 to 8148	Increase ↑ 1.81 to 12.78		Increase ↑ -2.60 to 11.48	Decrease ↓ 7.50 to 4.76	
Wind resource (-30% to 10%)	Conservative	Decrease ↓ 108.15 to 57.17	Increase ↑ 3.62 to 4.76	CD → moves to right	Increase ↑ -1348 to 1400	Increase ↑ 1.81 to 6.05	CD → moves to right	Increase ↑ -4.32 to 6.29	- 4.76/3.62	Typically, no effect for most of the wake models at 70 €/MWh ← CD moves to left for lower/higher strike prices
	Optimistic	Decrease ↓ 97.99 to 53.70	- 4.76		Increase ↑ -1283 to 2988	Increase ↑ 1.81 to 12.78		Increase ↑ -1.96 to 7.24	Decrease ↓ 6.05 to 4.76	
Additional losses (5% to 20%)	Conservative	Increase ↑ 61.70 to 73.27	- 4.76	-	Decrease ↓ 760 to -277	- 4.76 to 3.62	← CD moves to left	Decrease ↓ 5.16 to 2.58	Increase ↑ 3.62 to 4.76	CD → moves to right
	Optimistic	Increase ↑ 57.39 to 68.15	- 4.76		Decrease ↓ 1893 to 104	Decrease ↓ 9.10 to 4.76		Decrease ↓ 6.24 to 3.66	- 4.76	
Operational life (15 to 35 years)	Conservative	Decrease ↓ 79.80 to 58.55	Increase ↑ 3.62 to 4.76	CD → moves to right	Increase ↑ -485 to 1250	Increase ↑ 2.64 to 6.05	CD → moves to right	Increase ↑ 0.56 to 5.67	- 3.62	-
	Optimistic	Decrease ↓ 74.55 to 54.46	- 4.76		Increase ↑ -344 to 2888	Increase ↑ 3.62 to 10.86		Increase ↑ 1.99 to 6.64	- 4.76	
Nominal discount rate (WACC) (5% to 10%)	Conservative	Increase ↑ 59.20 to 107.23	Decrease ↓ 4.76 to 2.64	← CD moves to left	Decrease ↓ 1175 to -496	Decrease ↓ 6.05 to 2.64	← CD moves to left	- -	- -	-
	Optimistic	Increase ↑ 55.04 to 103.29	Decrease ↓ 6.05 to 4.76		Decrease ↓ 2884 to -398	Decrease ↓ 12.78 to 2.64		- -	- -	
inflation rate (1.5% to 5%)	Conservative	Decrease ↓ 67.63 to 53.73	- 4.76	CD → moves to right	Increase ↑ 143 to 2596	Increase ↑ 4.76 to 7.50	CD → moves to right	- -	- -	-
	Optimistic	Decrease ↓ 62.90 to 49.66	Increase ↑ 4.76 to 6.05		Increase ↑ 648 to 6137	Increase ↑ 6.05 to 12.78		- -	- -	
CapEx (-15% to +85%)	Conservative	Increase ↑ 58.14 to 90.95	Decrease ↓ 4.76 to 3.62	← CD moves to left	Decrease ↓ 1129 to -1300	Decrease ↓ 6.05 to 1.81	← CD moves to left	Decrease ↓ 6.24 to 0.15	- 3.62	-
	Optimistic	Increase ↑ 54.07 to 85.27	- 4.76		Decrease ↓ 2578 to -1215	Decrease ↓ 10.86 to 2.64		Decrease ↓ 7.41 to 1.00	- 4.76	
OpEx (-70% to +50%)	Conservative	Increase ↑ 41.64 to 77.98	Increase ↑ 2.64 to 4.76	CD → moves to right	Decrease ↓ 3289 to -728	Decrease ↓ 9.10 to 3.62	← CD moves to left	Decrease ↓ 9.59 to 1.17	Increase ↑ 2.64 to 4.76	CD → moves to right
	Optimistic	Increase ↑ 39.46 to 72.42	Increase ↑ 4.76 to 6.05		Decrease ↓ 5811 to -340	Decrease ↓ 12.78 to 4.76		Decrease ↓ 10.09 to 2.65	Increase ↑ 2.64 to 6.05	

The inference drawn in terms of sensitivities reflect the values based on the realistic method. In addition to several sensitivities performed, parameters like uncertainty in weather and royalty percentage were considered. Increase in Royalty essentially means a decrease in revenue and it's a factor added to strike price. On that note, an increase in royalty could be assumed as a decrease in strike price. However, the excel tool developed incorporates all the variables into account to obtain the final results. A key observation based on uncertainty in construction years or the wait time due to bad weather in the North Sea resulted in a fluctuation of capacity density between 3.62 and 4.76 MW/km^2.
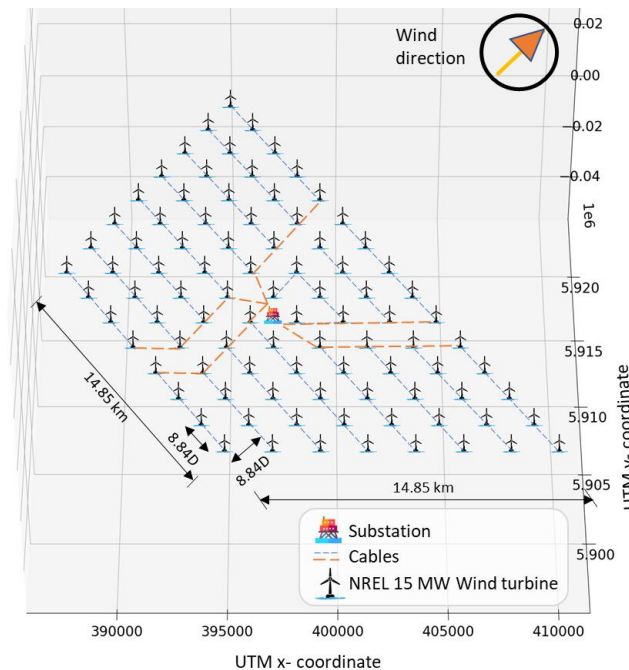
Figure 7.1 3D view of the wind farm on the proposed site with capacity density of 4.76 MW/km^2

The general findings based on analysis summary in Table 11 and sensitivity are stated below:

- Assuming the baseline setting and given flow conditions at the site, the suggested capacity density for the proposed offshore windfarm in the North Sea could be 4.76 MW/km^2 (refer to Figure 7.1). The suggested CD is based on the iteration with deflation (estimated at 2%) or increase in WACC (raised to 7%) or reduction in economic lifetime with overplanting (approx. 22 years).
- When any parameter is increased, the general trend is that capacity density lowers for the LCOE and IRR value. This is exceptional for OpEx increment where CD increases.
- OpEx is the key parameter that drives the maximum shift in optimal point for all the three economic indices.
- Strike price has the highest influence in terms of economic index variability for NPV and IRR, while wind resource is the primary reason for a broad range of results in LCOE and it is the second most influential parameter that affects the IRR extremes. OpEx and CapEx also show a wide range of variation in the economic index, when altered.
- According to the results obtained from the IRR analysis, although the NPV and IRR values show a similar pattern, the optimal capacity density does not. Instead, IRR follows NPV/WFP in a few cases. This disagreement could be explained by differences in variables such as annual energy production, CapEx, OpEx, annuity used in construction.

A concise summary of answers to each research question is presented under the trailing subsections.

7.1 Impact of capacity density on economic indices: NPV, LCOE, and IRR

- Conceptually, a higher capacity density offshore wind farm can lead to increased revenues, which improve NPV or IRR, and lower costs per unit of electricity generated, resulting in a lower LCOE. It's due to increased power generation potential, economies of scale, reduced transmission costs, and improved wind resource utilization. However, it's important to note that the specific impact of capacity density on economic indices also depends on operating and capital expenditures. All these factors, i.e., revenue, CapEx, and OpEx, together lead to an abrupt shift in the graph, yielding the optimal point for selected scenarios (or range in capacity density). Overplanting beyond a certain capacity density may not be an effective solution.

- The question of what the optimal capacity density of a windfarm should be depends on the type of economic index that one is planning to optimize. Numerous factors such as array efficiency, operational life, the real rate of interest (WACC and inflation), expenditures, local wind resource at the location, and uncertainties in the construction years influence the Levelized cost. Additionally, revenue influencing parameters like strike price/electricity price, and royalty contribute to changes in NPV and hence the IRR. With the assumed characteristics which are reasonable for an offshore wind project in North Sea, it can be inferred that the optimal capacity density point lies close to 4.76 MW/km^2 while optimizing for LCOE or NPV per windfarm rating, and towards the lower end of 3.62 MW/km^2 with the motive to optimize IRR.

- For a profitable business from the project management perspective a strike price or electricity price below 65 €/MWh could be unfavorable without any support scheme/ government subsidies or incentives. A lower strike price also indicates an extended payback period, or a greater number of operational years required to recover the expenditure. For an optimistic assumption at the baseline setting, a strike price of 70 €/MWh suggested an optimal capacity density between 4.76 and 6.05 MW/km^2 by the industry-recognized wake models Fuga and TurbOPark. This is a replicate situation of real-life problems that companies in the wind industry are facing today where one company bids for twice as high-capacity density being way too optimistic. NPV recommended by the optimistic wake model, IEA37SimpleBastankhahgaussian is exceptionally high for higher values of strike price and estimated severely low for lower strike prices using the conservative wake model (FugaBlockage).

- Taking into consideration all the parameters and sensitivity, the optimal CD is anticipated to lie between 3.62 to 6.05 MW/km^2 for a typical wind farm in the North Sea and in some extreme cases with lower strike prices (~50 €/MWh) below the LCOE, it could be as low as 2.64 MW/km^2.

- However, NPV is extremely receptive to parametric changes and the optimal capacity jump occurs instantly with a minor change in any of the input constraints. In such a case, validation of wake model is necessary to determine the accurate answer.

7.2 Guidelines for determining the optimal capacity density

- To identify the optimal capacity density of a wind farm, the initial procedure involves site assessment, turbine selection, energy yield estimation (including neighboring wind farm wake interactions), layout planning/optimization followed by cost-benefit analysis, and environmental impact assessment. It can further be explained with the following steps:

1) Develop scenarios: A set of scenarios with ranges in capacity densities are required for comparison. A suitable comparison could be based on optimizing the layout within the selected area for higher capacity densities.

2) Define the objective and relevant metrics: The optimal capacity density of a windfarm can vary depending on the specific context and objective of the project. For example, the objective may be to maximize the energy production, minimize the resource usage/expenditure, or maximize the profitability. For this research, optimal capacity density is the capacity density that corresponds to the lowest cost of energy, adds up to the maximum net present value and displays the highest rate of return.

3) Identify the constraints: The constraints are the parameters that determine the NPV, LCOE and IRR pertaining to the capacity density. Constraints such as wind resource (speed and direction), losses, CapEx, OpEx, WACC, inflation, construction and operational years, electricity price and royalty are some parameters that affect the sensitivity of these metrics.

4) Sensitivity Analysis: Create a mathematical model for each metric with the necessary constraints to simulate various possibilities and predict the impact of changes. The sensitivity analysis tool can be used to determine the values of the decision variables that maximize or minimize the objective function.

5) Result Validation: Testing the results of the optimization in the real world and measuring its performance can help in the development of future offshore windfarms. Selection of wake model is crucial in determining the outcome and therefore it is necessary to examine the relationship between theoretical prediction and actual dataset.

- The actual capacity density of a wind farm may also depend on its layout and regularity frameworks. To prevent wake effects and improve power output, turbines in a wind farm are placed apart from one another. Environmental aspects, for instance, bird and bat populations, noise pollution, and visual effects may also have an impact. Therefore, it is essential to consider these factors when deciding on a location and developing a design for the wind farm to operate sustainably and responsibly. Overall, finding the optimal capacity density requires a thorough analysis of several factors and a balance between energy production, cost, and environmental impact.

7.3 Wake model influence on the expected optimal capacity density

- The choice of the wake model has a significant impact on the estimated optimal capacity density, highlighting the importance of careful consideration in the selection process. The wake model that results in higher capacity factors, such as the IEA37SimpleBastankhahGaussian, BastankhahGaussian model, usually predicts a higher optimal capacity density in comparison to the Computational fluid dynamics wake model (Fuga, FugaBlockage). The conservative wake model evaluates higher power losses and therefore a lower optimal capacity density. Hence, it is crucial to select an appropriate wake model that meets the specific requirements of wind farm layout and analysis to achieve accurate predictions of the optimal capacity density.

- Typically, with higher capacity densities, the variation in the prediction of financial metrics to be optimized (whether LCOE, NPV, or IRR) from different wake models increases. This difference is more evident when capacity density surpasses 4 MW/km^2. Due to the variation of economic indices, the minima for LCOE or maxima in NPV and IRR stand apart in some cases with the variation in wake models. For instance, while LCOE displays the same optimal capacity density at the baseline setting, NPV and IRR indicate different values. NPV shows a significant difference, with the optimistic wake model estimating maximum NPV at 9.10 MW/km^2, while the conservative wake model predicts maxima at 4.76 MW/km^2. The difference in optimal values for IRR is not as pronounced. The optimistic wake model matches the optimal capacity density for LCOE and NPV, whereas the conservative wake model shows two values 3.62 and 4.76 MW/km^2 (as an alternative).

- The results show that a higher capacity density produces a better NPV if the revenue/ strike price is high or, on the contrary, if TotEx is low (particularly in the OpEx segment). Other factors such as a longer operational life expectancy, increased inflation or higher wind speeds than anticipated, reduced losses (wake, array losses etc.), and a lower WACC may also highly impact the NPV as well as the LCOE, and a similar pattern can be expected for the optimal values.

7.4 Impact of wind resource the optimal capacity density

- In general, optimizing for LCOE and NPV, the optimal capacity density tends to increase with higher wind resource availability. It's perhaps because regions with higher wind speeds and consistent wind patterns can accommodate more wind turbines without compromising performance. When considering wake models, the models that display lower wake losses and higher capacity factors exhibit a higher optimal point.

- When examining the minimal LCOE resulting from a 30% reduction in wind speed, wake models such as IEA37SimpleBastankhahGaussian, BastankhahGaussian, and Jensen, PyWake models that forecast lower wake, anticipate the same optimal capacity density of 4.76 MW/km^2 as when the wind resource increases to 10% (refer to Table 17 in the appendix). On the other hand, the remaining wake models predict an optimal capacity density of 3.62 MW/km^2 at reduced wind resources (30%). A descending order of WR shift points is evident, such as the shift occurring at values of -6%, -9%, -20%, -30%, and -30% for FugaBlockage, Fuga, TurboGaussian, TurbOpark, and local Jensen, respectively.

- The NPV shows an erratic change for the wind resource when the agreed strike price falls above the LCOE (refer to Table 18 in the appendix). From a profitability standpoint, at a strike price of 70 €/MWh, conservative wake models such as TurboGaussian, Fuga, and FugaBlockage demonstrate an optimal value of 4.76 MW/km^2, whereas Jensen and its derivatives (Original Jensen, local Jensen, TurbOpark) show an optimal value of 6.05 MW/km^2. Wake models with the highest capacity factors, such as IEA37SimpleBastankhahGaussian and BastankhahGaussian, indicate an optimal value of 9.10 MW/km^2. If the wind resource is reduced by 25%, 75% of the wake models (except the optimistic and conservative) suggest an optimal value of 2.64 MW/km^2. However, when the wind is further reduced by 30%, all wake models predict an optimal capacity density between 1.81 (alternative option as 2.64 MW/km^2). Furthermore, when the windspeed is increased by 10%, the range of variation between optimistic and conservative wake models is between 6.05 and 9.10 MW/km^2.

- At a strike price below LCOE, for instance, at 50 €/MWh, all the wake models predict negative values for NPV and an optimal CD of 2.64 MW/km^2 (refer to Table 19 in the appendix). With increased wind resources, the NPV slightly improves, and the optimal CD shifts to a higher value of 3.62 or 4.76 MW/km^2 (for optimistic wake models), except for FugaBlockage. If the wind resource is reduced by 20%, all models suggest a CD of 1.81 MW/km^2. A further decrease results in a lower optimal capacity density.

- Wind resource has very little influence on the optimal point for IRR and remains consistent within the selected wake model. For IRR at a strike price of 70 €/MWh, when wind speed decreases by 30%, the optimistic wake model yields 6.05 MW/km^2 (refer to Table 20 in the appendix). However, 75% of the other models, including the conservative FugaBlockage model, show a value of 4.76 MW/km^2. Industry-specific wake models (TurbOPark and Fuga) result in the same optimal point (4.76 MW/km^2) regardless of wind resource changes. Interestingly, several PyWake models show a lower internal rate of return at wind speeds below 5%.

- However, when considering a lower strike price of 50 €/MWh, the internal rate of return remains below the real interest rate even with a 10% increase in wind resources (refer to Table 21 in the appendix). On average, most models predict an optimal capacity density of 4.76 MW/km^2 for a strike price equivalent to 70 €/MWh. Deduction in strike price leads to similar outcomes for all wake models with lower capacity factors (such as FugaBlockage, Fuga, TurboGaussian, and TurboOpark). If the wind speed reduces from the forecasted value by 15%, the optimal point shifts from 4.76 to 6.05 MW/km^2 for Jensen and local Jensen wake model. Wake models like IEA37SimpleBastankhahGaussian and BastankhahGaussian predict a higher optimal point of 6.05 MW/km^2 consistently.
- Nevertheless, it should be emphasized that factors like spatial limitations and environmental concerns can also restrict the maximum capacity density attainable, even in regions with abundant wind resources. Furthermore, the optimal capacity density can fluctuate based on the particular wind turbine technology and design employed.

8. Conclusion

This study establishes comprehensive guidelines involved in determining the optimal capacity density for a typical offshore windfarm in the North Sea ensuring a holistic approach. The key aspects involved in the decision-making of a windfarm development include wind resource assessment, turbine selection, layout design, energy production estimation, financing, and the optimization of economic indicators - LCOE, NPV and IRR.

A method for identifying the capacity density under different scenarios and economic frameworks has been developed under this work. The general observation reported with the baseline setting shows that upon scaling the number of turbines within a designated area, LCOE experiences a sharp decline until reaching a certain threshold, resulting in a dip in the LCOE curve or the optimized LCOE. Beyond this, the curve rises upward suggesting an increase in the cost of energy. Based on the input parameters considered in this study, the optimized value of LCOE could lie between 59-63 €/MWh. This indicates that a strike price or electricity price below 65 €/MWh could be unfavorable without any support scheme/ government subsidies or incentives. The LCOE estimate matches the projection according to the literature survey [21]. The work also indicates that rationalizing the OpEx estimation leads to a significant reduction in LCOE up to 47-50 €/MWh.

The study found that different windfarm operators may claim different capacity densities depending on their assumptions, methodologies and technologies used for estimation and reporting of the financial metrics. Some may use a more conservative approach for the wind resource, turbine performance, wake effects or models while the others may use optimistic assumptions. Moreover, some operators may have more advanced or sophisticated methods for wind farm simulation and power production estimation, leading to more accurate and precise capacity density estimates. If the focus is on minimization of levelized energy cost, overplanting may not be such a good option beyond 4.76 MW/km^2. On the other hand, if the focus is on profitability, it depends on the company-specific wake model employed. The choice of capacity density can be seen as a strategic economic decision. Choosing a relatively high capacity density of around 9.10 MW/km^2 results in a larger spread of NPV (-100M€ to 1600 M€) at a lower IRR. On the contrary, choosing a more common capacity density around 4.76 MW/km^2 results in the lowest LCOE, highest IRR and smaller spread in NPV (600 to 1100 M€). It also illustrates that developers using optimistic wake models might be more inclined to higher capacity densities if they are optimizing for NPV. However, the impact of wake-induced turbulence on the operational lifespan of wind turbines plays a key role. A sensitivity analysis for NPV utilizing the turbine's operational life reveals that if the operational life falls below 22 years, the optimistic model indicates a shift in the optimal capacity density from 9.10 to 6.05 MW/km^2. Therefore, validation of wake model is crucial for an accurate prediction of the optimal capacity density.

A part of this study is to demonstrate the sensitivity of input parameters that have inherent uncertainty and their immediate impact on the resulting optimal capacity density. The question of what the optimal capacity density of a windfarm should be depends on the type of economic index that one plans to optimize. The Net Present Value is influenced by the revenue generated, which is determined by factors such as the strike price or electricity price. Additionally, the number of construction years also plays a role. Therefore, optimizing for the Levelized Cost of Energy does not necessarily guarantee the highest NPV at that specific point. However, if the strike price is close to LCOE of the project, then the simple calculation of NPV suggests that the maxima of NPV corresponds with minima of LCOE.

OpEx is the key parameter that drives the maximum shift in optimal point for all the three economic indices. Strike price is the second most influential parameter for IRR sensitivity. The NPV sensitivity conveys a wide range in the optimal capacity density as compared to the LCOE and IRR sensitivity analyses. It is more evident in the optimistic wake model as compared to the conservative wake

model. NPV recommended by the optimistic wake model, IEA37SimpleBastankhahgaussian is exceptionally high for higher values of strike price and estimated extremely low for lower strike prices using the conservative wake model (FugaBlockage). It also shows multiple maxima for a few iterated cases (such as inflation, WACC and no. of operation years), thereby illustrating the possibility of having more than one optimal point or a range of optimal solutions for CD. To investigate the robustness of the result with NPV a simple parameter variation (± 10% of variable parameters) is sufficient in determination of the optimal spacing or capacity density.

In general, optimizing for LCOE and NPV, the optimal capacity density tends to decrease with lower wind resource availability and vice versa. Regions with higher wind speeds and consistent wind patterns can accommodate more wind turbines without compromising performance. The selected site has tremendous potential and higher average wind speed as compared to the offshore locations currently operating in the North Sea. Taking into account the wind resource, projections of inflation, WACC and the company-specific wake model a CD close to 4.76 MW/km^2 is perhaps the best choice for the given site. The payback period for the selected windfarm (having 4.76 MW/km^2 CD) would be 18-20 years (predicted by the conservative and optimistic wake model), assuming the baseline setting with a strike price of 70 €/MWh and no termination of CfDs until at least the stated payback period. Although it is necessary to emphasize here that each site may have its own optimal capacity density based on various factors and input assumptions.

Both NPV and IRR methods are used in conjunction as decision gates for a potential investment, but sometimes conflicts the assessment as observed in many cases within this work. Although a higher IRR is considered favorable, a company may choose a project with a lower IRR, if it is still above the real interest rate. This is due to other intangible benefits such as a broader strategic plan (larger project with a lower IRR generates higher cash flows) or impeding competition that outweighs the lower financial return [17]. Based on a comprehensive analysis of various parameters and their impact on sensitivity, the optimal capacity density is anticipated to lie between 3.62 and 6.05 MW/km^2 for a typical wind farm located in the North Sea. In some extreme cases where the strike prices are below levelized energy cost (50 €/MWh), the optimal capacity density could be as low as 2.64 MW/km^2.

Limitations in the study included validation of cost estimates, wake model and computation requirement for FugaBlockage wake model. The overall cost extrapolated from the ECN studies seem high compared to presently reported cost results because the ECNs in-house cost model is developed based on a nominal power 5-8 MW. Moreover, the empirical constant, superposition models, and wake deficit model implemented in the PyWake code are sourced from public references, with the exception of the look-up table for Fuga and FugaBlockage. To account for the uncertainties associated with the wake model, the final conclusion on the optimum range is primarily focused on the two most widely used wake models in the industry, namely Fuga and TurbOPark.

The open-source tool has limitations on FugaBlockage model when larger number of turbines are employed and is infeasible to simulate considering the computation time. This could be addressed by utilizing the power of cloud computing cloud computing. The power of cloud computing allows for the use of multiple computing resources simultaneously, which can drastically decrease the time required to perform simulations. Additionally, the cloud offers the flexibility to scale resources up or down based on demand, making it a cost-effective solution for simulation projects that require a large amount of computing power. Overall, parallel computing on the cloud is an efficient and effective solution for solving heavy simulation problems.

Recommendations for Future Research

To further evaluate the optimal capacity density of a windfarm, there are several aspects to consider.

Influence of specific power and generator rating on the optimal capacity density

The specific power of a wind turbine is crucial to consider when planning and selecting wind turbines for a wind farm. For the same output power, a different rotor size alters the rotor swept area and, as a result, the specific power of a wind turbine. Turbines with lower power densities, i.e., larger rotors and smaller generators, produce electricity at lower wind speeds, and consequently, the power curve and thrust coefficient characteristics change [40]. Larger rotor diameters can increase the energy output of a wind turbine, up to a certain point. However, they also bring some technical and economic challenges, such as increased loads on the turbine structure, transportation and installation difficulties, and higher costs. The optimal size of the rotor depends on various site-specific factors, and finding the balance between energy production and costs is a key challenge for the wind industry. It would be fascinating to explore how specific power or wind turbine power density influences the optimal capacity density. Alternatively, turbines with different generator ratings may also be considered and the process can be iterated to find the variation.

Implementing use of technical tools and software for layout optimization

The performance and profitability of a wind farm can be improved with a more advanced layout optimization method using powerful software tools. It can aid in maximizing energy production or capacity factor, reducing costs, improving safety, reducing environmental impact, and further help optimize the economic indices, specifically for scenarios with higher capacity densities.

Electricity price hourly variation as a part of the sensitivity analysis

The revenue includes a fixed strike price and a CfD policy mechanism to simplify the calculation of financial metrics. Energy policies and regulations are subject to change, and new policies may replace or supplement CfDs in the future, for example, an auction-based system or feed-in tariffs, as a means of promoting renewable energy deployment. Also, with technological advancements, the cost of generating renewable energy may decrease and become competitive with traditional fossil fuel sources, making subsidiaries less necessary. Although the popularity of CfDs has grown in recent years, it may not be an effective way to understand and evaluate the actual economics of wind. This accentuates the need for understanding electricity price volatility using methods such as historical analysis, market modeling, machine learning, expert judgment, and impact of geopolitical situation or energy crisis.

Regularity frameworks and Spatial planning risk mitigation

A key variable in the economic calculation is adaptation cost or the cost incurred due to spatial planning risk. These expenses arise from adjusting wind farms to meet user requirements or vice versa. For example, wind turbines may need to be shut down during bird migration, "Building with Nature" techniques such as installing scour protection may need to be implemented to encourage the growth of reef-building species, or wind farm design may need to be adapted to accommodate shipping routes. When it comes to minor shipping routes, ships navigate around the wind farm to adjust, whereas, for major lanes, the wind farm's design is adjusted by constructing a shipping lane through the farm. It could also entail movement of a couple of turbines to respect the helicopter zone of an oil & gas platform. These estimates increase the uncertainty range in LCOE, NPV, and IRR,

emphasizing the need to interpret the values relative to one another rather than their absolute value [5],[41].

Effect of rotor tilt in floating offshore wind turbines

Turbines installed in water deeper than 55 meters require floating turbines, which are presently expensive compared to bottom-mounted turbines. This cost difference is anticipated to persist until around 2030 [5]. Although the cost of floating turbines is included in the sensitivity variation when calculating CapEx, these turbines face a significant challenge with reduced power and changes in wake pattern due to the rotor tilt. Tilting the rotor blades can alter the aerodynamic forces acting on them, which can adversely or favorably reflect in power, depending on the specific situation. It is an important aspect of the wake loss calculation and can be incorporated into sensitivity analysis.

Balancing transmission losses and costs through electrical infrastructure improvements

Currently, most offshore wind farms are located near the shore, within 80 km, and are built with alternating current (AC), as it is the most cost-effective option. However, those located further away are typically connected through either an AC booster station or a direct current (DC) connection, which can be expensive. To make wind energy more affordable in isolated remote offshore locations emerging methods such as the hub and spoke (H&S) concept need consideration [5]. Hub and spoke (H&S) concept refers to a system for connecting offshore wind farms to onshore electricity grids using a central hub that acts as a connection point for multiple wind farms. Single cable transmits the electricity to the onshore grid from the "hub" [42]. It can ultimately affect both the transmission cost and losses, and finding a balance between the two parameters could be worth investigating.

Wake losses from neighboring windfarms

When wind farms are planned in clusters can significantly impact each other, leading to turbine interaction losses and increased wake-induced fatigue loads for downstream turbines. This can cause premature damage or reduced lifetimes of the assets and negate any marginal gains, potentially resulting in increased LCOE [8]. As the industry has not experienced this before, it may require several technical innovations to overcome these challenges. The optimal capacity densities of clustered wind farms in North sea can be contextualized as a future work [5].

Automate and cross link PyWake simulation with the sensitivity analysis tool

Implementation of several other PyWake models like Zong Gaussian and Niyaifar could be included in the work. A tool (API: Application Programming Interface) can be developed to automate and ease the process for wind farm developers by cross-linking PyWake simulation with the sensitivity analysis tool.

List of References

[1]   "Dudgeon offshore wind farm officially opened." https://www.equinor.com/news/archive/21nov2017-dudgeon-opening (accessed Nov. 03, 2022).

[2]   "Nine countries pledge to turn the North Sea into Europe's biggest green power plant," *State of Green*, København, Apr. 25, 2023.

[3]   "Ostend declaration of energy ministers on the North Seas as Europe's green power plant," Ostend, Apr. 24, 2023.

[4]   L. Ramirez, "Offshore wind in Europe - key trends and statistics 2022," 2023, p. 53, Accessed: May 15, 2023. [Online]. Available: https://windeurope.org/intelligence-platform/product/offshore-wind-in-europe-key-trends-and-statistics-2022/.

[5]   E. C. M. Ruijgrok, E. J. Van Druten, and B. H. Bulder, "Cost evaluation of north sea offshore wind post 2030," Deventer, 2019. Accessed: May 15, 2023. [Online]. Available: https://northseawindpowerhub.eu/knowledge/cost-evaluation-of-north-sea-offshore-wind-post-2030-towards-spatial-planning-february.

[6]   R. Borrmann, K. Rehfeld, A.-K. Wallasch, and S. Lüers, "Capacity densities of European offshore wind farms," Hamburg, 2018. Accessed: Nov. 03, 2022. [Online]. Available: https://vasab.org/wp-content/uploads/2018/06/BalticLINes_CapacityDensityStudy_June2018-1.pdf.

[7]   W. Vanheusden and B. Baetens, "LCOE offshore wind in the Princess zone (Analysis of various density scenarios)," 2021. [Online]. Available: https://economie.fgov.be/sites/default/files/Files/Energy/LCOE-offshore-wind-in-the-Princess-zone.pdf.

[8]   P. Enevoldsen and M. Z. Jacobson, "Data investigation of installed and output power densities of onshore and offshore wind turbines worldwide," *Energy Sustain. Dev.*, vol. 60, pp. 40–51, Feb. 2021, doi: 10.1016/J.ESD.2020.11.004.

[9]   M. Tauzowski, J. Collins, C. Ribeiro, and A. Cowan, M, "Capacity density offshore wind farms in Europe - Technical challenges and mitigations," Brussels, 2022. Accessed: May 15, 2023. [Online]. Available: https://windeurope.org/tech2022/programme/posters/PO102/.

[10]   S. Mathew, *Wind energy: Fundamentals, resource analysis and economics*. Springer Berlin Heidelberg, 2007.

[11]   H. Bidaoui, I. El Abbassi, A. El Bouardi, and A. Darcherif, "Wind speed data analysis using Weibull and Rayleigh distribution functions, case Study: five cities Northern Morocco," *Procedia Manuf.*, vol. 32, pp. 786–793, Jan. 2019, doi: 10.1016/J.PROMFG.2019.02.286.

[12]   "Offshore Wind Turbine Documentation." https://nrel.github.io/turbine-models/IEA_15MW_240_RWT.html#link-to-tabular-data (accessed Nov. 11, 2022).

[13]   E. Gaertner *et al.*, "Definition of the IEA Wind 15-Megawatt Offshore Reference Wind Turbine Technical Report," 2020. Accessed: May 15, 2023. [Online]. Available: www.nrel.gov/publications.

[14]   M. Martín, L. V. Cremades, and J. M. Santabàrbara, "Analysis and modelling of time series of surface wind speed and direction," *Int. J. Climatol.*, vol. 19, no. 2, pp. 197–209, 1999.

[15]   "Wind farm costs." https://guidetoanoffshorewindfarm.com/wind-farm-costs (accessed May 15, 2023).

[16]   "Interactive guide." https://guidetoanoffshorewindfarm.com/guide (accessed May 15, 2023).

[17]   J. Fernando, W. Kenton, A. Hayes, and C. Majaski, "Corporate finance," 2023. https://www.investopedia.com/terms/c/capitalexpenditure.asp#toc-what-are-capital-expenditures-capex (accessed May 15, 2023).

[18]   A. Dalla Riva *et al.*, "Wind Technology, Cost, and Performance Trends in Denmark, Germany, Ireland, Norway, Sweden, the European Union, and the United States: 2008-2016," 2018.

Accessed: May 15, 2023. [Online]. Available: https://www.nrel.gov/docs/fy19osti/71844.pdf.

[19] "Policy paper - Contracts for Difference," 2022. https://www.gov.uk/government/publications/contracts-for-difference/contract-for-difference (accessed May 15, 2023).

[20] "The CFD Scheme." https://www.lowcarboncontracts.uk/the-cfd-scheme (accessed May 15, 2023).

[21] M. David *et al.*, "Offshore Wind-Opportunities for the Norwegian Industry," Oslp, 2020. Accessed: May 15, 2023. [Online]. Available: https://www.regjeringen.no/contentassets/07635c56b2824103909fab5f31f81469/offshore-wind-opportunities-for-the-norwegian-industry.pdf.

[22] G. Brindley, L. Ramirez, P. Tardieu, and C. Zipf, "Financing and investment trends 2021," 2021, p. 32, Accessed: May 15, 2023. [Online]. Available: https://windeurope.org/intelligence-platform/product/financing-and-investment-trends-2021-webinar/.

[23] D. Annas and P. Karlsson, "Norwegian Renewable Energy Producer Statkraft AS Upgraded To 'A' Amid Elevated Power Prices; Outlook Stable," p. 10, 2022, Accessed: May 15, 2023. [Online]. Available: www.spglobal.com/ratingsdirect.

[24] O. K. Helgesen, M. Aanestad, and M. Holter, "World's largest offshore wind farm 'unprofitable' for Equinor, say government-funded researchers," Stavanger and Oslo, Nov. 24, 2021.

[25] C. Richard, "Offshore wind leaders warn CfD changes may be needed as UK sector grows," *Windpower Monthly*, London, Sep. 29, 2021.

[26] S. P. PRATT and R. J. GRABOWSKI, "Weighted Average Cost of Capital," in *Cost of Capital Applications and Examples*, John Wiley & Sons, Inc., p. 794.

[27] E. F. Brigham and J. F. Houston, *Fundamentals of Financial Management*, Eleventh E. Thomson South-Western, 2007.

[28] M. H. Hansen and O. C. Handegård, "Historical development and outlook of offshore wind. Dudgeon Offshore Wind Farm case study.," uis, 2022.

[29] J. Berk *et al.*, *Corporate Finance*, Third. Pearson Education, 2017.

[30] "Inflation, consumer prices (annual %) - Norway." https://data.worldbank.org/indicator/FP.CPI.TOTL.ZG?end=2021&locations=NO&start=1960&view=chart (accessed May 15, 2023).

[31] A. O'Neill, "Norway - Inflation rate 2028." Statista, 2023, Accessed: May 15, 2023. [Online]. Available: https://www.statista.com/statistics/327359/inflation-rate-in-norway/.

[32] "Valuation - Net Present Value (NPV), Internal Rate of Return (IRR) ; Economics - Fisher Equation." Corporate Finance Institute, 2023, Accessed: May 15, 2023. [Online]. Available: https://corporatefinanceinstitute.com/resources/valuation/net-present-value-npv/.

[33] "Simple Levelized Cost of Energy (LCOE) Calculator Documentation." National Renewable Energy Laboratory, Accessed: May 15, 2023. [Online]. Available: https://www.nrel.gov/analysis/tech-lcoe-documentation.html.

[34] W. Short, D. J. Packey, and T. Holt, "A Manual for the Economic Evaluation of Energy Efficiency and Renewable Energy Technologies," Colorado, 1995. Accessed: May 15, 2023. [Online]. Available: https://www.nrel.gov/docs/legosti/old/5173.pdf.

[35] B. . Bulder, G. Bedon, and E. T. . Bot, "Optimal wind farm power density analysis for future offshore wind farms," Netherlands, 2018. Accessed: Nov. 10, 2022. [Online]. Available: https://www.humsterlandenergie.nl/resources/LInks-duurzaam/Linkpagina/Optimal-wind-farm-power-density-analysis-for-future-offshore-wind-farms.pdf.

[36] "Annual report and Form 20-F- Equinor," 2021. Accessed: May 15, 2023. [Online]. Available: https://www.equinor.com/investors/annual-reports.

[37] "Inflation rates in Norway." https://www.worlddata.info/europe/norway/inflation-rates.php (accessed May 15, 2023).

[38] "PyWake 2.4.0," 2018. https://topfarm.pages.windenergy.dtu.dk/PyWake/index.html

(accessed Nov. 03, 2022).

[39]   R. Lacal-Arántegui, J. M. Yusta, and J. A. Domínguez-Navarro, "Offshore wind installation: Analysing the evidence behind improvements in installation time," *Renew. Sustain. Energy Rev.*, vol. 92, pp. 133–145, Sep. 2018, doi: 10.1016/J.RSER.2018.04.044.

[40]   L. Hartman, "Wind Turbines: the Bigger, the Better | Department of Energy," *U.S. Department of Energy, Office of Energy Efficiency and Renewable Energy, operated by the Alliance for Sustainable Energy LLC*, 2022. https://www.energy.gov/eere/articles/wind-turbines-bigger-better (accessed May 15, 2023).

[41]   J. F. FeyertagI and B. Bowie, "The financial costs of mitigating social risks: costs and effectiveness of risk mitigation strategies for emerging market investors.," london, 2021. doi: 10.4324/9781003139614-39.

[42]   "Hub-and-spoke," *North Sea Wind Power Hub*. https://northseawindpowerhub.eu/key-concepts (accessed May 15, 2023).

[43]   "Resource your source for renewable energy information," *Int. Renew. Energy Agency*, p. 14, 2015, Accessed: May 15, 2023. [Online]. Available: https://dashboard.irena.org/download/methodology.pdf.

9. Appendices

Wind distribution

Table 12 Wind distribution according to sectors at reference height 160m

SN	Probability Distribution F (%)	scale factor (c) A (m/s)	shape factor (k) k	Mean wind speed (m/s)
Mean	100	11.227	1.9921	9.95
N	7.326	9.643	1.9632	8.55
NNE	7.836	9.384	2.2272	8.311
ENE	7.889	9.339	2.3788	8.278
E	6.81	9.397	2.2792	8.325
ESE	6.369	9.846	2.1247	8.72
SSE	6.02	10.147	2.101	8.987
S	7.038	11.273	1.9157	10
SSW	13.04	14.212	2.1953	12.586
WSW	12.658	13.567	2.2486	12.017
W	9.54	12.283	2.0915	10.879
WNW	7.703	10.804	1.9564	9.579
NNW	7.77	10.379	2.0259	9.196

Hexagonal layout
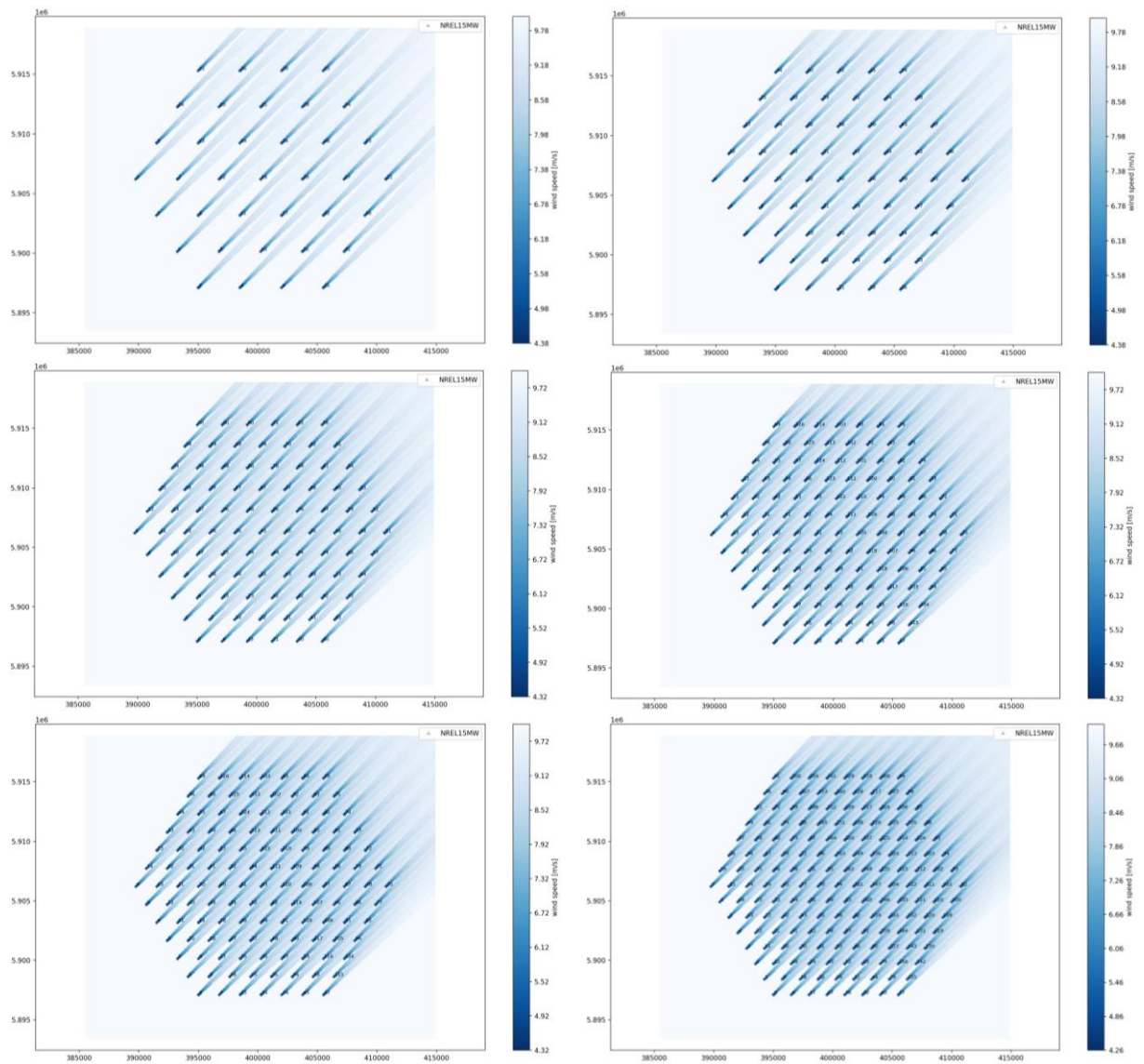
Figure 9.1 Different capacity density scenarios with Hexagonal layout

Sensitivity analysis tool

Figure 9.2 Sensitivity analysis tool

PyWake simulation Results with Trapezoidal layout

Table 13 PyWake simulation Results for capacity factor using different capacity density and windspeeds[12]

Wind Resource Increment (%)	Capacity Density	NOJ_CF	NOJlocal_CF	TurboNOJ_CF	BastankhahGaussian_CF	IEA37SBG _CF	TurboGaussian_CF	Fuga_CF	FugaBlockage_CF
-30	12.78	0.272737151	0.254830292	0.249897828	0.290184549	0.306550694	0.248057265	0.224558679	0.205128
-30	10.86	0.284313434	0.268951566	0.26610082	0.301188383	0.314639702	0.260399193	0.240876546	0.229828
-30	9.10	0.295821562	0.283306648	0.282030991	0.311729321	0.32251347	0.273237459	0.257784985	0.255307
-30	7.50	0.307146407	0.297509697	0.297389312	0.321753883	0.330122043	0.286504963	0.274919348	0.272667
-30	6.05	0.318151289	0.311212328	0.311804455	0.331076904	0.337332963	0.300020963	0.291893195	0.290038
-30	4.76	0.328660235	0.324049549	0.324995719	0.339613259	0.344034194	0.313506337	0.308143125	0.306726048
-30	3.62	0.338514366	0.33578598	0.336766922	0.347249724	0.350169121	0.326605316	0.323261378	0.322309857
-30	2.64	0.347439047	0.345890381	0.34676268	0.353865425	0.355636164	0.338532649	0.336476662	0.33583904
-30	1.81	0.355078762	0.354237681	0.354899283	0.359342022	0.360264651	0.348987754	0.347651618	0.347300224
-30	1.14	0.3611436	0.360774984	0.361079634	0.363505944	0.363908097	0.35724281	0.356454219	0.35645051
-30	0.62	0.365330997	0.365217299	0.365235875	0.366288542	0.366397641	0.363269085	0.362870644	0.362870644
-25	12.78	0.3140549	0.295227705	0.289772268	0.332046529	0.349680588	0.287248946	0.261899007	0.261899007
-25	10.86	0.326264942	0.310192742	0.307030888	0.343694582	0.358126745	0.300418147	0.2795203	0.2795203
-25	9.10	0.338362659	0.325325669	0.323891876	0.354809363	0.366327412	0.314052274	0.2976436	0.2976436
-25	7.50	0.35022173	0.340223557	0.340047597	0.365339202	0.374233529	0.328082426	0.315878859	0.315878859
-25	6.05	0.361711607	0.35452685	0.355131628	0.375085989	0.381705187	0.342310994	0.333825024	0.333825024
-25	4.76	0.372643412	0.367875838	0.368867962	0.383973248	0.388627247	0.356456668	0.350911331	0.349442479
-25	3.62	0.382867995	0.380044759	0.381074938	0.391892932	0.394949833	0.370155373	0.366732246	0.365750412
-25	2.64	0.392098446	0.390492766	0.391408077	0.39872901	0.400572985	0.382607842	0.380518767	0.379863705
-25	1.81	0.399977042	0.3991048	0.399793485	0.404368347	0.405323598	0.393501633	0.392147909	0.391787878
-25	1.14	0.40621654	0.405835116	0.406149049	0.40864284	0.409057748	0.40209345	0.401297042	0.401293238
-25	0.62	0.410513306	0.410395938	0.410413945	0.411492472	0.411604051	0.40835279	0.407950461	0.407950461
-20	12.78	0.354509714	0.335103579	0.329220098	0.372720802	0.391325719	0.326035641	0.299264149	0.299264149
-20	10.86	0.36714045	0.350649022	0.347232847	0.384816527	0.399982514	0.33980812	0.317897204	0.317897204
-20	9.10	0.379617397	0.366293158	0.364728403	0.396316068	0.408368102	0.354004546	0.336928329	0.336928329
-20	7.50	0.391804764	0.381623887	0.38139743	0.407170686	0.416434989	0.368556094	0.35595087	0.35595087
-20	6.05	0.40358056	0.396277756	0.396885932	0.417173739	0.424038845	0.383252323	0.374558285	0.374558285
-20	4.76	0.414746524	0.409906568	0.410927978	0.426259126	0.431063343	0.397814828	0.392184348	0.390688655
-20	3.62	0.425165733	0.422297773	0.42335949	0.434326004	0.437466073	0.411877477	0.408433857	0.407438307
-20	2.64	0.434543728	0.432909688	0.43385217	0.441265449	0.443150088	0.424640404	0.422553357	0.421891818
-20	1.81	0.442526839	0.441638983	0.442343021	0.446971603	0.447942791	0.435784856	0.434436087	0.434073414
-20	1.14	0.448835132	0.448447684	0.448765731	0.451284487	0.451704944	0.4445647	0.443773675	0.443769841
-20	0.62	0.45316882	0.453049886	0.453067154	0.454153344	0.454265527	0.450948539	0.450548975	0.450548975
-15	12.78	0.393555326	0.373869562	0.367655133	0.41171787	0.431010077	0.363857732	0.336075953	0.336075953
-15	10.86	0.406417041	0.389757166	0.386144731	0.424083895	0.439751115	0.378026066	0.355439418	0.355439418
-15	9.10	0.419087783	0.405675443	0.404007979	0.43579965	0.448200187	0.392571888	0.375089614	0.375089614
-15	7.50	0.431424183	0.421209961	0.420939562	0.446820186	0.456311847	0.407428033	0.394611551	0.394611551
-15	6.05	0.443314314	0.435999261	0.436603222	0.456934363	0.463939949	0.422375148	0.413601074	0.413601074
-15	4.76	0.454553785	0.449710944	0.450746802	0.466087352	0.47096855	0.437141554	0.431505767	0.430004252

---

[12] The capacity factor reported for the FugaBlockage model, when the capacity density ≥ 6.05 MW/km², is directly sourced from Fuga except for the case with wind resource -30%, -10%, 0%, and 10%. This is due to computation time and memory requirements. the capacity factor using FugaBlockage model for rest of the cases is expected to be higher than what is presented in the table.

-15	3.62	0.46501922	0.46214777	0.463225263	0.474186794	0.477362837	0.451364106	0.447946551	0.446951036
-15	2.64	0.474412807	0.47277412	0.473729719	0.481132299	0.483029829	0.464252935	0.462194988	0.46153591
-15	1.81	0.482389545	0.481498988	0.482208237	0.486826523	0.487799704	0.475487534	0.474160949	0.473800469
-15	1.14	0.488680066	0.488292195	0.488610022	0.491119254	0.491539322	0.484328968	0.483553276	0.483549463
-15	0.62	0.492992048	0.492873265	0.492889676	0.49396894	0.494080231	0.49074565	0.490353858	0.490353858
-10	12.78	0.430781721	0.411066921	0.404614426	0.448685049	0.468406061	0.400270842	0.371853247	0.354846
-10	10.86	0.443712443	0.427090497	0.423337169	0.461167562	0.477126752	0.414651191	0.391688433	0.381947
-10	9.10	0.456420185	0.443081109	0.441338086	0.472955182	0.485539684	0.429360467	0.411698344	0.408893
-10	7.50	0.468755897	0.458627571	0.458320287	0.484007324	0.493601777	0.444334377	0.431466885	0.428988
-10	6.05	0.480618468	0.473374924	0.47396857	0.494111848	0.501167196	0.459348227	0.450598561	0.448604
-10	4.76	0.491800228	0.487009172	0.488046771	0.503225401	0.508121612	0.474139732	0.468561451	0.467071108
-10	3.62	0.502191761	0.499349287	0.500429102	0.511264745	0.514437521	0.488352616	0.484996301	0.484011739
-10	2.64	0.511495426	0.509870896	0.510827679	0.518138741	0.520026492	0.501214968	0.499205906	0.49855627
-10	1.81	0.519378103	0.518495116	0.519201183	0.523759116	0.524723139	0.512408141	0.511116193	0.510761638
-10	1.14	0.52558306	0.525199191	0.52551332	0.527986239	0.528401236	0.521208001	0.520454705	0.520450953
-10	0.62	0.529827922	0.529710629	0.529726113	0.530787262	0.530896519	0.527583307	0.527202835	0.527202835
-9	12.78	0.437980551	0.418285661	0.411796017	0.455811515	0.475589983	0.407352285	0.378848444	0.378848444
-9	10.86	0.45090817	0.434314711	0.430539425	0.46830106	0.484295949	0.421755308	0.398749487	0.398749487
-9	9.10	0.463607067	0.450298792	0.448543717	0.480087934	0.492691572	0.43647753	0.418803255	0.418803255
-9	7.50	0.475927275	0.465827923	0.465514106	0.491132473	0.50073427	0.451455349	0.438594185	0.438594185
-9	6.05	0.487769883	0.480548872	0.481139848	0.501222699	0.508278484	0.466463387	0.457729122	0.457729122
-9	4.76	0.498926865	0.494151514	0.495188133	0.510317532	0.515210328	0.481241473	0.475680837	0.47419443
-9	3.62	0.509291586	0.506458088	0.507536966	0.518335588	0.5215037	0.495435074	0.49209433	0.491113036
-9	2.64	0.518566805	0.516946959	0.517902743	0.525187609	0.527071122	0.508276619	0.506279145	0.505632077
-9	1.81	0.526422053	0.525541595	0.526246173	0.53078716	0.531748246	0.519448189	0.518164296	0.517811287
-9	1.14	0.53260329	0.532220656	0.5325337	0.534996763	0.535410286	0.528229333	0.527481144	0.527477408
-9	0.62	0.536830342	0.536713476	0.53672877	0.537785224	0.537893965	0.534588927	0.534211035	0.534211035
-8	12.78	0.445092328	0.425425022	0.41890154	0.462845026	0.482672136	0.414360837	0.385783465	0.385783465
-8	10.86	0.458011741	0.441452952	0.43765767	0.475336645	0.491360211	0.428780466	0.405741468	0.405741468
-8	9.10	0.470696909	0.457424176	0.455658016	0.487118195	0.499735543	0.443509606	0.42583041	0.42583041
-8	7.50	0.482997024	0.472930081	0.472610008	0.498150942	0.507756054	0.458485371	0.445635488	0.445635488
-8	6.05	0.494815374	0.487619285	0.488207413	0.508223184	0.515276525	0.473481823	0.464766062	0.464766062
-8	4.76	0.505943673	0.501185574	0.502220811	0.517296091	0.522183546	0.488240962	0.482699749	0.481217776
-8	3.62	0.516278049	0.513454447	0.514531966	0.525290137	0.528452392	0.502410109	0.499085871	0.498108158
-8	2.64	0.525521769	0.523907146	0.524861557	0.532117951	0.533996551	0.515226236	0.513240851	0.512596547
-8	1.81	0.53334709	0.532469456	0.53317229	0.537694927	0.538652753	0.526372263	0.525096733	0.524745371
-8	1.14	0.539502702	0.539121428	0.539433285	0.541885748	0.542297665	0.535131619	0.534388708	0.534384989
-8	0.62	0.543710685	0.543594285	0.543609387	0.544660841	0.544769035	0.541473317	0.54109809	0.54109809
-7	12.78	0.452115219	0.432482798	0.425928707	0.469784124	0.489651337	0.421294249	0.39265566	0.39265566
-7	10.86	0.465021542	0.448503285	0.444689921	0.482273056	0.498318512	0.435724637	0.412661987	0.412661987
-7	9.10	0.477688322	0.464455607	0.462679307	0.494044899	0.506670726	0.450454899	0.432777715	0.432777715
-7	7.50	0.489963975	0.479932675	0.479606617	0.505061855	0.514666409	0.465422895	0.452589016	0.452589016
-7	6.05	0.501753988	0.494585065	0.495170177	0.515112602	0.522160741	0.480402241	0.471707922	0.471707922
-7	4.76	0.512849903	0.508110507	0.50914398	0.524160545	0.52904082	0.495137165	0.489617041	0.488139975
-7	3.62	0.523150593	0.520337752	0.521413508	0.532128011	0.535283275	0.509276935	0.505970073	0.504996236
-7	2.64	0.532359937	0.530751044	0.531703729	0.538929512	0.540802563	0.522063267	0.520090428	0.51944907
-7	1.81	0.540152984	0.539278452	0.539979302	0.544482272	0.545436535	0.533180012	0.531913127	0.531563509
-7	1.14	0.546281185	0.54590139	0.546211966	0.548653131	0.549063318	0.541914672	0.541177191	0.54117349

-7	0.62	0.550468926	0.550353026	0.550367936	0.551414104	0.551521723	0.548236408	0.547863922	0.547863922
-6	12.78	0.45904751	0.439456915	0.432875358	0.476627462	0.496526514	0.428150392	0.399462492	0.399462492
-6	10.86	0.471936081	0.455463904	0.451634319	0.489109141	0.505169937	0.442585911	0.419508777	0.419508777
-6	9.10	0.484580029	0.471391557	0.469606035	0.500867081	0.513496355	0.45731173	0.439643197	0.439643197
-6	7.50	0.496827066	0.48683445	0.486502676	0.511864434	0.521464715	0.472266486	0.459453107	0.459453107
-6	6.05	0.508584875	0.501445222	0.502027161	0.521890352	0.52893065	0.487223456	0.478553357	0.478553357
-6	4.76	0.519644906	0.514925574	0.515956914	0.530910453	0.535781796	0.501929146	0.496431675	0.49495996
-6	3.62	0.529908758	0.527107489	0.528181096	0.538848913	0.541996109	0.516034865	0.512746184	0.511776499
-6	2.64	0.539081019	0.537478332	0.538428954	0.545622124	0.547489024	0.528787246	0.526827373	0.526189132
-6	1.81	0.54683959	0.545968422	0.54666706	0.551149131	0.552099545	0.53987117	0.538613185	0.5382654
-6	1.14	0.552938708	0.552560504	0.552869709	0.555298927	0.555707266	0.548578383	0.54784647	0.547842789
-6	0.62	0.557105112	0.556989746	0.557004462	0.558045079	0.558152097	0.554878206	0.554508531	0.554508531
-5	12.78	0.465887607	0.446345421	0.439739455	0.483373798	0.503296701	0.434927253	0.406201541	0.406201541
-5	10.86	0.478753977	0.462333123	0.458489127	0.495843848	0.511913668	0.449362488	0.426279684	0.426279684
-5	9.10	0.491370863	0.478230612	0.47643676	0.507583879	0.520211762	0.464078531	0.446424998	0.446424998
-5	7.50	0.503585343	0.493634262	0.493297036	0.518557995	0.528150446	0.479014814	0.46622621	0.46622621
-5	6.05	0.515307281	0.508198871	0.508777489	0.528555922	0.535585859	0.493944383	0.485301129	0.485301129
-5	4.76	0.526328124	0.521630128	0.522658987	0.53754546	0.542406203	0.508616067	0.503142709	0.501676766
-5	3.62	0.536552168	0.53376323	0.534834322	0.54545263	0.548590737	0.522683299	0.519413541	0.518448268
-5	2.64	0.545684805	0.544088771	0.545037007	0.552195696	0.554055875	0.535397794	0.533451268	0.532816304
-5	1.81	0.553406838	0.552539279	0.55323549	0.557695511	0.558641809	0.546445548	0.545196695	0.544850827
-5	1.14	0.559475315	0.559098804	0.559406555	0.561823219	0.562229602	0.555122716	0.554396496	0.554392835
-5	0.62	0.56361936	0.563504558	0.563519081	0.564553902	0.564660293	0.561398788	0.561031986	0.561031986
-4	12.78	0.472634028	0.453146488	0.446519082	0.490021988	0.509961028	0.441622928	0.412870497	0.412870497
-4	10.86	0.485473958	0.469109377	0.465252722	0.502476221	0.518548984	0.456052679	0.432972669	0.432972669
-4	9.10	0.498059761	0.48497147	0.483170156	0.514194519	0.526816366	0.470753837	0.453121369	0.453121369
-4	7.50	0.510237945	0.500331071	0.499988653	0.525141944	0.534723158	0.485666649	0.472906881	0.472906881
-4	6.05	0.521920548	0.514845224	0.515420381	0.535108881	0.542126054	0.500564034	0.491950096	0.491950096
-4	4.76	0.532899086	0.528223614	0.529249659	0.54406529	0.54891385	0.515197179	0.509749299	0.508289521
-4	3.62	0.543080528	0.54030463	0.54137286	0.551939021	0.555067074	0.52922172	0.525971569	0.525010951
-4	2.64	0.55217116	0.550582196	0.551527742	0.558650204	0.560503128	0.541894606	0.539961773	0.539330236
-4	1.81	0.559854727	0.558991008	0.559684588	0.564121488	0.565063417	0.55290303	0.551663519	0.551319644
-4	1.14	0.565891109	0.565516389	0.565822608	0.568226155	0.568630478	0.561547702	0.560827287	0.560823646
-4	0.62	0.570011849	0.56989764	0.569911969	0.570940765	0.571046508	0.567798295	0.567434422	0.567434422
-3	12.78	0.479285398	0.459858404	0.453212437	0.496570983	0.516518721	0.44823562	0.419467158	0.419467158
-3	10.86	0.492094853	0.475791206	0.471923596	0.509005395	0.525075252	0.4626549	0.4395858	0.4395858
-3	9.10	0.504645756	0.491612935	0.489804999	0.520698317	0.533309674	0.477336285	0.459730668	0.459730668
-3	7.50	0.516784105	0.506923936	0.50657658	0.531615767	0.54118249	0.492220858	0.479493778	0.479493778
-3	6.05	0.5284241	0.521383582	0.521955148	0.541548879	0.548550999	0.507081509	0.498499218	0.498499218
-3	4.76	0.539357401	0.534705561	0.535728475	0.550469739	0.555304612	0.521671816	0.516250686	0.514797444
-3	3.62	0.54949362	0.546731423	0.547796457	0.558308016	0.561425102	0.53564969	0.532419775	0.531464038
-3	2.64	0.558540015	0.556958514	0.55790108	0.564985692	0.566830857	0.54827745	0.546358624	0.545730651
-3	1.81	0.566183322	0.565323657	0.566014414	0.570427197	0.571364523	0.559243565	0.558013582	0.557671773
-3	1.14	0.572186257	0.571813419	0.572118031	0.574507938	0.574910107	0.567853434	0.567138921	0.567135302
-3	0.62	0.576282815	0.576169224	0.576183359	0.577205922	0.577310994	0.574076922	0.573716028	0.573716028
-2	12.78	0.485840443	0.46647957	0.459817832	0.503019821	0.522969093	0.454763637	0.425989434	0.425989434
-2	10.86	0.498615592	0.482377264	0.478500343	0.515430591	0.531491924	0.469167665	0.446117251	0.446117251
-2	9.10	0.511127974	0.49815391	0.496340167	0.527094668	0.53969127	0.48382461	0.466251357	0.466251357

76

-2	7.50	0.523223144	0.51341201	0.513059966	0.537979031	0.547528156	0.498676402	0.485985657	0.485985657
-2	6.05	0.534817445	0.527813334	0.52838119	0.547875639	0.554860528	0.513495997	0.504947541	0.504947541
-2	4.76	0.545702755	0.541075574	0.542095057	0.556758672	0.561578435	0.528039394	0.522646197	0.521199838
-2	3.62	0.555791291	0.55304341	0.554104936	0.564559607	0.567664866	0.541966845	0.53875774	0.537807096
-2	2.64	0.564791369	0.563217694	0.564157007	0.57120226	0.573039194	0.554546161	0.552641624	0.552017343
-2	1.81	0.572392743	0.571537333	0.572225087	0.576612827	0.577545331	0.565467161	0.564246875	0.563907197
-2	1.14	0.578360978	0.577990106	0.578293044	0.580668828	0.581068754	0.574040059	0.573331536	0.573327939
-2	0.62	0.582432543	0.582319596	0.582333538	0.583349671	0.583454054	0.580234921	0.579877049	0.579877049
-1	12.78	0.492297991	0.473008494	0.466333685	0.50936763	0.529311541	0.46120539	0.432435335	0.432435335
-1	10.86	0.505035196	0.488866304	0.484981665	0.521751113	0.537798531	0.475589591	0.452565302	0.452565302
-1	9.10	0.517505631	0.504593398	0.502774636	0.533383046	0.545960814	0.490217639	0.472681997	0.472681997
-1	7.50	0.529554465	0.519794534	0.519438046	0.544231372	0.553759939	0.505032328	0.492381368	0.492381368
-1	6.05	0.541100168	0.534133951	0.534697983	0.554088949	0.56105454	0.519806768	0.511294201	0.511294201
-1	4.76	0.551934901	0.547333334	0.548349101	0.562932018	0.567735324	0.534299404	0.528935236	0.527496084
-1	3.62	0.561973455	0.559240462	0.560298181	0.570693845	0.573786465	0.548172888	0.544985116	0.544039762
-1	2.64	0.570925277	0.569359767	0.570295567	0.577300065	0.579128325	0.560700637	0.558810639	0.558190169
-1	1.81	0.578483166	0.577632197	0.578316779	0.582678622	0.583606098	0.571573887	0.570363445	0.570025958
-1	1.14	0.584415543	0.584046714	0.584347914	0.586709128	0.58710673	0.580107779	0.579405321	0.579401746
-1	0.62	0.588461368	0.588349087	0.588362835	0.589372362	0.589476037	0.586272588	0.585917776	0.585917776
0	12.78	0.498656963	0.479443792	0.472758522	0.515613618	0.535545541	0.467559385	0.438802977	0.423869359
0	10.86	0.511352778	0.495257181	0.491366361	0.527966341	0.543994676	0.481919385	0.458928334	0.450323468
0	9.10	0.523778024	0.510930492	0.509107473	0.539563002	0.552118035	0.49651429	0.479021247	0.476249
0	7.50	0.535777549	0.526070837	0.525710144	0.5503725	0.559877688	0.511287769	0.498679852	0.496257
0	6.05	0.547271925	0.54034498	0.540905085	0.560188666	0.567132996	0.526013172	0.517538418	0.515606
0	4.76	0.558053661	0.553478591	0.554490373	0.568989766	0.573775342	0.540451409	0.535117284	0.533685643
0	3.62	0.568040087	0.56532251	0.566376142	0.576710836	0.579790056	0.554267587	0.551101626	0.550161742
0	2.64	0.576941848	0.57538482	0.576316862	0.583279315	0.585098486	0.566740832	0.564865597	0.564249047
0	1.81	0.584454817	0.583608463	0.584289713	0.588624869	0.589547128	0.577563859	0.576363391	0.576028152
0	1.14	0.590350265	0.589983553	0.590282955	0.592629188	0.593024391	0.58605684	0.585360511	0.585356961
0	0.62	0.594369664	0.59425807	0.594271626	0.595274384	0.595377335	0.592190265	0.591838546	0.591838546
1	12.78	0.504916373	0.485784182	0.47909097	0.521757072	0.541670645	0.473824227	0.44509058	0.44509058
1	10.86	0.517567537	0.501548843	0.497653327	0.534075732	0.550080039	0.48815585	0.465204824	0.465204824
1	9.10	0.529944535	0.517164375	0.515337834	0.545634152	0.558162731	0.502713568	0.485267859	0.485267859
1	7.50	0.541891952	0.532240326	0.53187566	0.556402187	0.565881316	0.517441939	0.504880139	0.504880139
1	6.05	0.55333244	0.546446042	0.547002123	0.566174705	0.573095914	0.532114632	0.523679491	0.523679491
1	4.76	0.564058919	0.559511161	0.560518704	0.57493196	0.579698605	0.546495039	0.541191896	0.539768046
1	3.62	0.573991217	0.571289545	0.572338824	0.582610739	0.585675843	0.560250774	0.557107052	0.556172809
1	2.64	0.582841244	0.58129299	0.582221045	0.589140263	0.590949959	0.572666757	0.570806482	0.570193953
1	1.81	0.590307966	0.589466389	0.590144158	0.594451901	0.595368768	0.583437246	0.582246866	0.581913924
1	1.14	0.596165502	0.595800974	0.596098524	0.5984294	0.598822132	0.591887535	0.591197391	0.591193864
1	0.62	0.600157848	0.60004696	0.600060324	0.601056164	0.601158378	0.597988335	0.597639737	0.597639737
2	12.78	0.511075323	0.492028478	0.485329755	0.527797356	0.547686479	0.479998614	0.45129646	0.45129646
2	10.86	0.523678753	0.507740335	0.503841551	0.540078814	0.556054363	0.494297875	0.471393349	0.471393349
2	9.10	0.536004622	0.523294316	0.521464962	0.551596183	0.564094763	0.508814564	0.491420678	0.491420678
2	7.50	0.547897303	0.538302489	0.537934078	0.562320268	0.571770793	0.52349413	0.510981344	0.510981344
2	6.05	0.559281505	0.552436829	0.552988798	0.572047038	0.578943369	0.538110645	0.529716796	0.529716796
2	4.76	0.569950619	0.565430922	0.566433986	0.580758696	0.585505279	0.552429992	0.547158693	0.545742898
2	3.62	0.579826929	0.577141613	0.57818629	0.588393759	0.591444076	0.566122337	0.563001242	0.562072794

2	2.64	0.588623677	0.587084465	0.588008316	0.594883207	0.596683067	0.578478476	0.576633332	0.576024915
2	1.81	0.59604293	0.595206277	0.595880427	0.600160091	0.601071402	0.589194263	0.588014066	0.587683469
2	1.14	0.601861652	0.60149937	0.601795016	0.604110191	0.604500389	0.597600197	0.596916284	0.596912782
2	0.62	0.605826372	0.605716208	0.60572938	0.606718168	0.606819631	0.603667218	0.603321764	0.603321764
3	12.78	0.517133002	0.498175593	0.491473702	0.533733907	0.553592735	0.486081336	0.457419034	0.457419034
3	10.86	0.52968579	0.513830788	0.509930114	0.545975185	0.561917457	0.500344439	0.47749258	0.47749258
3	9.10	0.541957815	0.529319665	0.527488182	0.557448845	0.56991405	0.514816448	0.497478637	0.497478637
3	7.50	0.553793297	0.544256886	0.543884952	0.568126639	0.577546146	0.529443713	0.516982661	0.516982661
3	6.05	0.565118974	0.558317099	0.558864874	0.577805693	0.584675485	0.544000776	0.535649784	0.535649784
3	4.76	0.575728761	0.571237813	0.572236172	0.586470121	0.59119558	0.558256027	0.553017364	0.551609867
3	3.62	0.58554736	0.582878813	0.583918652	0.594060148	0.59709505	0.57188222	0.568784098	0.56786159
3	2.64	0.594289399	0.59275948	0.593678923	0.600508487	0.602298177	0.5841761	0.582346235	0.581742013
3	1.81	0.601660062	0.600828472	0.601498873	0.605749849	0.606655455	0.594835167	0.593665236	0.593337025
3	1.14	0.607439147	0.607079168	0.607372865	0.609672025	0.61005963	0.603195199	0.602517554	0.602514076
3	0.62	0.611375722	0.611266299	0.61127928	0.612260894	0.612361593	0.609227369	0.608885078	0.608885078
4	12.78	0.523088681	0.504224533	0.497521727	0.539566234	0.559389174	0.492071271	0.463456815	0.463456815
4	10.86	0.535588088	0.519819422	0.515918181	0.551764508	0.567669194	0.506294604	0.483501279	0.483501279
4	9.10	0.54780372	0.535239853	0.533406899	0.56319195	0.575620571	0.520718473	0.503440757	0.503440757
4	7.50	0.559579696	0.550103151	0.549727909	0.573821251	0.583207454	0.535290129	0.522883368	0.522883368
4	6.05	0.570844758	0.564086674	0.564630182	0.58345075	0.590292436	0.549784661	0.54147798	0.54147798
4	4.76	0.581393398	0.576931828	0.57792527	0.59206643	0.596769766	0.563972965	0.558767661	0.557368687
4	3.62	0.591152691	0.588501293	0.589536074	0.599610198	0.602629101	0.577530423	0.574455581	0.573539143
4	2.64	0.599838711	0.598318313	0.599233157	0.606016481	0.607795692	0.589759788	0.587945328	0.587345379
4	1.81	0.607159758	0.606333358	0.606999888	0.611221623	0.612121385	0.600360256	0.599200658	0.598874872
4	1.14	0.612898458	0.612540832	0.612832537	0.615115399	0.615500357	0.608672949	0.608001601	0.607998149
4	0.62	0.616806417	0.616697748	0.61671054	0.61768487	0.617784796	0.614669278	0.614330164	0.614330164
5	12.78	0.528941712	0.510174393	0.50347284	0.545293913	0.565075619	0.497967387	0.469408412	0.469408412
5	10.86	0.541385159	0.525705538	0.521805004	0.557446511	0.573309505	0.512147517	0.489418301	0.489418301
5	9.10	0.553542009	0.541054386	0.539220595	0.568825369	0.58121436	0.526519966	0.509306142	0.509306142
5	7.50	0.565256326	0.555840986	0.555462647	0.579404112	0.588754849	0.541032892	0.528682818	0.528682818
5	6.05	0.576458829	0.569745439	0.570284612	0.588982339	0.595794443	0.555461995	0.547200974	0.547200974
5	4.76	0.586944635	0.582513016	0.583501342	0.597547861	0.60222814	0.569580682	0.564409399	0.563019154
5	3.62	0.596643154	0.59400925	0.595038766	0.605044246	0.608046604	0.583066994	0.580015704	0.579105456
5	2.64	0.605271949	0.603761283	0.60467135	0.611407606	0.613176049	0.595229746	0.593430795	0.592835186
5	1.81	0.612542448	0.611721352	0.612383902	0.616575893	0.617469685	0.60576987	0.60462066	0.604297331
5	1.14	0.618240083	0.61788486	0.618174534	0.620440841	0.620823103	0.614033893	0.613368863	0.613365437
5	0.62	0.622119005	0.622011105	0.622023708	0.622990657	0.623089799	0.619993464	0.619657539	0.619657539
6	12.78	0.534691523	0.516024359	0.50932614	0.550916589	0.570651957	0.503768734	0.475272525	0.475272525
6	10.86	0.547076593	0.531488522	0.527589915	0.563020985	0.578838377	0.517902402	0.495242586	0.495242586
6	9.10	0.559172421	0.546762847	0.544928825	0.574349032	0.586695503	0.53222033	0.515073981	0.515073981
6	7.50	0.570823074	0.56147016	0.561088927	0.58487528	0.59418851	0.546671585	0.53438044	0.53438044
6	6.05	0.581961212	0.575293337	0.575828114	0.594400636	0.601181771	0.561032539	0.552818427	0.552818427
6	4.76	0.592382628	0.58798148	0.588964503	0.602914697	0.607571045	0.575079113	0.56994245	0.568561125
6	3.62	0.602019021	0.599402925	0.600426982	0.610362665	0.613347973	0.588492033	0.58546453	0.584560582
6	2.64	0.610589493	0.609088749	0.609993873	0.616682313	0.618439724	0.600586219	0.598802864	0.598211657
6	1.81	0.617808596	0.616992911	0.617651376	0.62181317	0.622700877	0.611064384	0.609925604	0.609604762
6	1.14	0.623464556	0.623111777	0.623399385	0.625648907	0.626028429	0.619278505	0.618619809	0.618616408
6	0.62	0.627314064	0.627206944	0.62721936	0.62817884	0.628277192	0.625200478	0.624867748	0.624867748

7	12.78	0.540337622	0.521773698	0.515080812	0.556433968	0.576118131	0.509474447	0.48104795	0.48104795
7	10.86	0.552662044	0.537167837	0.533272327	0.568487779	0.584255853	0.523558565	0.500973166	0.500973166
7	9.10	0.56469476	0.552364888	0.550531219	0.579762922	0.592064136	0.537819043	0.520743539	0.520743539
7	7.50	0.576279882	0.566990507	0.566606579	0.590234865	0.599508663	0.552205857	0.539975736	0.539975736
7	6.05	0.587351985	0.580730368	0.581260695	0.599705864	0.606454729	0.566496115	0.558330064	0.558330064
7	4.76	0.597707578	0.593337368	0.594314916	0.608167262	0.612798863	0.580468245	0.575366744	0.573994512
7	3.62	0.607280606	0.604682604	0.605701021	0.615565867	0.618533654	0.593805685	0.590802174	0.589904624
7	2.64	0.615791756	0.614301109	0.615201135	0.621841084	0.62358722	0.605829496	0.604061804	0.603475054
7	1.81	0.6229587	0.622148522	0.622802806	0.626933999	0.627815516	0.61624421	0.615115889	0.614797563
7	1.14	0.628572437	0.628222143	0.628507652	0.630740185	0.631116927	0.624407296	0.62375494	0.623751566
7	0.62	0.632392197	0.632285868	0.632298099	0.633250035	0.633347587	0.630290897	0.629961367	0.629961367
8	12.78	0.545879585	0.527421765	0.520736127	0.561845822	0.581474143	0.515083745	0.486733569	0.486733569
8	10.86	0.558141238	0.542743022	0.538851732	0.5738468	0.58956203	0.529115385	0.506609154	0.506609154
8	9.10	0.570108894	0.55786023	0.556027475	0.585067077	0.597320447	0.543315651	0.526314165	0.526314165
8	7.50	0.581626754	0.572401921	0.57201549	0.595483024	0.604715579	0.557635424	0.545468278	0.545468278
8	6.05	0.592631276	0.586056588	0.586582415	0.60489829	0.611613666	0.571852602	0.563735672	0.563735672
8	4.76	0.602919733	0.598580883	0.599552791	0.613305919	0.617912013	0.585748119	0.580682265	0.579319287
8	3.62	0.612428267	0.609848613	0.610861223	0.620654298	0.623604131	0.599008142	0.596028798	0.595137734
8	2.64	0.62087919	0.619398797	0.62029358	0.626884439	0.628619077	0.610959906	0.609207926	0.608625683
8	1.81	0.627993289	0.627188705	0.627838722	0.631938951	0.632814183	0.621309794	0.620191953	0.619876164
8	1.14	0.633564317	0.633216542	0.633499924	0.635715287	0.636089214	0.629420803	0.62877479	0.628771443
8	0.62	0.637354035	0.637248507	0.637260553	0.638204879	0.638301626	0.635265327	0.634938998	0.634938998
9	12.78	0.551317063	0.532967993	0.526291436	0.567151983	0.58672005	0.520595922	0.492328356	0.492328356
9	10.86	0.563513966	0.54821369	0.544327695	0.579098014	0.594757055	0.53457232	0.512149747	0.512149747
9	9.10	0.575414747	0.563248664	0.561417358	0.590261586	0.602464667	0.548709771	0.531785281	0.531785281
9	7.50	0.586863745	0.577704359	0.577315611	0.600619965	0.609809573	0.562960063	0.55085771	0.55085771
9	6.05	0.597799266	0.591272103	0.59179339	0.609978224	0.616658971	0.577101938	0.569035101	0.569035101
9	4.76	0.608019383	0.603712268	0.604678388	0.61833107	0.622910952	0.590918825	0.585889054	0.584535474
9	3.62	0.617462397	0.61490132	0.615907967	0.62562844	0.628559919	0.604099641	0.601144607	0.600260111
9	2.64	0.625852279	0.624382281	0.625271689	0.631812923	0.63353586	0.615977817	0.614241583	0.613663889
9	1.81	0.632912921	0.632114011	0.63275968	0.636828626	0.637697488	0.626261616	0.625154263	0.624841032
9	1.14	0.638440813	0.638095588	0.638376816	0.640574852	0.640945931	0.634319594	0.63367992	0.6336766
9	0.62	0.642200234	0.642095515	0.642107378	0.643044036	0.643139974	0.640124399	0.639801269	0.639801269
10	12.78	0.556649775	0.538411893	0.531746175	0.572352342	0.591855962	0.526010354	0.497831369	0.484952742
10	10.86	0.568780082	0.553579528	0.549699854	0.58424144	0.599841124	0.539928897	0.517594223	0.510120923
10	9.10	0.580612305	0.568530042	0.5667007	0.595346588	0.607497076	0.554001088	0.537156383	0.534493
10	7.50	0.591990963	0.582897833	0.58250695	0.605645936	0.614790999	0.568179615	0.556143738	0.553837
10	6.05	0.602856179	0.596377075	0.596893782	0.614946017	0.62159107	0.582244113	0.574228259	0.572402
10	4.76	0.613006864	0.608731814	0.609692006	0.623243153	0.62779617	0.595980503	0.5909872	0.589643148
10	3.62	0.622383428	0.619841131	0.62084167	0.630488807	0.633401564	0.609080461	0.606149856	0.605271997
10	2.64	0.63071154	0.629252066	0.630135975	0.636627114	0.638338166	0.620883631	0.619163163	0.618590056
10	1.81	0.637718187	0.63692502	0.637566269	0.641603652	0.642466068	0.631100187	0.630003323	0.629692667
10	1.14	0.643202567	0.642859921	0.643138972	0.645319543	0.645687747	0.639104266	0.638470922	0.638467628
10	0.62	0.646931472	0.646827569	0.646839252	0.647768194	0.647863317	0.644868769	0.644548834	0.644548834

Sensitivity Analysis Results

Table 14 LCOE sensitivity Analysis Results

	OpEx Change with Resolution of 1%			CapEx Change with Resolution of 1%			Operational years		
	OpEx Change %	Corresponding CD MW/km²	LCOE €/MWh	CapEx Change %	Corresponding CD MW/km²	LCOE €/MWh	Operation years	Corresponding CD MW/km²	LCOE €/MWh
Optimistic Wake Model	-70	4.76	39	-15	4.76	54	15	4.76	75
	34	6.05	68	85	4.76	85	35	4.76	54
	50	6.05	72						
Conservative Wake Model	-70	2.64	42	-15	4.76	58	15	3.62	80
	-67	3.62	43	18	3.62	69	22	4.76	68
	-15	4.76	59	85	3.62	91	35	4.76	59
	50	4.76	78						

	WACC with Resolution of 0.5%			Inflation with Resolution of 0.1%			Additional losses with Resolution of 0.5%		
	WACC %	Corresponding CD MW/km²	LCOE €/MWh	Inflation %	Corresponding CD MW/km²	LCOE €/MWh	Additional losses %	Corresponding CD MW/km²	LCOE €/MWh
Optimistic Wake Model	5.0	6.05	55	1.5	4.76	63	5.0	4.76	57
	5.5	4.76	57	3.4	6.05	55	20.0	4.76	68
	10	4.76	76	5	6.05	50			
Conservative Wake Model	5.0	4.76	59	1.5	4.76	68	5.0	4.76	62
	7.5	3.62	70	5.0	4.76	54	20.0	4.76	73
	10	3.62	81						

	Wind resource variation with Resolution of 5%		
	Wind resource variation %	Corresponding CD MW/km²	LCOE €/MWh
Optimistic Wake Model	-30	4.76	98
	10	4.76	54
Conservative Wake Model	-30	3.62	108
	-5	4.76	67
	10	4.76	57

Table 15 NPV sensitivity Analysis Results

	OpEx Change with Resolution of 1%			CapEx Change with Resolution of 1%			Operational years		
	OpEx Change %	Corresponding CD MW/km²	NPV M€	CapEx Change %	Corresponding CD MW/km²	NPV M€	Operation years	Corresponding CD MW/km²	NPV M€
Optimistic Wake Model	-70	12.78	5811	-15	10.86	2578	15	3.62	-344
	-25	10.86	2920	-7	9.10	2020	16	4.76	-220
	-11	9.10	2133	15	6.05	703	20	6.05	345
	20	6.05	631	26	4.76	256	22	9.10	648
	40	4.76	-50	49	3.62	-478	32	10.86	2415
	50	4.76	-340	61	2.64	-770	35	10.86	2888
				85	2.64	-1215			
Conservative Wake Model	-70	9.10	3289	-15	6.05	1129	15	2.64	-485
	-44	6.05	2024	-9	4.76	894	17	3.62	-340
	-15	4.76	1034	19	3.62	-17	21	4.76	13
	28	3.62	-207	39	2.64	-514	33	6.05	1084
	50	3.62	-728	74	1.81	-1158	35	6.05	1250
				85	1.81	-1300			

	WACC with Resolution of 0.5%			Inflation with Resolution of 0.1%			Strike Price with Resolution of 5 €/MWh		
	WACC %	Corresponding CD MW/km²	NPV M€	Inflation %	Corresponding CD MW/km²	NPV M€	Strike Price	Corresponding CD MW/km²	NPV M€
Optimistic Wake Model	5.0	12.78	2884	1.5	6.05	648	40	1.81	-1400
	5.5	10.86	2158	1.7	9.10	797	45	2.64	-1160
	6.0	9.10	1596	3.0	10.86	2178	51	3.62	-778
	7.0	6.05	674	3.5	12.78	2927	55	4.76	-452
	8.0	4.76	192	5.0	12.78	6137	61	6.05	180
	9.5	3.62	-299				65	9.10	701
	10.0	2.64	-398				75	10.86	2530
							79	12.78	3362
							100	12.78	8148
Conservative Wake Model	5.0	6.05	1175	1.5	4.76	143	40	1.81	-1439
	5.5	4.76	852	3.2	6.05	975	50	2.64	-964
	7.5	3.62	-22	4.5	7.50	2025	60	3.62	-303
	9.0	2.64	-361	5.0	7.50	2596	64	4.76	19
	10	2.64	-496				75	6.05	1088
							90	9.10	2963
							100	9.10	4507
							130	10.86	9169
							165	12.78	15120

	Additional losses with Resolution of 0.5%			Wind resource variation with Resolution of 5%		
	Additional losses %	Corresponding CD MW/km²	NPV M€	Wind resource variation %	Corresponding CD MW/km²	NPV M€
Optimistic Wake Model	5.0	9.10	1893	-30	1.81	-1283
	14.5	6.05	621	-25	2.64	-982
	20.0	4.76	104	-20	3.62	-633
				-15	4.76	-197
				-10	6.05	288
				-5	9.10	872
				4	10.86	2133
				10	12.78	2988
Conservative Wake Model	5.0	4.76	760	-30	1.81	-1348
	16.5	3.62	-77	-20	2.64	-827
	20.0	3.62	-277	-10	3.62	-183
				-7	4.76	21
				4	6.05	917
				10	6.05	1400

Table 16 IRR sensitivity Analysis Results

	OpEx Change with Resolution of 5%			CapEx Change			Operational years		
	OpEx Change %	Corresponding CD MW/km²	IRR %	CapEx Change %	Corresponding CD MW/km²	IRR %	Operation years	Corresponding CD MW/km²	IRR %
Optimistic Wake Model	-70	2.64	10.09	-15	4.76	7.41	15	4.76	1.99
	-45	4.76	8.39	85	4.76	1.00	35	4.76	6.64
	40.0	6.05	3.31						
	50.0	6.05	2.65						
Conservative Wake Model	-70	2.64	9.59	-15	3.62	6.24	15	3.62	0.56
	-30	3.62	6.74	85	3.62	0.15	35	3.62	5.67
	5	4.76	4.48						
	50	4.76	1.17						

	Additional losses with Resolution of 0.5%			Wind resource variation with Resolution of 10%			Strike Price with Resolution of 5 €/MWh		
	Additional losses %	Corresponding CD MW/km²	IRR %	Wind resource variation %	Corresponding CD MW/km²	IRR %	Strike Price	Corresponding CD MW/km²	IRR %
Optimistic Wake Model	5.0	4.76	6.24	-30.0	6.05	-1.96	40	7.50	-2.60
	20.0	4.76	3.66	-20.0	4.76	1.59	45	6.05	-0.70
				10.0	4.76	7.24	60	4.76	3.58
							100	4.76	11.48
							150	2.64	20.08
Conservative Wake Model	5.0	3.62	5.16	-30.0	4.76	-4.32	40	4.76	-4.44
	7.5	4.76	4.75	-20.0	4.76/3.62	0.05	70	3.62	4.80
	20.0	4.76	2.58	10.0	4.76/3.62	6.28/6.29	95	2.64	9.71
							100	2.64	10.66
							150	2.64	19.20

Sensitivity analysis based on wind resource variation using different wake models.

Table 17 LCOE correlation with wind resource

Wind Resource	NOJ		NOJlocal		TurboNOJ		BastankhahGaussian		IEA37SBG		TurboGaussian		Fuga		FugaBlockage	
	CD	LCOE	CD	LCOE	CD	LCOE	CD	LCOE	CD	LCOE	CD	LCOE	CD	LCOE	CD	LCOE
%	MW/km²	€/MWh	MW/km²	€/MWh	MW/km²	€/MWh	MW/km²	€/MWh	MW/km²	€/MWh	MW/km²	€/MWh	MW/km²	€/MWh	MW/km²	€/MWh
-30	4.76	103	3.62	104	3.62	104	4.76	99	4.76	98	3.62	107	3.62	108	3.62	108
-25	4.76	90	4.76	92	4.76	91	4.76	88	4.76	87	3.62	94	3.62	95	3.62	95
-20	4.76	81	4.76	82	4.76	82	4.76	79	4.76	78	3.62	85	3.62	85	3.62	86
-15	4.76	74	4.76	75	4.76	75	4.76	72	4.76	72	4.76	77	3.62	78	3.62	78
-10	4.76	69	4.76	69	4.76	69	4.76	67	4.76	66	4.76	71	3.62	72	3.62	72
-9	4.76	68	4.76	68	4.76	68	4.76	66	4.76	65	4.76	70	3.62	71	3.62	71
-8	4.76	67	4.76	67	4.76	67	4.76	65	4.76	65	4.76	69	4.76	70	3.62	70
-7	4.76	66	4.76	66	4.76	66	4.76	64	4.76	64	4.76	68	4.76	69	3.62	69
-6	4.76	65	4.76	65	4.76	65	4.76	63	4.76	63	4.76	67	4.76	68	3.62	68
-5	4.76	64	4.76	65	4.76	64	4.76	63	4.76	62	4.76	66	4.76	67	4.76	67
-4	4.76	63	4.76	64	4.76	64	4.76	62	4.76	61	4.76	65	4.76	66	4.76	66
-3	4.76	63	4.76	63	4.76	63	4.76	61	4.76	61	4.76	65	4.76	65	4.76	65
-2	4.76	62	4.76	62	4.76	62	4.76	61	4.76	60	4.76	64	4.76	65	4.76	65
-1	4.76	61	4.76	62	4.76	61	4.76	60	4.76	59	4.76	63	4.76	64	4.76	64
0	4.76	60	4.76	61	4.76	61	4.76	59	4.76	59	4.76	62	4.76	63	4.76	63
1	4.76	60	4.76	60	4.76	60	4.76	59	4.76	58	4.76	62	4.76	62	4.76	62
2	4.76	59	4.76	60	4.76	60	4.76	58	4.76	58	4.76	61	4.76	62	4.76	62
3	4.76	59	4.76	59	4.76	59	4.76	57	4.76	57	4.76	60	4.76	61	4.76	61
4	4.76	58	4.76	58	4.76	58	4.76	57	4.76	56	4.76	60	4.76	60	4.76	60
5	4.76	57	4.76	58	4.76	58	4.76	56	4.76	56	4.76	59	4.76	60	4.76	60
6	4.76	57	4.76	57	4.76	57	4.76	56	4.76	55	4.76	59	4.76	59	4.76	59
7	4.76	56	4.76	57	4.76	57	4.76	55	4.76	55	4.76	58	4.76	59	4.76	59
8	4.76	56	4.76	56	4.76	56	4.76	55	4.76	55	4.76	58	4.76	58	4.76	58
9	4.76	55	4.76	56	4.76	56	4.76	55	4.76	54	4.76	57	4.76	58	4.76	58
10	4.76	55	4.76	55	4.76	55	4.76	54	4.76	54	4.76	57	4.76	57	4.76	57

Table 18 NPV correlation with wind resource at strike price of 70 €/MWh

Wind Resource	NOJ		NOJlocal		TurboNOJ		BastankhahGaussian		IEA37SBG		TurboGaussian		Fuga		FugaBlockage	
	CD	NPV	CD	NPV	CD	NPV	CD	NPV	CD	NPV	CD	NPV	CD	NPV	CD	NPV
%	MW/km²	M€	MW/km²	M€	MW/km²	M€	MW/km²	M€	MW/km²	M€	MW/km²	M€	MW/km²	M€	MW/km²	M€
-30	1.81	-1309	1.81	-1313	1.81	-1310	1.81	-1288	1.81	-1283	1.81	-1340	1.81	-1346	1.81	-1348
-25	2.64	-1044	2.64	-1056	2.64	-1049	2.64	-996	2.64	-982	2.64	-1113	1.81	-1124	1.81	-1126
-20	2.64	-735	2.64	-747	2.64	-740	3.62	-663	3.62	-633	2.64	-807	2.64	-822	2.64	-827
-15	3.62	-367	3.62	-394	3.62	-384	4.76	-258	4.76	-197	3.62	-498	3.62	-531	2.64	-539
-10	4.76	68	4.76	7	4.76	20	4.76	213	6.05	288	3.62	-141	3.62	-174	3.62	-183
-9	4.76	158	4.76	98	4.76	111	4.76	303	6.05	399	4.76	-66	3.62	-105	3.62	-115
-8	4.76	247	4.76	187	4.76	200	6.05	398	6.05	508	4.76	23	3.62	-38	3.62	-47
-7	4.76	335	4.76	275	4.76	288	6.05	506	6.05	616	4.76	110	4.76	40	4.76	21
-6	4.76	421	4.76	361	4.76	374	6.05	612	6.05	722	4.76	196	4.76	127	4.76	108
-5	6.05	509	4.76	446	4.76	459	6.05	716	9.10	872	4.76	281	4.76	212	4.76	193
-4	6.05	612	4.76	530	4.76	543	6.05	818	9.10	1022	4.76	365	4.76	296	4.76	277
-3	6.05	714	4.76	612	4.76	625	6.05	918	9.10	1169	4.76	447	4.76	378	4.76	360
-2	6.05	813	6.05	704	6.05	713	9.10	1028	9.10	1314	4.76	528	4.76	459	4.76	441
-1	6.05	911	6.05	803	6.05	812	9.10	1171	9.10	1456	4.76	607	4.76	539	4.76	521
0	6.05	1008	6.05	900	6.05	908	9.10	1311	9.10	1596	4.76	685	4.76	618	4.76	599
1	6.05	1102	6.05	995	6.05	1004	9.10	1449	9.10	1733	6.05	771	4.76	695	4.76	677
2	9.10	1230	6.05	1088	6.05	1097	9.10	1584	9.10	1868	6.05	865	4.76	770	4.76	752
3	9.10	1365	6.05	1180	6.05	1189	9.10	1717	9.10	2000	6.05	957	4.76	845	4.76	827
4	9.10	1498	6.05	1270	6.05	1279	9.10	1847	10.86	2133	6.05	1047	4.76	918	6.05	917
5	9.10	1628	6.05	1358	6.05	1367	9.10	1975	10.86	2280	6.05	1136	6.05	1007	6.05	1007
6	9.10	1756	9.10	1474	7.50	1454	9.10	2101	10.86	2425	6.05	1222	6.05	1094	6.05	1094
7	9.10	1882	9.10	1602	9.10	1560	9.10	2224	10.86	2567	6.05	1308	6.05	1180	6.05	1180
8	9.10	2004	9.10	1726	9.10	1685	9.10	2344	10.86	2706	9.10	1396	6.05	1265	6.05	1265
9	9.10	2125	9.10	1849	9.10	1807	9.10	2462	10.86	2842	9.10	1519	6.05	1347	6.05	1347
10	9.10	2243	9.10	1969	9.10	1927	9.10	2577	12.78	2988	9.10	1639	6.05	1428	6.05	1400

Table 19 NPV correlation with wind resource at strike price of 50 €/MWh

Wind Resource	NOJ		NOJlocal		TurboNOJ		BastankhahGaussian		IEA37SBG		TurboGaussian		Fuga		FugaBlockage	
CD	NPV	CD	NPV	CD	NPV	CD	NPV	CD	CD	NPV	CD	NPV	CD	NPV	CD	
%	MW/km²	M€	MW/km²	M€	MW/km²	M€	MW/km²	M€	%	MW/km²	M€	MW/km²	M€	MW/km²	M€	MW/km²
-30	1.14	-1770	1.14	-1771	1.14	-1770	1.14	-1765	1.14	-1764	1.14	-1779	1.14	-1781	1.14	-1781
-25	1.81	-1656	1.81	-1659	1.81	-1656	1.81	-1640	1.81	-1636	1.14	-1678	1.14	-1680	1.14	-1680
-20	1.81	-1504	1.81	-1507	1.81	-1504	1.81	-1488	1.81	-1484	1.81	-1528	1.81	-1533	1.81	-1534
-15	1.81	-1362	1.81	-1365	1.81	-1362	1.81	-1346	1.81	-1342	1.81	-1386	1.81	-1391	1.81	-1392
-10	1.81	-1230	1.81	-1233	1.81	-1230	2.64	-1204	2.64	-1194	1.81	-1255	1.81	-1259	1.81	-1260
-9	2.64	-1202	1.81	-1208	2.64	-1205	2.64	-1167	2.64	-1157	1.81	-1229	1.81	-1234	1.81	-1235
-8	2.64	-1165	2.64	-1174	2.64	-1169	2.64	-1131	2.64	-1121	1.81	-1205	1.81	-1209	1.81	-1211
-7	2.64	-1130	2.64	-1138	2.64	-1133	2.64	-1096	2.64	-1086	1.81	-1181	1.81	-1185	1.81	-1186
-6	2.64	-1095	2.64	-1103	2.64	-1098	2.64	-1061	2.64	-1051	2.64	-1149	2.64	-1159	2.64	-1162
-5	2.64	-1061	2.64	-1069	2.64	-1064	2.64	-1027	2.64	-1017	2.64	-1114	2.64	-1124	2.64	-1128
-4	2.64	-1027	2.64	-1035	2.64	-1030	2.64	-993	2.64	-984	2.64	-1080	2.64	-1090	2.64	-1094
-3	2.64	-994	2.64	-1002	2.64	-997	2.64	-960	2.64	-951	2.64	-1047	2.64	-1057	2.64	-1060
-2	2.64	-961	2.64	-970	2.64	-965	2.64	-928	2.64	-919	2.64	-1015	2.64	-1025	2.64	-1028
-1	2.64	-930	2.64	-938	2.64	-933	2.64	-896	2.64	-887	2.64	-983	2.64	-993	2.64	-996
0	2.64	-898	2.64	-906	2.64	-902	2.64	-865	2.64	-856	2.64	-951	2.64	-961	2.64	-964
1	2.64	-868	2.64	-876	2.64	-871	2.64	-835	3.62	-817	2.64	-921	2.64	-930	2.64	-933
2	2.64	-838	2.64	-846	2.64	-841	3.62	-798	3.62	-777	2.64	-890	2.64	-900	2.64	-903
3	2.64	-808	2.64	-816	2.64	-811	3.62	-759	3.62	-738	2.64	-861	2.64	-870	2.64	-873
4	2.64	-779	2.64	-787	2.64	-782	3.62	-721	3.62	-700	2.64	-832	2.64	-841	2.64	-844
5	3.62	-742	2.64	-759	3.62	-753	3.62	-684	3.62	-663	2.64	-803	2.64	-813	2.64	-816
6	3.62	-705	3.62	-723	3.62	-716	3.62	-647	3.62	-626	2.64	-775	2.64	-785	2.64	-788
7	3.62	-668	3.62	-686	3.62	-679	3.62	-611	3.62	-591	2.64	-748	2.64	-757	2.64	-760
8	3.62	-633	3.62	-651	3.62	-644	3.62	-576	3.62	-556	2.64	-722	2.64	-731	2.64	-734
9	3.62	-598	3.62	-616	3.62	-609	3.62	-542	3.62	-521	3.62	-690	2.64	-704	2.64	-707
10	3.62	-564	3.62	-582	3.62	-575	3.62	-508	4.76	-483	3.62	-656	3.62	-676	2.64	-682

Optimal capacity density of offshore wind farms

Table 20 IRR correlation with wind resource at strike price of 70 €/MWh

Wind Resource	NOJ		NOJlocal		TurboNOJ		BastankhahGaussian		IEA37SBG		TurboGaussian		Fuga		FugaBlockage	
	CD	IRR	CD	IRR	CD	IRR	CD	IRR	CD	IRR	CD	IRR	CD	IRR	CD	IRR
%	MW/km2	%	MW/km2	%	MW/km2	%	MW/km2	%	MW/km2	%	MW/km2	%	MW/km2	%	MW/km2	%
-30	4.76	-2.94	4.76	-3.21	4.76	-3.15	6.05	-2.28	6.05	-1.96	4.76	-3.87	4.76	-4.22	4.76	-4.32
1st Alternative	-	-	-	-	-	-	4.76	-2.33	7.5	-2.07	-	-	-	-	3.62	-4.41
2nd Alternative	-	-	-	-	-	-			4.76	-2.10	-	-	-	-	-	-
-25	4.76	-0.73	4.76	-0.94	4.76	-0.90	4.76	-0.23	6.05	0.01	4.76	-1.48	4.76	-1.75	4.76	-1.82
Alternative									4.76	-0.04					3.62	-1.85
-20	4.76	0.99	4.76	0.81	4.76	0.85	4.76	1.41	4.76	1.59	4.76	0.33	4.76	0.11	4.76/3.62	0.05
15	4.76	2.39	4.76	2.23	4.76	2.27	4.76	2.77	4.76	2.93	4.76	1.80	4.76	1.60	4.76/3.62	1.56
10	4.76	3.58	4.76	3.43	4.76	3.46	4.76	3.92	4.76	4.07	4.76	3.03	4.76	2.85	4.76/3.62	2.82
-5	4.76	4.59	4.76	4.46	4.76	4.49	4.76	4.91	4.76	5.04	4.76	4.08	4.76	3.92	4.76/3.62	3.88
0	4.76	5.47	4.76	5.34	4.76	5.37	4.76	5.76	4.76	5.88	4.76	4.99	4.76	4.84	4.76/3.62	4.80
5	4.76	6.22	4.76	6.11	4.76	6.14	4.76	6.49	4.76	6.61	4.76	5.77	4.76	5.64	4.76/3.62	5.60
10	4.76	6.88	4.76	6.78	4.76	6.80	4.76	7.13	4.76	7.24	4.76	6.45	4.76	6.33	4.76/3.62	6.29/6.28

Table 21 IRR correlation with wind resource at strike price of 50 €/MWh

Wind Resource	NOJ		NOJlocal		TurboNOJ		BastankhahGaussian		IEA37SBG		TurboGaussian		Fuga		FugaBlockage	
	CD	IRR	CD	IRR	CD	IRR	CD	IRR	CD	IRR	CD	IRR	CD	IRR	CD	IRR
%	MW/km2	%	MW/km2	%	MW/km2	%	MW/km2	%	MW/km2	%	MW/km2	%	MW/km2	%	MW/km2	%
-30	#N/A	#N/A	#N/A	#N/A	#N/A	#N/A	#N/A	#N/A	#N/A	#N/A	#N/A	#N/A	#N/A	#N/A	#N/A	#N/A
-25	6.05	-7.74	6.05	-8.40	4.76	-8.32	6.05	-6.70	7.50	-6.24	4.76	-9.63	#N/A	#N/A	#N/A	#N/A
-20	6.05	-4.94	6.05	-5.34	4.76	-5.30	6.05	-4.24	6.05	-3.91	4.76	-6.09	4.76	-6.47	4.76	-6.57
-15	6.05	-3.07	6.05	-3.38	4.76	-3.33	6.05	-2.53	6.05	-2.26	4.76	-3.95	4.76	-4.22	4.76	-4.29
-10	6.05	-1.67	4.76	-1.90	4.76	-1.86	6.05	-1.21	6.05	-0.99	4.76	-2.38	4.76	-2.60	4.76	-2.66
-5	6.05	-0.55	4.76	-0.73	4.76	-0.70	6.05	-0.15	6.05	0.05	4.76	-1.15	4.76	-1.34	4.76	-1.39
0	6.05	0.37	4.76	0.23	4.76	0.26	6.05	0.72	6.05	0.90	4.76	-0.15	4.76	-0.31	4.76	-0.35
5	4.76	1.16	4.76	1.04	4.76	1.07	6.05	1.46	6.05	1.62	4.76	0.69	4.76	0.54	4.76	0.51
Alternative	6.05	1.14														
10	4.76	1.83	4.76	1.72	4.76	1.74	6.05	2.08	6.05	2.23	4.76	1.39	4.76	1.26	4.76	1.23
Alternative	6.05	1.79														

Sammendrag

Dette arbeidet presenterer en intuitive litteraturstudie for å identifisere den optimale tettheten av vindturbiner i en vindpark lokalisert til havs.En klimatologisk studie på vind er analysert ved hjelp av tidsserieanalyse, og installasjon av National Renewable Energy Laboratory (NREL) 15-MW vindturbin (WT). Foreløpige simuleringer av PyWake ved bruk av ulike kjølvannsmodeller blir undersøkt for å finne forholdet mellom netto årlig energiproduksjon (AEP) og kapasitetstettheten til vindparken.

ENE503: ENERGY RESEARCH PROJECT

Written by:

Akansha Jha
M.Sc Renewable Energy

Supervised by:

Sathyajith Mathew, Department of Engineering Sciences, UiA
Stefan Goossens, Offshore Wind Technology, Equinor ASA
Dhruvit Berawala, Offshore Wind Technology, Equinor ASA

University of Agder
Faculty of Technology and Science
Department of Engineering Science

11. November 2022

Optimal capacity density analysis for future offshore wind farms

Akansha Jha

Supervised by
Sathyajith Mathew*, Stefan Goossens[†], and Dhruvit Berawala[†]
*Department of Engineering Sciences, University of Agder, Grimstad, Norway. Email: sathyajith.mathew@uia.no
[†]Wind Energy Technology, Equinor ASA, Stavanger, Norway. Email: SGOO@equinor.com, DSB@equinor.com

Abstract - This work presents an intuitive literature study on identifying the optimum capacity density of a wind farm at a specified offshore location. A climatological study on wind is analyzed using time-series analysis, and installing National Renewable Energy Laboratory (NREL)15-MW wind turbine (WT) at the site. Preliminary simulations on PyWake using various wake models are examined to obtain the relationship between net Annual Energy Production (AEP) and the capacity density of wind farm.

I. INTRODUCTION

Norway is targeting 30 GW offshore wind capacity by 2040 [1]. Several large-scale offshore wind projects are planned to meet this target. One of the challenges for this large-scale development would be the "resource rich" sea space that is required for this large-scale development. Hence, possibilities of enhancing the current capacity densities (nameplate power capacity per unit land or water area) of offshore project are to be investigated. Further, with higher capacity densities, investments required for inter-cabling and for power transmission infrastructure can also be minimised [2].Over the years numerous estimations have been developed to determine power obtained from the installed area and the optimum space required to extract most production out of the given area [2][3]. Aspects restraining wind growth include limited remaining high-windspeed locations near load centers, transmission constraints, competition between wind farms and other land and water uses, permitting processes and social opposition. This study deduces solution based on i) wake loss prediction with a selected layout ii) basic layout optimization in comparison with the previous layout.

It is crucial to accurately estimate the WT wakes and the economics associated [4]. The average power loss due to WT wakes in case of large offshore wind farm (OSWF) is approximately 10 to 20 % of the annual energy production (AEP). When the wind flows through the rotors, turbulence generated are transported downstream which may affect the lifetime and maintenance cost. Wind varies as the cube of the WS and, therefore, an improper estimation of velocity field in a wind farm can lead to redundant errors in the prediction of net AEP [5]. The work extensively focuses on 67 National Renewable Energy Laboratory (NREL) 15-MW turbines placed in a pre-determined pattern to a probable future location with available wind data. The pilot simulation run involves placement of these turbines to an original wind farm layout, Dudgeon situated in Great Yarmouth, UK implementing PyWake models- N.O.Jensen (NOJ), Local Jensen, Turbo Jensen (TOP), BastankhahGaussian(BP), IEA37SimpleBastankhahGaussian (IEA37SBG), Turbo Gaussian, Fuga, FugaBlockage and sequentially increasing the distance between each turbines from their primary position to obtain the relation between net AEP and capacity density. The upscaled area of the original layout is compared to the manually optimised layout using the basic model (Jensen) and the best possible capacity density is derived.

Conceptual rendering of a commercial-scale OSWF is performed on a chosen site in the North Sea. Moreover, there is currently no timeline or specific plan to develop the offshore wind project and the results performed are solely for the study and research purpose.

II. LITERATURE REVIEW

In this section, previous studies for estimating the theoretical capacity density are being reviewed. The term capacity density is most commonly used in the wind industry as the ratio of the wind farm's rated capacity to its ground area [2]. The mean installed and output power densities (wind farm power output per unit land or water area) are reported under TABLE I. from previous studies [3].

TABLE I. INSTALLED AND OUTPUT POWER DENSITY

Wind farm Type	Capacity Factor [%]	Installed Power Density [MW/km²]		Output Power Density [W/m²]	
	Mean	Mean	Range	Mean	Range
Onshore Europe	33.5	19.8	(6.2–46.9)	6.64	(2.3–8.2)
Onshore (outside Europe)	33.4	20.5	(16.5–48)	6.84	(4.81–11.2)
Offshore Europe	40.8	7.2	(3.3–20.2)	2.94	(1.15–6.32)

North Sea holds majority of the world's operating offshore wind farms (OSWFs). The European statistics represented above are from 11 OSWFs located in the North sea with

nameplate capacity of 3.1 (2.0–3.6) MW. The number of turbines per OSWF ranges from 27 to 175, with a mean of 8.8 m/s and the average wind speed range between 7.3 to 9.9 m/s. The capacity density in these OSWFs ranges between 3.3 to 20.2 MW/km^2 with a mean of 7.2 MW/km^2 according to a study stated by Peter Enevoldsen [3]. The ECN (Energy Center Netherlands) quantified the values for a 15MW wind turbine (WT) to be 5.06MW/km^2, approximately 4% higher as compared to 10MW WT [6]. In another study by Müller, mean capacity density of 5 MW/km² was derived and several other studies suggested a range between 4.9 to 5.4MW/km^2 [2]. However, the power density varied with specific power values (nameplate generation capacity rating per unit rotor swept area).

III. THEORICAL AND CONCEPTUAL FRAMEWORK

The hourly mean wind speeds and wind directions for an offshore location in North Sea at 10m and 100m above mean sea level was collected with a resolution of one hour. Extrapolation of WS at 160m hub height was performed using the exponential law or 'power law' expressed below. A shear table was later used to extrapolate more realistic values with Windpro^{TM}.

$$v_z = v_0 \left(\frac{z}{z_0}\right)^\alpha \tag{1}$$

where v_z is the wind speed caluated at height z, z_0 refers to wind speed at reference height at z_0 and α is the emperically derived coeffcent that depends on the stability of atmosphere.

A. Windrose

Wind velocity and direction can be represented in the form of windrose, a polar plot divided into equally spaced sectors, to visualize the distribution of wind in various directions at the candidate site. The typical information displayed in a wind rose graphical plot are the distribution of frequency, velocity and energy in different directions [7]. The polar diagram was developed using 'windrose' module in python^{TM}, divided into 16 sectors covering an angle of 22.5° each. The circular demonstration of the wind rose depicts the direction and the length of each "spoke" presents how often the wind blew from that direction. For 2021, the highest prevailing WD originated south-west (SW, azimuth 225 ° ± 22.5°) with 9.4% of occurrence and the maximum value of 28.6m/s, quite similar to the overall rose curve for cumulative wind data between 1990 and 2021with 10.2% and the maximum value of 35.3m/s (refer Fig. 1). SW and NE are dominant, but the strongest winds are from SSW in both the windrose plot.
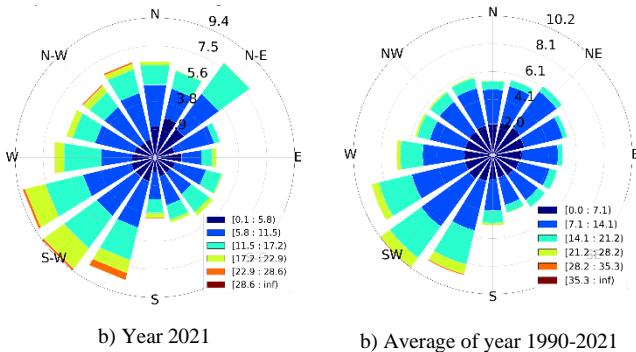

b) Year 2021   b) Average of year 1990-2021

Fig. 1.   Windrose plot at height 160m

B. Statistical models for data-analysis - Weibull Distribution

The statistical distribution of wind speeds differs at various location around the globe, depending upon local climatic conditions, the landscape, and its surface. Weibull distribution is considered as a special case of Pierson class III distribution where the variation in wind velocity are characterized by the probability density and cumulative density function. The probability distribution function refers to the fraction of time for which the wind flows with a specific wind speed represented as:

$$f(V) = \frac{k}{c}\left(\frac{V}{c}\right)^{k-1} e^{(-V/c)^k} \tag{2}$$

where k is the Weibull shape factor, c is the scale factor and V is the wind speed [8]. The cumulative distribution is the integral of the probability distribution function and indicates the percent of time for which the wind speed is less than or equal the wind speed V [7]. The relation is mathematically expressed as the integral of probability density functions with the following equation:

$$F(V \le V_0) = \int_0^\alpha f(V) = 1 - e^{(-V/c)^k} \tag{3}$$

Fig. 9 and Fig. 10 (under Appendix) shows the variation of Weibull probability and cumulative distribution function for the year 1990-2021. Fig. 8 under Appendix shows windrose plot for different years and it is interesting to note that 2010 was an outlier year with high dominancy of wind from E followed by NNW and 'k', 'c' and PDF values as 2.37, 12.16m/s and 7.87% respectively (refer Fig. 9 peak grey curve). For AEP calculation, the Weibull shape factor 'k' (mean 2.28, with range 2.15 to 2.45) and scale factor c (mean 13.91, with range 12.16 to 15.41 m/s) were obtained using the average values for 32 years (1990-2021) as the 2022 year had an incomplete dataset. The peak Probability distribution for the new Weibull corresponds to 6.76% indicating the probability that 592.30 hours of the year the velocity is equal or below 10.8m/s and production is 8.88 GWh (refer Fig. 2).

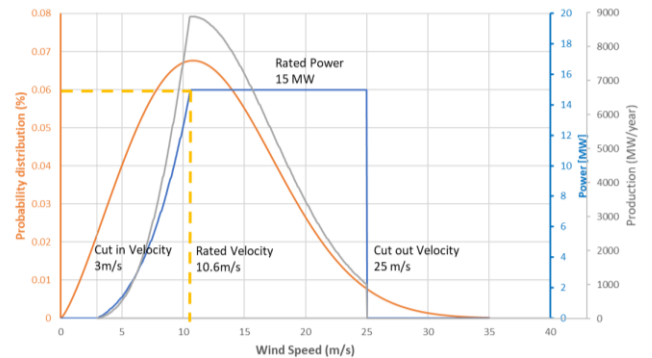### C. Power Cuve, Thrust Coefficient and Gross AEP

Fig. 2.   Power curve, weibull curve and theoretical annual production

Details of NREL 15MW WT with the rotor diameter 240m and hub height 160m, specified power and thrust coefficient values corresponding to the WS were collected (refer Fig. 2 and Fig. 11 under Appendix) [9]. The specific power was calculated as 332W/m^2. In general, WT with high specific power are used

in regions with high average wind speeds [2]. Python™ module 'sympy' and wera application (newton –raphson method) were used to obtain the gross annual energy production of 94.85 GWh and capacity factor of 72% from the available wind data (refer Fig. 12 under Appendix). Capacity factor (C$_F$) is one of the important index for evaluating performance of a WT and is defined as the ratio of actual energy produced to the energy that could have been produced if the WT operated at its rated power throughout the time period [7]. Gross AEP of WT can be calculated by any of the numerical method using equation:

$$E_t = \left[\int_{V_I}^{V_R} P(V) \cdot f(V) + P_r \int_{V_R}^{V_C} f(V) \right] \cdot 8760 \qquad (4)$$

$$P(V) \text{ or } P_v = P_R \left[\frac{V^n - V_I^n}{V_R^n - V_I^n} \right] \qquad (5)$$

where V_I (3 m/s), V_R (10.6 m/s), and V_C (25 m/s) are cut-in, rated, and cut-out wind speed respectively. P_R is the rated power and $P(V)$ can be obtained by finding velocity power proportionality 'n' using curve fitting module 'scipy' and the Power-velocity values of 15MW NREL WT.

D. Time series analysis and modelling of surface wind

Fig. 3 shows the variation of energy production w.r.t wind for the three regions. Fig. 13 under Appendix depicts the predicted average hourly production each month within the span of 32 years. It can be observed that the wind speed is seasonal, and the average value was highest in winters (Dec-Jan-Feb) and lowest in the summer (Jun-Jul-Aug). Furthermore, a plot between yearly average for production and wind speed is plotted under Fig. 14 (refer Appendix) to see the relation.
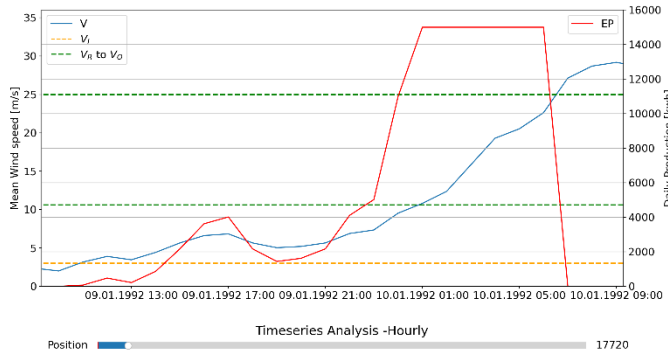
Fig. 3.   Timeseries analysis on hourly basis for wind data during 1990-2021

E. PyWake Overview and Wake Models

PyWake, is an open source python™ package developed by DTU Wind Energy for wind farm simulation, capable of evaluating wind farm flow fields, power production and AEP over a given layout of wind farm. One of the key features of PyWake is vectorization and use of numerical libraries which speedups the run. PyWake encapsulates predefined engineering wind farm wake models such as NOJ, Fuga, FugaBlockage, BP (BastankhahGaussian),   IEA37SBG(IEA37SimpleBastankhah Gaussian).Fig. 15 (under Appendix) illustrates the flowchart showcasing exchange of data within the PyWake wind farm model (WFM) for AEP calculation [10]. TABLE II. represents the key feature of wind farm models (WFMs) used in python™

programming. The default superposition model defines how deficits sum up, 'SquaredSum' indicates that it uses root-sum-square to construct the velocity field of the array.

TABLE II.   PYWAKE MODELS IMPLEMENTED

Wind farm models	Wake Deficit Model in Python™	Default Superposition Model	Default Empirical constants using in Coding
Original Jensen /Park (NOJ)	NOJDeficit	SquaredSum	k= 0.1[a] (used value k= 0.04)
Local Jensen	NOJLocal Deficit	LinearSum	a= [0.38, 4e-3]
Turbo Jensen/ TurbOpark (TOP)	TurboNOJ Deficit	LinearSum	A=.6, cTI= [1.5, 0.8]
Bastankhah Gaussian (BP)	Bastankhah Gaussian Deficit	SquaredSum	k= 0.0324555 [b]
IEA37Simple Bastankhah Gaussian (IEA37SBG)	IEA37Simple Bastankhah Gaussian Deficit	SquaredSum	k = 0.0324555 (beta=1/sqrt(8) ~ ct=0.9637188)
Turbo Gaussian	Turbo Gaussian Deficit	LinearSum (used-SquaredSum)	A=.04, cTI=[1.5, 0.8]
Fuga	FugaDeficit	LinearSum	-
Fuga Blockage	FugaDeficit	LinearSum	-

[a] k value employed in NOJ model for PyWake represents the wake expansion factor or wake decay coefficient, **k**

[b] k value in BastankhahGaussian and IEA37SimpleBastankhah Gaussian model for PyWake represents the wake expansion parameter.

1) Original Jensen Model

Original Jensen (NOJ) wake model (also known as Park), first developed by Niels Otto Jensen (1983) is based on conservation of mass and states that the wake behind a WT expands linearly from the rotor plane. Velocity deficit is only dependent on the distance downstream from the turbine and the expansion is a function of the wake decay coefficient or wake expansion factor, k which depends on ambient turbulence level and atmospheric stability. The initial velocity deficit is calculated from the turbine's C$_T$, and the semi-empirical coefficient k [11]. It was originally empirically calibrated (k = 0.04) for the far wake based on measurements by Katić, Højstru [4]. With uniform velocity profile shape Jensen is also referred as top-hat wake model and velocity deficit (difference between free stream and wake velocity at a downstream distance x) is represented by the following equation:

$$\Delta U = U \left[\frac{1 - \sqrt{1 - C_T}}{\left(1 + \frac{2kx}{D}\right)^2} \right] \qquad (6)$$

where D is the rotor diameter, U is the free stream wind velocity and C_T is used for thrust coefficient [12]. NOJ model in Pywake considers a default value of $k = 0.1$ but in theory, $k = 0.075$ for onshore and 0.04 or 0.05 for OSWFs.

2) Local Jensen Model

Local Jensen model incorporates 'NOJLocalDeficit' wake model which is very similar to NOJDeficit but the wake deficit is scaled with the effective wind speed instead of ambient WS. Wake expansion factor (k) is a function of the new introduced element Turbulence intensity (TI, default value 0.1) and follows a linear relation. TI is only required in specific wake models; refers to the standard deviation of wind speed signal /mean wind speed and depends on atmospheric stability and wind directions. The code used for Local Jensen accounts for 'STF2017TurbulenceModel' as added turbulence in the wake. The turbulence model by Steen Frandsen takes a pre-defined weight function input resulting into the bell-shape. According to IEC 61400-1 (International Electrotechnical Commission) edition 3 standard interpretation, 6% contribution from neighbouring wind turbines (WTs) is assumed when measuring the omni-directional effective turbulence intensity. The 6% ambient turbulence (I_0) maps to a full added turbulence in spread angle of 360º x 6% = 21.6º up to 10D (10 times Diameter) downstream [10].

3) Turbulence Optimized Park Model

TurboOpark or Turbo Jensen is a modified version of park model which assumes the wake expansion rate to be proportional to the local turbulence intensity in the wake [10]. The local turbulence intensity is described by the combination of atmospheric (I_0) and wake added turbulence ($I_w(x)$). The additional turbulence generated by shear on the wake edge is dependent on two inbuilt constants (c1= 1.5 and c2 = 0.8) stored in 'TurboNOJDeficit' wake model. Since the wake contribution to turbulence is highest at the rear of WT, the wake expansion is fastest at the point closest to WT. With increasing downstream distance, the cumulative turbulence intensity ($I(x)$) approaches I_0 asymptomatically and the wake expansion dissipates reaching a linear expansion at constant rate. The wake persists longer in TubOpark as compared to original Jensen model which leads to higher losses occurring in WT downstream [13]. Analytical expression for the wake diameter at distance x downstream of the turbine can be obtained as follows:

$$D_w(\text{x}) = \frac{AI_0 D}{\beta}\left(\sqrt{(\alpha + \beta\, x/D)^2 + 1} - \sqrt{1 + \alpha^2}\right. \\ \left. - \ln\left[\frac{\left(\sqrt{(\alpha + \beta\, x/D)^2 + 1} + 1\right)\alpha}{(\sqrt{1 + \alpha^2} + 1)(\alpha + \beta\, x/D)}\right]\right) + D \quad (7)$$

where auxiliary variables $\alpha = c_1 I_0$, and $\beta = c_2 I_0/\sqrt{C_T(V_{in})}$. V_{in} is the rotor-averaged inflow wind speed at the turbine position. A is the model constant tuned to a recommended value of 0.6. The python™ code implements superposition model as 'linearsum', 'STF2017TurbulenceModel' (similar to Local Jensen) and 'TurboNOJDeficit' as wake deficit model to obtain results. Study indicate that the TurbOPark model with the site-specific ambient turbulence intensity predicts the correct size of the power deficit for the selected value of A and the parameter is often tuned on location basis. [13].

4) BastankhahGaussian Model

Gaussian model proposed by Bastankhah and Porté-Agel (2014), also known as BP wake model incorporates mass and momentum conservation ignoring the viscous and pressure terms in the momentum equation. It assumes gaussian distribution for the velocity deficit in wake. Compared to the top-hat model, gaussian distribution provides a better, consistent and more accurate resemblance for far wakes and this has been proved with numerous measurements and numerical solutions. NOJ adopts a simple and low-computational cost wake model and hence tends to under and over predict power at the center and edges of the wake [12]. Similar to k in NOJ, a linear wake expansion is considered which depends on C_T, spatial coordinates and wake expansion parameter (k^*) [5]. Velocity deficit in this model is mathematically expressed as:

$$\Delta U = \text{U}\left(1 - \sqrt{1 - \frac{C_T}{8\left(k^*\frac{x}{D}+\varepsilon\right)^2}}\right) e^{\left\{-\frac{1}{2\left(k^*\frac{x}{D}+\varepsilon\right)^2}\left(\left(\frac{z-z_h}{D}\right)^2 + \left(\frac{y}{D}\right)^2\right)\right\}} \quad (8)$$

where $\varepsilon = \sqrt{\beta}/4$, and $\beta = (1 + \sqrt{1 - C_T})/2(\sqrt{1 - C_T})$. x, y , z are streamwise, spanwise and vertical coordinates, respectively. z_h is the hub height [12].

5) IEA37SimpleBastankhahGaussian Model

This method follows the same method as BastankhahGaussian assuming the value of $\beta = 1/\sqrt{8}$ and C_T as 0.9637188.

6) TurboGaussian Model

This model is implemented similar to Ørsted's TurbOPark model, wherein TurboGaussian wake A is tuned to a recommended value of 0.04 [10].

7) Fuga Model

Fuga is a linear flow solver based on steady-state Reynolds-Averaged Navier-Stokes equations (RANS) equation with simple turbulence closure and considers atmospheric stability. The new version also includes meandering effect [4][11]. It is considered one of the most robust computational fluid dynamics (CFD) based models due to its simplicity in wake modelling [14]. The model requires a look up table for the multiple wake case and linear summation to construct the velocity field of the array in PyWake. Fuga assumes a horizontally homogenous boundary layer suited for flat terrain and can model long distance wakes as they occur within and downstream from large OSWF installations [12].

8) FugaBlockage Model

All the aforementioned WFMs use 'PropogateDownwind' to determine wake deficits which is fast although blockage is neglected. FugaBlockage model simply iterates over all the turbines in downstream order and performs the calculation of effective wind speed at the current WT as the free stream wind speed minus the summation of the deficit from upstream sources. The 'All2AllIterative' WFM captured in FugaBlockage performs iteration until the effective wind speed converge. In each iteration it sums up the deficit from all WT sources and computes the deficit on each WT. In the first iteration, all WT see the free WS, resulting in equal CT and deficits. In the second iteration, the local effective wind speeds are updated based on the wake and blockage effects of the other WT. The CT and deficits are then recalculated due to change in local WS. The

third iteration follows a repetition till the flow field converges. So, the local wind speeds are updated based on the wake and blockage effects of the other WT and hence it predicts lower net AEP in effect [10].

IV. METHODOLOGY

PyWake implements the concept of 'Xarray' for handling multidimensional data to eliminate use of multiple for loops. The task is simplified for obtaining power which is a function of several parameters (WT, WD and WS). The simulations from the WFMs are averaged over wind direction sectors of 30° to compute AEP, i.e., sector frequencies are obtained from the 12 sectors (with 30° increments; starting from $0 \pm 15°$). However, it may be important to understand that model accuracy depends on the span of averaging sector which largely depends on the uncertainty in WD. Studies indicate the accuracy decreases with wind direction sectors below 10° [4]. Flowmap simulated through the results provides production at a specific direction and does not take into account the AEP. Mean wind speed of 10m/s was selected to perform the simulation with a resolution of 0.5m/s WS and 1° WD. The net AEP has negligible effect on further lowering these values , in contradiction it increases the computation time.

A. Dudgeon wind farm

As a preliminary run, a site was identified to obtain wind data and time-series analysis was performed by virtually installing only one type of turbine, i.e, 15MW on dudgeon layout to observe the wake losses from various PyWake models. Fig. 16 under Appendix) shows the flowmap for the initial selected layout using the original Jensen model.

B. Layout Optimisation

Aside from lowering land requirements thus land costs, the benefit of a higher installed power density is a reduction in the cost of transmission between turbines in a farm. A disadvantage is increased wake-losses for the turbines located downstream, which may affect lifespan and cause premature damage to components of the WT [3]. The newly designed layout having Row spacing by column spacing (RS x CS) of 5D x 5D with a flowmap indicating WS due to wake losses in NOJ model can be observed in Fig. 17 (under Appendix)). CS refers to the distance along the prevailing whereas RS is the spacing perpendicular to wind.

V. RESULTS AND DISCUSSIONS

Higher capacity densities imply greater potential installations of turbines over smaller ocean areas. Wake is highly influenced by the type of layout and turbine spacing, distance between each turbine and how they are placed which is further explained and analysed in this section.

A. Wake model analysis

Area of the initially selected Dudgeon layout is increased sequentially to observe changes in the wake. The Coordinate location of turbines are adjusted in such a way that the distance between each turbine (in both latitude-longitude direction) is increased gradually maintaining the aspect ratio and without distorting the original layout. The coordinates obtained in UTM were converted to decimals to obtain the area and finally the capacity density by assuming that the turbines are placed at far

corners of the selected space. Python[TM] library – 'plotly', and packages – 'utm', 'pyproj', 'shapely' were used to obtain the precise ocean surface. Spreading the same number of WTs over a wind farm substantially increases the power output among all WTs as each turbine experience less competition for available kinetic energy and this is evident with Fig. 4 and Fig. 5. Area of the OSWF in the scaled layout varies as the square of distance between each WT but the variation in losses significantly diminishes w.r.t spacing after a certain distance.

Different type of wake models are executed in this study. Jensen and its modified versions (Local Jensen, TurbOpark) show slightly close value of wake with Local Jensen predicting relatively high. The predicted power of the Turbo Jensen is reasonably close to the results from the original Jensen with slightly higher wake losses in the former model. Wake persistence is longer in Tubo Jensen leading to higher losses occurring in WT downstream and thereby reducing the overall net AEP. If in any case NOJ model overpredicts the wake losses when compared to the original dataset, the error can be mitigated by reducing the value of 'k', especially for the deeper turbines in array. Alternatively, wake expansion parameter A can be calibrated in TurbOpark model to ensure more accurate and validated results.
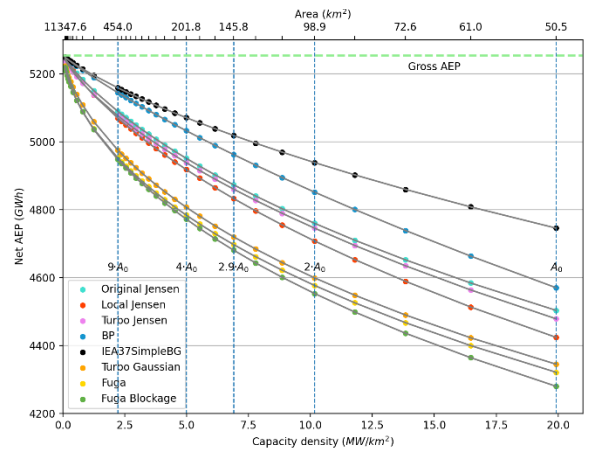
[c] Capacity Density of 0MW/km2 refers to very large spacing between the wind turbines in a wind farm in the current scenario.

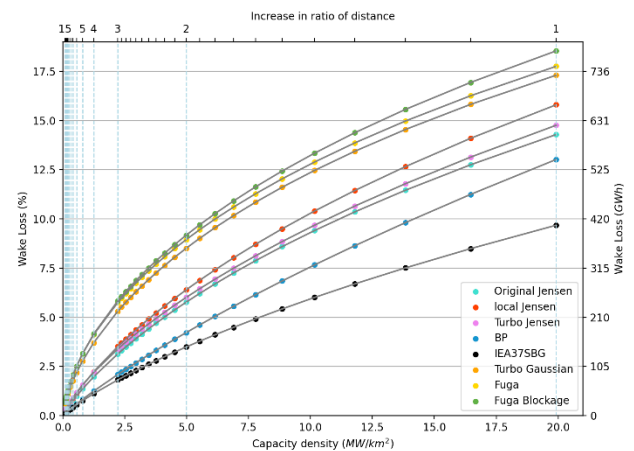Fig. 4. Net AEP vs Capacity density/Area for different wake models

Fig. 5. Wakeloss vs Capacity density/Scaled ratio for different wake models

Wake losses from Fuga, FugaBlockage and TurboGaussian tend to lie close to each other. Fuga, in general is expected to provide accurate predictions for larger wind farms [12]. FugaBlockage shows a higher net AEP in comparison to Fuga as it incorporates a global blockage model. The basic visual difference that can be seen in the WFMs while simulating is that WT is unaffected by downstream wake, in case of 'PropogateDownWind' which is not likely the case with 'All2AllIterative' used in FugaBlockage [10]. FugaBlockage and IEA37SBG predicts the highest and lowest wake losses for the specified layout respectively. In theory IEASBG assumes a C_T value of 0.9637188 leading to a higher net AEP and less wake losses. The selected WT NREL 15MW has maximum C_T ranging between 0.8 to 0.835. Hence, IEA37SBG may underestimate the result and prove not to be of value. Additionally, very few concepts on this model were publicly available to confirm the robustness of this model.

TABLE III. Net Annual Energy Production And Capacity Factor Values

Area Ratio A_{new} /$A_{original}$	Installed Capacity Density [MW/km²]	Output Power Density Range [W/m²]	Net AEP Range (neglecting IEA37SBGModel) [GWh]	Range of Capacity factor (C_F) [%]
1	19.92	9.78 - 10.34	4570.18 - 4280.05	49 - 52
4	4.98	2.71 - 2.85	5032.60 - 4772.38	54 -57
9	2.21	1.25 – 1.29	5144.85 - 4948.26	56 - 58
16	1.25	0.71 – 0.73	5188.89 - 5036.25	57 - 59
25	0.80	0.46 – 0.47	5210.75 - 5088.49	58 - 59

Net AEP, C_F, Installed and Output power density for scaled layout is listed under TABLE III. The values are calculated based on gross AEP of 5254.38GWh and gross C_F of 59.7% obtained with the simulation of current wind farm. With increase in turbine spacing for the fixed number of WTs, the wind farm's capacity density decreases and consequently the wake losses. This substantially increases the marginal gains in production up to a certain point when C_F reaches its peak value. As seen under TABLE III. , The C_F value doesn't have much significant improvement after increasing the area is increased nine times or further.

Turbine spacing is a critical concern due to the wake effect. To prevent early fatigue or issues concerning frequent maintenance of Wind Turbine Generation System (WTGS), OSWFs are typically spaced in the range of 5D to 15D in the direction of prevailing wind and minimum 3D perpendicular to it. Study indicates for the current specific power assumption of 332W/m2, the capacity density varies between a rough value of 5 to 8MW/ km² marked as a zone under Fig. 7[2]. The graph for comparison of new layout vs the previous dudgeon layout is developed using original Jensen model under Fig. 6 and Fig. 7.

TABLE IV. provides the comparison between original vs optimized layout for the maximum value of capacity density in the selected range. It can be inferred that the original layout of Dudgeon selected for the first attempt could have been improved with a better layout. For example, a new optimized layout with CS x RS spacing of 6D x 9D gave a higher net AEP with NOJ

method for the same capacity density (7.6 MW/km²) and specific power assumption of 332 W/m². Further better results can be observed when the spacing is altered to 9D x 6D. However, for practical purpose RS x CS of 9D x 5D (CD = 9.11 MW/ km², WL = 4.79%) to 7D x 5D (CD = 11.72 MW/ km², WL = 6.24% could prove to be a good fit for considerable improvement in net AEP corresponding to the optimised area but it largely depends on other factors which shall be carried out in the future analysis with thesis.
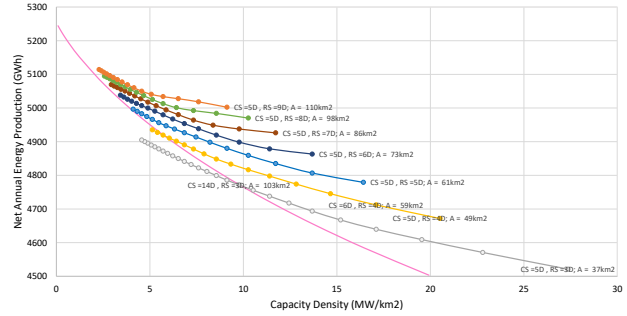
B. Layout comparison

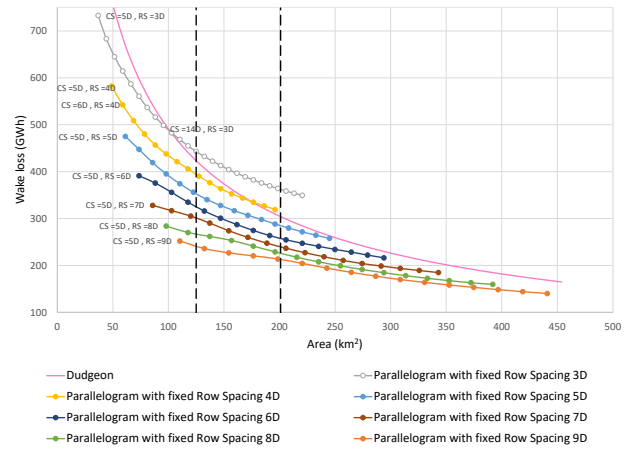Fig. 6. Net AEP vs Capacity Density for increment in column spacing

Fig. 7. Wake losses vs Area for increment in column spacing

TABLE IV. Comparison Of Layouts

Layout	Spacing		Net AEP (NOJ model) [GWh]	Wake losses (WL)		Capacity Factor (C_F)
	R	C		[GWh]	[%]	
Dudgeon	-	-	4847.19	407.20	7.75	55%
Optimized-1	6D	9D	4938.28	316.11	6.02	56%
Optimized-2	9D	6D	5018.41	235.98	4.49	57%

VI. Conclusion

The selected location for WT installation evidently has tremendous scope and great wind resource compared to the offshore locations currently operating. Capacity density can be improved with optimization of layout as well as turbine spacing. The natural upper limit for capacity density is not defined, so the optimised turbine spacing can be evaluated based on the minimizing wake losses and the area. Theoretical predicted

wake losses from the concluded turbine spacing of (9D to 7D) x 5D (4.79% - 6.24%) and capacity density of 9.11 – 11.72 MW/km² are significantly lower than the average values of wake losses from currently operating wind farms (10 - 20%).

Parameters affecting the wake includes -type of layout, turbine spacing, WT type, wind climate data. The probability distribution showed high dominancy of wind in 2010 from E followed by NNW. Investigation for a reliable and consistent method can quantify the WD uncertainty in large wind farms to ensure a reasonable comparison between actual power produced and numerical simulations [4]. The PyWake models implement different model parameters which dictates intensity of wake effect and can have impact on the production. Jensen implements an empirical constant - wake decay coefficient, k (standard value used for offshore, 0.04) and specific models like Local, Turbo Jensen and TurboGaussian considers Turbulence intensity, TI whereas BP and IEA37SBG employs wake expansion parameter (k^*- k used in PyWake). Need for tuning of these parameters, especially wake expansion parameter A according to the designed wind farm may arise in Turbo Jensen model for achieving more validated results. More research is needed to ensure that the models are appropriately calibrated and include the relevant physics. The wide variety of existing wake models in PyWake accentuates the need for clear guidelines on the best fit or criteria on how the wind industry shall use these models. The wake loss uncertainty can be reduced with calibration and understanding the model limitations. The best model that fits to calculate more accurate results at present can only be confirmed with a practical dataset.

Limitations in the research were data resolution and disregarding physical constraints with scaled and optimized layouts elaborated as follows. i) The true power prediction in the timeseries is lost without taking wind variation into account for hourly-wind data. ii)Although wake losses are optimized as much as possible, very often the projects are driven by other constraints (such as shipping lane, fishing, helicopter zone, etc.) and this leaves a very little room to optimize layout or wake losses. iii)The simulations from the wake models, i.e, Weibull probability, scale and shape parameter values are averaged over wind-direction sectors of 30° to compute AEP. Studies indicate that model accuracy changes with the span of averaging sector[4].

VII. FUTURE WORK

The objective of the future proposed project is to develop methods and perform extensive study on sensitivity of the input parameters to maximize the capacity densities of OSWFs, without sacrificing the plant capacity factor (C_F). The sensitivity analysis may include different scenarios for wind turbine type, number, rotor size, wind farm layout, climate etc. The thesis topic shall largely focus on identifying the optimal wind farm capacity density corresponding to a minimized Levelized Cost of Energy (LCoE) and establishing a relation between the respective cost associated while deviating from the nominal value of spacing between the wind turbines.

REFERENCES

[1] K. Stoltz and Karianne Kojen Andersen, "Norway sets 30GW offshore wind energy target | GCE Ocean Technology," May 11, 2022. https://www.gceocean.no/news/posts/2022/may/norway-sets-30gw-offshore-wind-energy-target/ (accessed Nov. 10, 2022).

[2] R. Borrmann, K. Rehfeld, A.-K. Wallasch, and S. Lüers, "Capacity densities of European offshore wind farms," Hamburg, 2018.

[3] P. Enevoldsen and M. Z. Jacobson, "Data investigation of installed and output power densities of onshore and offshore wind turbines worldwide," *Energy Sustain. Dev.*, vol. 60, pp. 40–51, Feb. 2021, doi: 10.1016/J.ESD.2020.11.004.

[4] M. Gaumond *et al.*, "Benchmarking of wind turbine wake models in large offshore windfarms," in *The science of Making Torque from Wind 2012*, 2012, vol. 7, no. 1, pp. 343–354.

[5] M. Bastankhah and F. Porté-Agel, "A new analytical model for wind-turbine wakes," *Renew. Energy*, vol. 70, pp. 116–123, Oct. 2014, doi: 10.1016/J.RENENE.2014.01.002.

[6] B. . Bulder, G. Bedon, and E. T. . Bot, "Optimal wind farm power density analysis for future offshore wind farms," Netherlands, 2018.

[7] S. Mathew, *Wind energy: Fundamentals, resource analysis and economics*. Springer Berlin Heidelberg, 2007.

[8] H. Bidaoui, I. El Abbassi, A. El Bouardi, and A. Darcherif, "Wind speed data analysis using Weibull and Rayleigh distribution functions, case Study: five cities Northern Morocco," *Procedia Manuf.*, vol. 32, pp. 786–793, Jan. 2019, doi: 10.1016/J.PROMFG.2019.02.286.

[9] "Offshore Wind Turbine Documentation." https://nrel.github.io/turbine-models/IEA_15MW_240_RWT.html#link-to-tabular-data (accessed Nov. 11, 2022).

[10] "PyWake 2.4.0," 2018. https://topfarm.pages.windenergy.dtu.dk/PyWake/index.html (accessed Nov. 03, 2022).

[11] M. Gaumond, P. E. Réthoré, S. Ott, A. Peña, A. Bechmann, and K. S. Hansen, "Evaluation of the wind direction uncertainty and its impact on wake modeling at the Horns Rev offshore wind farm," *Wind Energy*, vol. 17, no. 8, pp. 1169–1178, Aug. 2014, doi: 10.1002/WE.1625.

[12] A. C. de. B. Neiva, V. G. Guedes, C. L. S. Massa, and D. D. B. de Freitas, "A review of wind turbine wake models for microscale wind park simulation," 2019.

[13] N. G. Nygaard, S. T. Steen, L. Poulsen, and J. G. Pedersen, "Modelling cluster wakes and wind farm blockage," *J. Phys. Conf. Ser.*, vol. 1618, pp. 62–72, Sep. 2020, doi: 10.1088/1742-6596/1618/6/062072.

[14] T. Göçmen, P. Van Der Laan, P. E. Réthoré, A. P. Diaz, and G. C. Larsen, "Wind turbine wake models developed at the technical university of Denmark: A review," *Renew. Sustain. Energy Rev.*, vol. 60, pp. 752–769, Jul. 2016, doi: 10.1016/J.RSER.2016.01.113.
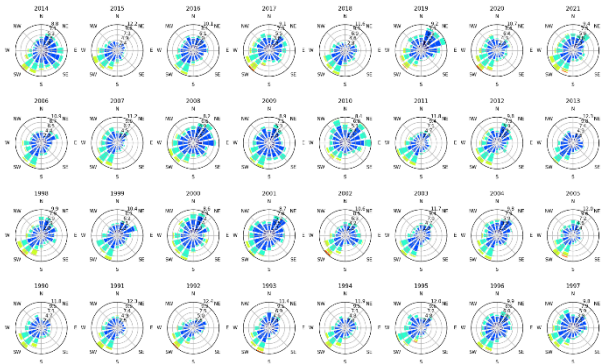
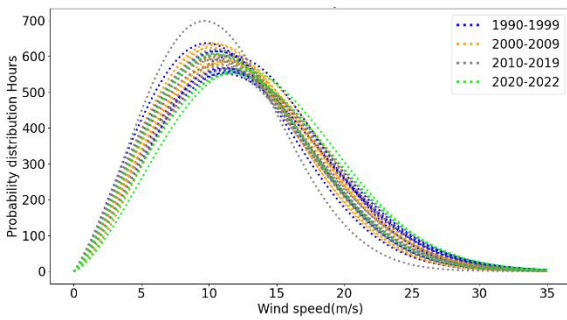Fig. 8. Windrose plot for each year between 1990-2021 at height 160m

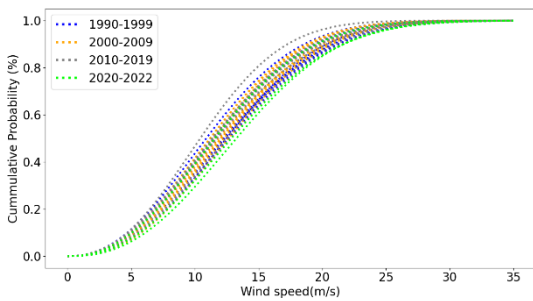Fig. 9. Weibull distribution for the year 1990 to 2022

Fig. 10. Weibull cummulative distribution for the year 1990 to 2022
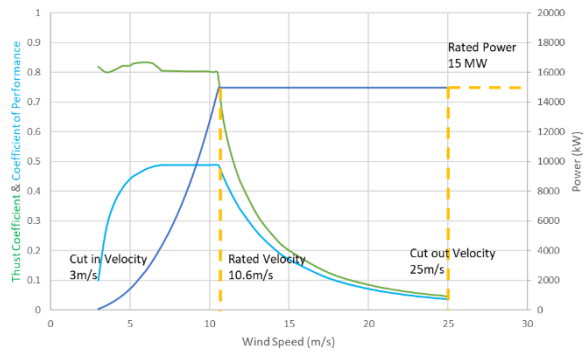

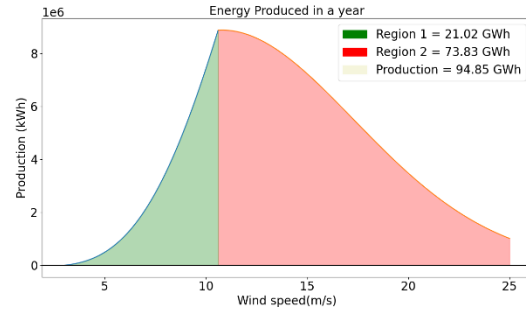Fig. 11. Coefficient of Performance, Thrust coefficient and Power for NREL 15MW wind turbine

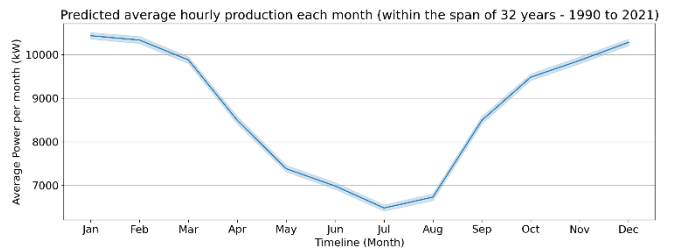Fig. 12. Annual energy production for the average value of shape and scale factor

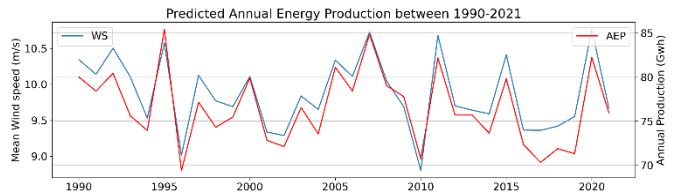Fig. 13. Predicted average hourly production each month within the span of 32 years

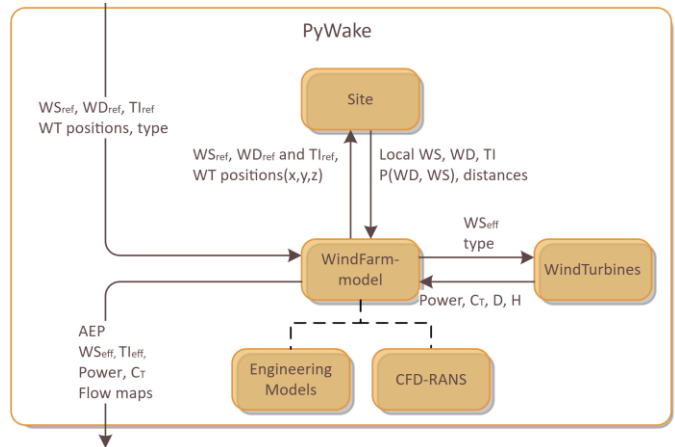Fig. 14. Predicted Annual energy production for between 1990-2021
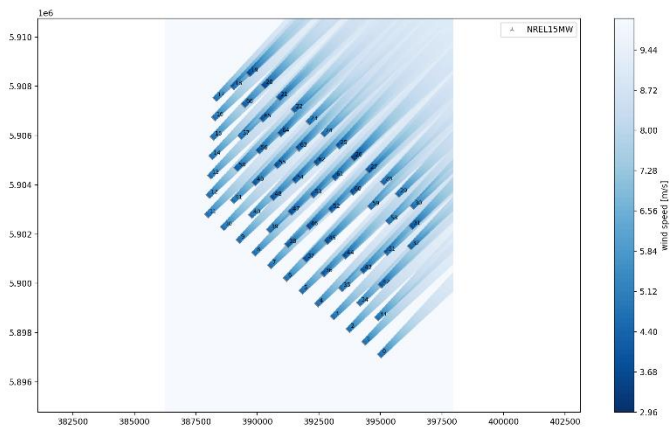

Fig. 15. Flowchart of PyWake simulation

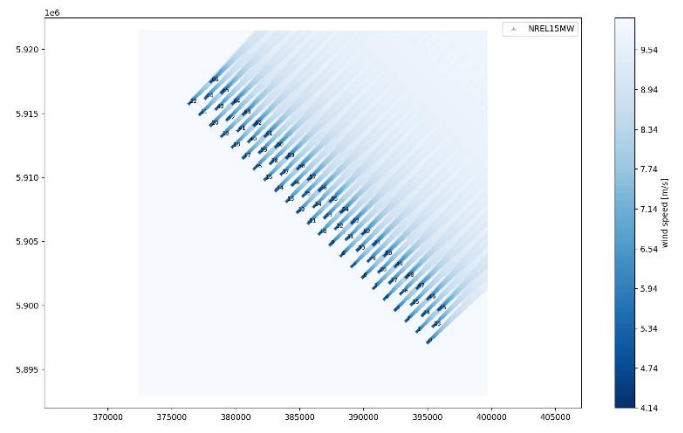Fig. 16. Flowmap of NREL 15MW WT placed in Dudgeon layout

Fig. 17. Flowmap of optimized layout with turbine spacing 5D x 5D